Solving Boundary Value Problems
on Composite Grids
with an Application to
Combustion

P.J.J. Ferket

SOLVING

BOUNDARY VALUE PROBLEMS

ON COMPOSITE GRIDS

WITH AN APPLICATION TO COMBUSTION

SOLVING
BOUNDARY VALUE PROBLEMS
ON COMPOSITE GRIDS
WITH AN APPLICATION TO COMBUSTION

Dit proefschrift is goedgekeurd door de promotoren:

prof.dr. R.M.M. Mattheij
en
prof.dr. P.W. Hemker

Copromotor: dr. A.A. Reusken

CONTENTS

1

SCOPE OF THE THESIS

1.1 INTRODUCTION

In many industrial and scientific disciplines there is a great interest in predicting the outcome of physical processes by computer simulations. For example, for the design of burners in industrial and domestic applications, the influence of variations in the composition of (natural) gas on the combustion process is studied. Subjects such as flame stability and the prediction of the composition of exhaust gases are of main importance. Other examples are in aerospace industry where the air flow around aeroplanes is studied to predict loads on the structure of a plane, in geophysical science where one studies the dispersion of pollutants in ground and surface water to predict the quality of water resources, and in petro-chemical industry where porous media flow simulation is used to predict the recovery of oil from a well. The basis of the simulations is a mathematical model describing the underlying physical process. Many physical processes are described by models involving partial differential equations inside a domain of definition, completed with conditions at the boundary of the domain. Such models are called *boundary value problems*.

Usually the boundary value problems describing a physical process are too complex to obtain an analytical solution, and they have to be solved numerically. To obtain a numerical solution, the partial differential equations and the boundary conditions are discretized using a grid consisting of a finite number of points. The discretization process leads to a system of algebraic equations. By solving this system one obtains a numerical approximation of the solution of the boundary value problem on the grid. Clearly the grid size needed for a reasonable representation of (an approximation of) the solution depends on the variations of the solution. The finer the grid is, the larger the system of algebraic equations and the higher the computational costs, i.e. CPU time and memory requirements, are.

Often the variations of the solution are large only in a part of the domain and small anywhere else. For such problems a uniform grid over the whole domain contains a large number of redundant grid points. To approximate the solution, a large system of algebraic equations has to be
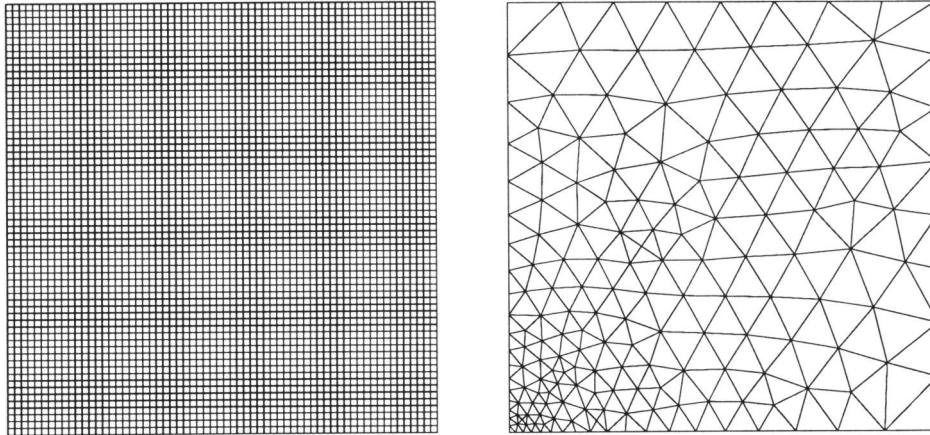
Figure 1.1   A uniform fine grid and a truly non-uniform refined grid.

solved and information has to be stored at a large number of grid points. In general the advantages of using a uniform grid, like simple data structures and the existence of simple, accurate discretization stencils and fast solution techniques for the resulting systems of algebraic equations, do not counterbalance the disadvantage of having so many redundant grid points, and the use of a global uniform grid is computationally inefficient. In such a situation adaptive grid methods prove to be beneficial, since these methods attempt to adapt locally the grid size to the behaviour of the solution.

Adaptive grid methods can be divided into two classes: methods using *a priori adapted* grids and *self-adaptive* grid methods. In many numerical simulations requiring local refinement, it is known in advance where the grid needs to be refined and at what scale. In this case a method using an a priori adapted grid can be applied. With the available information a locally refined grid is generated. Then, an approximation of the solution is computed on this adapted grid. In many other cases, however, the knowledge of where to refine has to be obtained dynamically from features of the emerging solution. In self-adaptive grid methods a posteriori error estimates on a given grid are used to decide where to adapt this grid. The grid adaptation process is performed recursively, starting from a coarse basis grid. Clearly, self-adaptive grid methods are more complex than methods using a priori adapted grids. In this thesis we study the solution of boundary value problems on a priori adapted grids.

In order to construct a grid which is adapted to the local behaviour of the solution, a local grid refinement technique is applied. A great variety of local grid refinement techniques exists. The counterpart of global uniform grid refinement is pointwise grid refinement. The pointwise grid refinement technique leads to a truly non-uniform refined grid. In such a grid there is hardly any structure in the position of the grid points. A grid point may be positioned anywhere inside the domain and the distance between the grid points can be as small or as large as the variations in the solution require. Such grids are mainly used in finite element computations. In Figure 1.1 both a

a)

b)
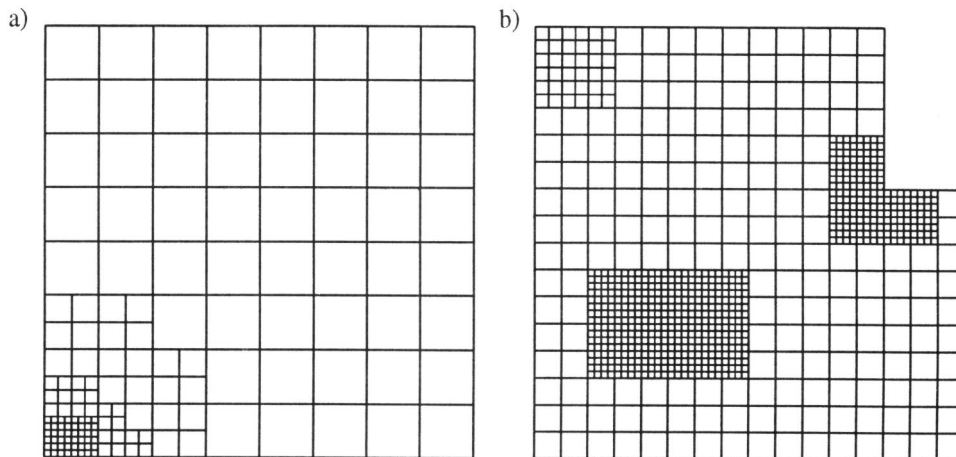
Figure 1.2 Composite grids.

global uniform fine grid and a truly non-uniform grid are shown. Clearly, truly non-uniform grids can be very well adapted to the variations of the solution in any part of the domain. An important disadvantage is that such truly non-uniform grids result in rather complex data structures. The data structure problem is even more pronounced for three space dimensions.

1.2 COMPOSITE GRIDS

Compromising between the extremes of globally uniform grid refinement and pointwise adaptive grid refinement, each with its obvious advantages and disadvantages, leads to the use of locally uniform grid refinement techniques. In these techniques a coarse basis grid, covering the whole domain, is locally uniformly refined in certain parts of the domain. Locally uniform grid refinement techniques result in *composite grids* with locally refined regions. In Figure 1.2 two composite grids are shown. In Figure 1.2.a the locally refined regions are nested, which is typical for composite grids resulting from a self-adaptive local uniform grid refinement technique. The grid in Figure 1.2.b is a typical example of an a priori adapted composite grid.

Locally uniform grid refinement methods have been proposed in many different varieties. They are used to solve elliptic partial differential equations in [18],[29],[48], hyperbolic partial differential equations in [1],[4],[28] and parabolic partial differential equations in [24],[64]. Self-adaptive locally uniform grid refinement methods resulting in a sequence of locally nested grids are combined with a multigrid solution technique in [7],[9]. In [43],[44] a self-adaptive multigrid method with locally uniform grid refinement for solving the Euler equations is developed. There also the discretization of steady conservation laws in the neighbourhood of coarse and fine grid interfaces is studied.

In this thesis we consider the solution of boundary value problems on a certain class of a priori

Figure 1.3   Global coarse grid with a rectangular and an L-shaped region of local refinement.

adapted composite grids. Here we briefly describe typical examples from this class of composite grids. In these examples we consider the case of two space dimensions and only one region of local refinement.

The composite grids which we consider result from a uniform basis grid with grid size H covering a domain of definition by uniform refinement in a subregion of the domain, the so-called *region of local r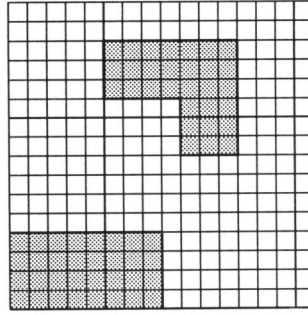efinement*. The uniform basis grid is called the *global coarse grid*. The region of local refinement is assumed to be the union of a set of neighbouring coarse grid cells[1]. It is assumed that at least one grid point of the global coarse grid lies in the interior of this region. In Figure 1.3 two examples of local refinement regions satisfying the above assumptions are shown. The part of the global coarse grid inside the region of local refinement is uniformly refined by a factor $\sigma \in I\!N$, the so-called *refinement factor*. The uniform grid with grid size $h = H/\sigma$, covering the region of local refinement, is called the *local fine grid*. The composite grid is composed of the global coarse grid and the local fine grid. In Figure 1.4 examples of a global coarse grid, a local fine grid and a composite grid are shown.

In this thesis we study the solution of boundary value problems on composite grids as described above. It is assumed that the variations of the solution of the boundary value problem are relatively large in a small part of the domain, so that a locally strongly refined composite grid (i.e. $\sigma \gg 1$) is needed for numerically approximating the solution. For discretizing the boundary value problem, *finite difference methods* will be used.

The composite grids described above have several attractive properties. Since they are highly structured, data structures are very simple. The position of all grid points can be determined from a small number of parameters. So, the composite grids are very manageable in a practical implementation. In some part of the domain the grid can be locally refined to any scale required by the variations of the solution. So, the solution can be efficiently and accurately approximated on the composite grid. Since the composite grid is composed of uniform subgrids, discretization of the boundary value problem is standard in the greater part of the domain. At most grid points accurate, uniform difference stencils can be used. Only at certain grid points on and near the coarse

---

[1] Here a coarse grid cell is a square of size H generated by four grid points of the global coarse grid.
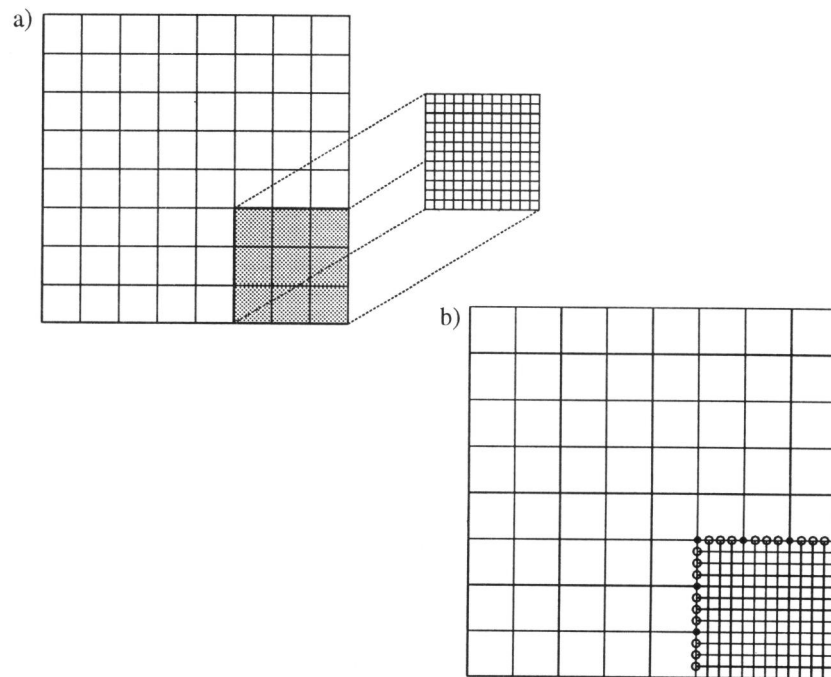
Figure 1.4 a) Global coarse grid and local fine grid; refinement factor 4. b) Composite grid with interface grid points (•) and slave points (○).

and fine grid interface the discretization process is non-standard and needs special care.

A large part of the computational work for numerically approximating the solution of a boundary value problem consists of solving systems of algebraic equations. In this thesis we study iterative methods which predominantly use the uniform subgrids underlying the composite grid. In these methods systems of algebraic equations are solved on the uniform subgrids only. Often systems of algebraic equations resulting from discretization on uniform grids can be solved very efficiently.

Although in the examples above we consider two-dimensional composite grids composed of two uniform subgrids, it should be emphasized that the methods and many of the results presented in this thesis can be generalized to several other situations in a straightforward way. For the main results we will give comments on possible generalizations. Here we already mention that the assumption of one local fine grid is not restrictive. The methods and analysis in chapters 2-5 can be easily generalized to composite grids composed of a global coarse grid and a number of local fine grids, covering disjoint regions of local refinement. An example of such a grid is given in Figure 1.2.b. We do not consider composite grids composed of a global coarse grid and a nested sequence of local grids as in Figure 1.2.a. Instead of gradual refinement by a sequence of nested uniform subgrids, where the refinement factor for two consecutive grids is only 2, we consider an abrupt refinement by only one local fine grid. Finally we mention that the methods in chapters 2

and 5 and the analysis in Chapter 3 can be easily generalized for three space dimensions.

1.3   CONTENTS OF THE THESIS

In the literature ([7],[30],[46]) one can find three basic iterative methods for approximating the solution of boundary value problems on composite grids. In Chapter 2 these three methods are introduced and compared. We believe that a uniform presentation and analysis of these methods is a novelty. The methods are described for a model linear elliptic boundary value problem and a model composite grid. The boundary value problem is discretized using finite difference methods. In the local defect correction (LDC) method the boundary value problem is discretized both on the uniform global coarse grid and on the uniform local fine grid. The right hand sides of the discrete equations on the uniform subgrids are adapted in an iterative process. Each iteration step yields approximations of the solution of the boundary value problem on the uniform subgrids. In the LDC method no discretization of the boundary value problem on the composite grid is needed. The fast adaptive composite grid (FAC) method is of a different nature. This is an iterative method for solving an a priori given discretization of the boundary value problem on the composite grid. The solution of the composite grid discretization is approximated by solving systems of algebraic equations on the uniform global coarse grid and on the uniform local fine grid. The multi-level adaptive technique (MLAT) is a multigrid approach on grids with local refinements. Like in the LDC method the boundary value problem is discretized only on the uniform global coarse grid and on the uniform local fine grid. For solving the systems of algebraic equations on the local fine grid, a two-grid method is used.

Both for the LDC method and for the MLAT method the composite grid discretization, which is actually solved by the method, is an implicit result of the method itself. These composite grid discretizations are the key to an analysis of the LDC method and the MLAT method. In Chapter 3 the composite grid discretization related to the LDC method is derived. Also an expression for the iteration matrix of the LDC method is derived. In order to compare the LDC method and the FAC method, the latter is applied to the composite grid discretization related to the LDC method. It is shown that then, with a suitable choice of the initial approximation in the FAC method, the LDC iterates and the FAC iterates are the same. For the MLAT method the composite grid discretization which is actually solved by the method is derived too. The composite grid discretizations related to the LDC method and the MLAT method are compared. It is shown that the composite grid discretization related to the MLAT method depends on the restriction operator used in MLAT for restricting local fine grid approximations to grid points of the global coarse grid.

In Chapter 4 the composite grid discretizations related to the LDC method and the MLAT method are studied. Global discretization error estimates are derived for these two composite grid discretizations, as well as for a third composite grid discretization, which is characterized by the use of non-uniform finite difference stencils at the grid points on the coarse and fine grid interface. First the composite grid discretizations are compared for the one-dimensional Poisson problem. It is shown that already for this simple one-dimensional problem, the composite grid discretization related to the LDC method has important advantages compared to the other two composite grid discretizations. It is concluded that, from a discretization point of view, in the MLAT method

trivial injection should be used for restricting local fine grid approximations to grid points of the global coarse grid. The favourable properties of the composite grid discretization related to the LDC method remain valid for two space dimensions. For the two-dimensional Poisson problem a sharp global discretization error bound, which is valid without restrictions on the coarse grid size H, the fine grid size h and the refinement factor $\sigma = H/h$, is derived. This is a new result for finite difference discretization error estimation on composite grids in which the two grid sizes H and h are essentially independent.

In chapters 2-4 linear boundary value problems are considered. In Chapter 5 two methods for solving nonlinear boundary value problems on composite grids are described. The first one, the nonlinear LDC method, is a combination of an outer local defect correction iteration with inner Newton iterations for solving systems of nonlinear equations on the uniform subgrids. Sufficient conditions are given for the nonlinear LDC method to be well-defined, i.e. for all systems of non-linear equations in the nonlinear LDC method to have a locally unique solution. It is shown that the nonlinear LDC method is closely related to a composite grid discretization of the boundary value problem. In the second method, called the Newton-FAC method, this composite grid discretization is solved by an outer Newton iteration and inner FAC iterations for solving Jacobian systems on the composite grid.

In Chapter 6 the numerical simulation of flat flames on composite grids is considered. The numerical simulation of a combustion process typically requires the use of locally strongly refined grids, since the chemically active layer, where the variations in the variables are large, is relatively small compared to the size of the computational domain. The governing equations for reacting gas flow in general and for burner stabilized flat flames in particular are summarized. A one-dimensional combustion model problem is derived and the nonlinear LDC method from Chapter 5 is applied to this model problem. Properties of the nonlinear LDC method are illustrated by numerical results. For example, the errors in the approximations resulting after 0, 1 and 2 local defect correction steps are considered, as well as the error in the approximation obtained in the limit by the nonlinear LDC method.

2

INTRODUCTION OF ITERATIVE METHODS ON COMPOSITE GRIDS

In this chapter we describe three iterative methods for solving boundary value problems on composite grids: local defect correction (due to Hackbusch [30]), the fast adaptive composite grid method (due to McCormick [46]) and the multi-level adaptive technique (due to Brandt [7]). A basic feature of the methods is that the greater part of the work is carried out on uniform subgrids. The methods are all described for the same model setting.

The model boundary value problem and the model composite grid are introduced in Section 2.1. The local defect correction method is presented in Section 2.2. First the method is introduced for the model setting. Then some typical features of the method are illustrated by numerical results and important generalizations are discussed. In the local defect correction method boundary value problems are discretized on uniform subgrids only, not on the composite grid. The discrete problem on the composite grid which is actually solved by the method is not a priori given, but it is an implicit result of the iterative process. On the other hand, the fast adaptive composite grid method is an iterative method for solving an a priori given discrete problem on a composite grid. The fast adaptive composite grid method is presented in Section 2.3. The multi-level adaptive technique, which is presented in Section 2.4, is derived from the multigrid method for approximately solving boundary value problems. As for the local defect correction method, the discrete problem on the composite grid which is actually solved by the multi-level adaptive technique is an implicit result of the iterative process. In Section 2.5 we discuss the similarities and the differences between the three iterative methods. We use several results from Chapter 3, in which the three methods are analysed.

2.1   MODEL PROBLEM

In this section we introduce a simple model problem to be used for clarifying the iterative methods in the sections following. The model problem is suitable for introducing the basic concepts of the methods without the concern of technical and notational details.

The *model boundary value problem* is the two-dimensional Poisson problem on the unit square

with Dirichlet boundary conditions,

$$-\Delta u = f \qquad \text{in } \Omega := (0, 1) \times (0, 1), \tag{2.1a}$$

$$u = \varphi \qquad \text{on } \partial\Omega. \tag{2.1b}$$

Here f is a given function on Ω, φ a given function on the boundary $\partial\Omega$ of the domain Ω and $\Delta := \frac{\partial^2}{\partial x^2} + \frac{\partial^2}{\partial y^2}$, the Laplace operator. The closure of Ω is defined by $\bar{\Omega} := \Omega \cup \partial\Omega$. We assume that the boundary value problem (2.1) has a unique solution, $u^\star \in C^2(\Omega) \cap C(\bar{\Omega})$, and that the variations of the solution are relatively large in some part of the domain and relatively small in the remainder of the domain. The part of the domain where the variations of the solution are relatively large is called the *high activity region*.

The model composite grid $\Omega^{H,h}$ is composed of a global coarse grid and a local fine grid. The *global coarse grid* Ω^H is a uniform grid with grid size H covering the domain Ω:

$$\Omega^H := \hat{\Omega}^H \cap \Omega, \tag{2.2}$$

with

$$\hat{\Omega}^H := \{(x, y) \in {I\!R}^2 \mid x/H \in {I\!N}, \ y/H \in {I\!N}\}. \tag{2.3}$$

We assume that $1/H \in {I\!N}$. The *local fine grid* Ω_l^h is a uniform grid with grid size $h < H$, covering the *region of local refinement* $\Omega_l := (0, \gamma_1) \times (0, \gamma_2) \subset \Omega$:

$$\Omega_l^h := \hat{\Omega}^h \cap \Omega_l, \tag{2.4}$$

with

$$\hat{\Omega}^h := \{(x, y) \in {I\!R}^2 \mid x/h \in {I\!N}, \ y/h \in {I\!N}\}. \tag{2.5}$$

We assume that $\gamma_1/H \in {I\!N}$, $\gamma_2/H \in {I\!N}$ and $H/h \in {I\!N}$. The *interface* Γ is defined as the part of the boundary $\partial\Omega_l$ of Ω_l which lies inside Ω,

$$\Gamma := \partial\Omega_l \cap \Omega. \tag{2.6}$$

We assume that the high activity region of the boundary value problem (2.1) lies inside the subregion Ω_l. The *composite grid* $\Omega^{H,h}$ is defined by

$$\Omega^{H,h} := \Omega^H \cup \Omega_l^h, \tag{2.7}$$

and is shown in Figure 2.1.

The *refinement factor* σ is defined as the ratio of the coarse grid size H and the fine grid size h,

$$\sigma := H/h. \tag{2.8}$$

Since we have assumed that $H/h \in {I\!N}$, the refinement factor is an integer. In this thesis the refinement factor is an important parameter. We are particularly interested in composite grids with *large* refinement factors.
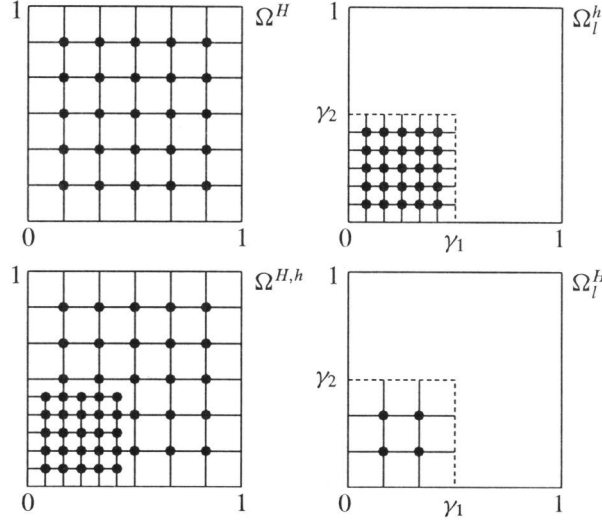
Figure 2.1   The uniform grids Ω^H, Ω_l^h and Ω_l^H, and the composite grid $\Omega^{H,h}$ for $H = 1/6$, $\sigma = 2$ and $\gamma_1 = \gamma_2 = 1/2$.

Remark 2.1   Often *sequences of locally nested uniform grids of decreasing grid size* are used for solving boundary value problems. The grid size ratio of two consecutive grids is usually small (e.g., 2). In this thesis we consider a global coarse grid Ω^H and *one* local fine grid Ω_l^h and a *large* refinement factor $\sigma = H/h$ (e.g., $\sigma = 16$). □

Besides the uniform global coarse grid Ω^H and the uniform local fine grid Ω_l^h, another two uniform grids are used in this chapter. The *local coarse grid* Ω_l^H is defined by

$$\Omega_l^H := \hat{\Omega}^H \cap \Omega_l, \tag{2.9}$$

with $\hat{\Omega}^H$ from (2.3). The local coarse grid Ω_l^H is a uniform grid with grid size H, covering the subregion Ω_l (see Figure 2.1). Since $H/h \in I\!N$, all grid points of Ω_l^H are grid points of the local fine grid Ω_l^h too. The local coarse grid Ω_l^H will be used in the local defect correction method. The *global fine grid* Ω^h is defined by

$$\Omega^h := \hat{\Omega}^h \cap \Omega, \tag{2.10}$$

with $\hat{\Omega}^h$ from (2.5). The global fine grid Ω^h is a uniform grid with grid size h covering Ω.

We conclude this section with some definitions and notation concerning functions on grids. We recall that a grid is a set of points.

Definition 2.2   A *grid function* on a grid V is a mapping $v : V \to I\!R$. The *set of all grid functions* on a grid V is denoted by $\mathcal{F}(V)$.

Definition 2.3   The *restriction* $w_{|V} : V \to I\!R$ of a (grid) function $w : W \to I\!R$ to the grid $V \subset W$ is defined by

$$w_{|V}(\mathbf{x}) := w(\mathbf{x}) \qquad \mathbf{x} \in V.$$

Definition 2.4 The *maximum norm* of a grid function $v \in \mathcal{F}(V)$ is defined by

$$\|v\|_\infty := \max_{\mathbf{x} \in V} |v(\mathbf{x})|.$$

Definition 2.5 For an ordering of the grid points of a grid V, say $\mathbf{x}_1, \mathbf{x}_2, \ldots, \mathbf{x}_l$, the *vector representation* of a grid function $v \in \mathcal{F}(V)$ is defined by

$$\mathbf{v} := (v(\mathbf{x}_1), v(\mathbf{x}_2), \ldots, v(\mathbf{x}_l))^T.$$

The component of the vector $\mathbf{v}$ corresponding to a grid point $\mathbf{x} \in V$ is denoted by $\mathbf{v}(\mathbf{x})$.

The notion of grid functions and vector representations will be used throughout the remainder of this thesis.

2.2 THE LOCAL DEFECT CORRECTION (LDC) METHOD

In this section we describe the *local defect correction* (LDC) method. In Subsection 2.2.1 the LDC method is introduced for the model boundary value problem and the model composite grid from the previous section. Some properties of the method are illustrated by numerical results in Subsection 2.2.2. The LDC method introduced here is a special case of a general local defect correction technique due to Hackbusch [30]. Important generalizations of the LDC method are considered in Subsection 2.2.3.

2.2.1 Description of the Method

The common approach for solving a boundary value problem on a grid consists of two steps. First the boundary value problem is discretized on the grid and then the resulting system of equations is solved. In the LDC method we do not a priori define discrete equations on the composite grid $\Omega^{H,h}$. The LDC method is an iterative process and in each step systems of linear equations resulting from discretizing the boundary value problem (2.1) on the global coarse grid Ω^H and on the local fine grid Ω^h_l are defined and solved. The solutions of the discrete problems are used to define an approximation of the solution of the boundary value problem (2.1) on the composite grid $\Omega^{H,h}$.

For discretizing on the uniform subgrids *finite difference methods* are used (see e.g. [32],[50]). At each grid point the differential equation is approximated by an *algebraic equation* in which the derivatives have been replaced by appropriate *difference quotients*. For discretizing the Poisson problem (2.1) central differences in the x and y direction are used:

$$-\Delta u(x, y) \doteq H^{-2}[4u(x, y) - u(x+H, y) - u(x-H, y) - u(x, y+H) - u(x, y-H)], \quad (2.11)$$
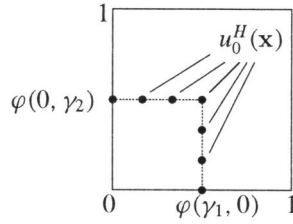
Figure 2.2 Values used to define artificial Dirichlet boundary values on the interface; $H = 1/6$, $\gamma_1 = \gamma_2 = 1/2$.

for a uniform grid with grid size H. The formula on the right hand side of (2.11) is the well-known *five-point formula* for the Laplace operator. Difference quotients at grid points close to the boundary involve points on the boundary. Since we consider Dirichlet boundary conditions, the values of the solution are given at the boundary points (cf. (2.1b)).

In the LDC method one starts by discretizing the boundary value problem on the global coarse grid Ω^H. This yields the *basic discretization*

$$L^H u_0^H = f^H \qquad \text{on } \Omega^H, \tag{2.12}$$

which describes a system of linear equations for the unknowns $\{u_0^H(\mathbf{x}) \mid \mathbf{x} \in \Omega^H\}$. The Dirichlet boundary values from (2.1b) are incorporated in the grid function f^H. The *finite difference operator* L^H is a linear mapping, $L^H : \mathcal{F}(\Omega^H) \to \mathcal{F}(\Omega^H)$. If we prescribe an ordering of the grid points $\mathbf{x} \in \Omega^H$ then the grid functions u_0^H and f^H can be represented by vectors and the finite difference operator can be represented by a matrix. In this chapter we mainly use the notation of grid functions and operators.

The grid function u_0^H is an approximation of the solution of the boundary value problem (2.1). This grid function is used for discretizing the boundary value problem (2.1) on the local fine grid Ω_l^h. At each grid point $\mathbf{x} \in \Omega_l^h$ the differential operator in (2.1) is approximated using the five-point formula for the Laplace operator, now for the grid size h. Difference quotients at grid points close to the boundary $\partial\Omega$ involve points on the boundary. The values of the solution at the boundary points are given (cf. (2.1b)). Difference quotients at grid points *close to the interface* involve points on the interface. The values at these interface points are determined from the coarse grid values $u_0^H(\mathbf{x})$, $\mathbf{x} \in \Omega^H \cap \Gamma$, and the the boundary values $\varphi(\gamma_1, 0)$, $\varphi(0, \gamma_2)$, by interpolation. In this way *artificial Dirichlet boundary values* are defined on the interface (see Figure 2.2). The discrete problem on the local fine grid Ω_l^h is denoted by

$$L_l^h u_{l,0}^h = f_l^h(u_0^H) \qquad \text{on } \Omega_l^h, \tag{2.13}$$

which describes a system of linear equations for the unknowns $\{u_{l,0}^h(\mathbf{x}) \mid \mathbf{x} \in \Omega_l^h\}$. The Dirichlet boundary values on $\partial\Omega_l \cap \partial\Omega$ (cf. (2.1b)) and the artificial Dirichlet boundary values on the interface Γ are incorporated in the grid function $f_l^h \in \mathcal{F}(\Omega_l^h)$. The dependence of f_l^h on the approximation u_0^H is denoted explicitly in (2.13). The finite difference operator L_l^h is a linear mapping, $L_l^h : \mathcal{F}(\Omega_l^h) \to \mathcal{F}(\Omega_l^h)$.

The approximations u_0^H from (2.12) and $u_{l,0}^h$ from (2.13) are used to define a *composite grid approximation* $u_0^{H,h}$ of the solution of the boundary value problem (2.1),

$$u_0^{H,h}(\mathbf{x}) := \begin{cases} u_{l,0}^h(\mathbf{x}) & \mathbf{x} \in \Omega_l^h \\ u_0^H(\mathbf{x}) & \mathbf{x} \in \Omega^{H,h} \backslash \Omega_l^h \end{cases}.$$

By solving the local fine grid problem (2.13) we aim at improving the approximation of the solution of the boundary value problem in the subregion Ω_l. However, the Dirichlet boundary values on the interface result from the basic discretization (2.12). Hence the accuracy of the approximation $u_{l,0}^h$ is restricted by the accuracy of the approximation u_0^H *on the interface*. In general, local phenomena inside Ω_l cause the approximations $u_0^H(\mathbf{x})$ to be relatively inaccurate both at grid points which lie inside Ω_l and at grid points which lie outside Ω_l. Therefore the accuracy of the approximation $u_0^{H,h}$ is usually not in agreement with the added resolution (see Subsection 2.2.2).

In the local defect correction method the local fine grid approximation $u_{l,0}^h$ is used to *correct the basic discretization* (2.12) in the following way. The global coarse grid approximation u_0^H and the local fine grid approximation $u_{l,0}^h$ are combined to define the global coarse grid function w^H,

$$w^H(\mathbf{x}) := \begin{cases} u_{l,0}^h(\mathbf{x}) & \mathbf{x} \in \Omega_l^H \\ u_0^H(\mathbf{x}) & \mathbf{x} \in \Omega^H \backslash \Omega_l^H \end{cases}.$$

Substituting this grid function in the basic discretization yields a *residual grid function* or *defect*,

$$d^H := L^H w^H - f^H.$$

The values of this defect at grid points inside Ω_l are used to update the right hand side f^H of the basic discretization,

$$\bar{f}^H(\mathbf{x}) := \begin{cases} f^H(\mathbf{x}) + d^H(\mathbf{x}) & \mathbf{x} \in \Omega_l^H \\ f^H(\mathbf{x}) & \mathbf{x} \in \Omega^H \backslash \Omega_l^H \end{cases}.$$

The updated coarse grid problem reads

$$L^H u_1^H = \bar{f}^H(u_{l,0}^h, u_0^H) \qquad \text{on } \Omega^H. \tag{2.14}$$

The dependence of $\bar{f}^H$ on the approximations $u_{l,0}^h$ and u_0^H is denoted explicitly in (2.14).

Remark 2.6 Suppose that the subregion Ω_l coincides with the domain (i.e. $\Omega_l = \Omega$). Then the values of u_1^H are equal to the values of the (global) fine grid approximation at all grid points of the global coarse grid. Hence, given the fine grid approximation, we have defined in (2.14) an optimal correction for the basic discretization (2.12). $\qquad \square$

Equation (2.14) yields an approximation u_1^H of the solution of the boundary value problem (2.1) on the global coarse grid Ω^H. Like the approximation u_0^H, the approximation u_1^H is used to define artificial Dirichlet boundary values on the interface. The related discrete problem on the local fine grid Ω_l^h reads (cf. (2.13))

$$L_l^h u_{l,1}^h = f_l^h(u_1^H) \qquad \text{on } \Omega_l^h. \tag{2.15}$$

The approximations u_1^H from (2.14) and $u_{l,1}^h$ from (2.15) are used to define a composite grid approximation $u_1^{H,h}$ of the solution of the boundary value problem (2.1),

$$u_1^{H,h}(\mathbf{x}) := \begin{cases} u_{l,1}^h(\mathbf{x}) & \mathbf{x} \in \Omega_l^h \\ u_1^H(\mathbf{x}) & \mathbf{x} \in \Omega^{H,h} \backslash \Omega_l^h \end{cases} .$$

In the *local defect correction method* the steps described above are performed iteratively. First, an initialization step is carried out by solving the basic discretization (2.12) and the related discrete problem on the local fine grid (2.13). Then, at each iteration step, an updated discrete problem on the global coarse grid (cf. (2.14)) and a related discrete problem on the local fine grid (cf. (2.15)) are solved.

LDC algorithm

Initialization:

Solve the basic discretization

$$L^H u_0^H = f^H \qquad \text{on } \Omega^H. \tag{2.16a}$$

Solve the local discrete problem

$$L_l^h u_{l,0}^h = f_l^h(u_0^H) \quad \text{on } \Omega_l^h. \tag{2.16b}$$

Define the composite grid approximation

$$u_0^{H,h}(\mathbf{x}) := \begin{cases} u_{l,0}^h(\mathbf{x}) & \mathbf{x} \in \Omega_l^h \\ u_0^H(\mathbf{x}) & \mathbf{x} \in \Omega^{H,h} \backslash \Omega_l^h \end{cases} . \tag{2.16c}$$

Iteration, $i = 1, 2, \ldots$:

Correct the right hand side of the basic discretization

$$w^H(\mathbf{x}) := \begin{cases} u_{l,i-1}^h(\mathbf{x}) & \mathbf{x} \in \Omega_l^H \\ u_{i-1}^H(\mathbf{x}) & \mathbf{x} \in \Omega^H \backslash \Omega_l^H \end{cases} ,$$

$$\bar{f}^H(\mathbf{x}) := \begin{cases} f^H(\mathbf{x}) + (L^H w^H - f^H)(\mathbf{x}) & \mathbf{x} \in \Omega_l^H \\ f^H(\mathbf{x}) & \mathbf{x} \in \Omega^H \backslash \Omega_l^H \end{cases} . \tag{2.16d}$$

Solve the global discrete problem

$$L^H u_i^H = \bar{f}^H(u_{l,i-1}^h, u_{i-1}^H) \quad \text{on } \Omega^H. \tag{2.16e}$$

Solve the local discrete problem

$$L_l^h u_{l,i}^h = f_l^h(u_i^H) \qquad \text{on } \Omega_l^h. \tag{2.16f}$$

Define the composite grid approximation

$$u_i^{H,h}(\mathbf{x}) := \begin{cases} u_{l,i}^h(\mathbf{x}) & \mathbf{x} \in \Omega_l^h \\ u_i^H(\mathbf{x}) & \mathbf{x} \in \Omega^{H,h} \backslash \Omega_l^h \end{cases} . \tag{2.16g}$$

In each step of the LDC iteration two systems of linear equations, one on the global coarse grid Ω^H and one on the local fine grid Ω_l^h, are defined and solved. The *system of linear equations on the composite grid $\Omega^{H,h}$* which is actually solved by the LDC method is an implicit result of the iterative process. In Section 3.2 we derive this system and we consider the convergence behaviour of the LDC method.

We emphasize that in the LDC method boundary value problem discretizations are used on *uniform subgrids* only. Discretizing on uniform grids is relatively easy compared to discretizing on non-uniform grids. The data structure for a uniform grid is much simpler than for a non-uniform grid and on a uniform grid simple and accurate finite difference approximations can be used. Furthermore, the systems of linear equations which have to be solved are defined on uniform grids. For systems of linear equations on uniform grids, fast iterative solution methods exist.

2.2.2 Numerical Results

In this subsection we illustrate some features of the LDC method by numerical results. We consider both one-dimensional and two-dimensional problems. For one-dimensional problems the interface consists of one or two points, and no interpolation on the interface is needed.

First we consider the *one-dimensional Poisson problem*

$$-u_{xx}(x) = f(x), \quad 0 < x < 1,$$
$$u(0) = \varphi_0, \ u(1) = \varphi_1. \tag{2.17}$$

The function f and the values φ_0 and φ_1 are such that the two-point boundary value problem has the solution

$$u^\star(x) = \frac{1}{2}(\tanh(25(x - 0.33)) + 1).$$

Boundary value problem (2.17) contains a high activity region near $x = 0.33$. For solving this boundary value problem we use a global grid with grid size $H = 1/16$ and a local grid, covering the subregion $\Omega_l = (3/16, 8/16)$, with grid size $h = 1/64$. The second derivative in (2.17) is approximated using central differences. In Figure 2.3 several approximations resulting from the LDC method are shown. We observe that the approximation u_0^H which results from solving the basic discretization is not only inaccurate at grid points near the high activity region, but also at grid points outside the subregion Ω_l. Hence the artificial Dirichlet boundary values at the interface grid points are inaccurate and solving the related local fine grid discretization does not yield a significantly more accurate approximation $u_0^{H,h}$ on the composite grid. However, inside Ω_l the grid function $u_0^{H,h}$ approximates the behaviour of the continuous solution quite well. In the local defect correction step this information about the problem inside Ω_l is used to update the basic

Figure 2.3 Approximations of the continuous solution (solid line) of the one-dimensional Poisson problem (2.17) resulting from the LDC method with $H = 1/16$, $\sigma = 4$, $\Omega_l = (3/16, 8/16)$. a) coarse grid approximation u_0^H; b) composite grid approximation $u_0^{H,h}$; c) coarse grid approximation u_1^H; d) composite grid approximation $u_1^{H,h}$.

discretization. After solving the updated basic discretization a much more accurate approximation u_1^H on the global coarse grid results. After solving the related local fine grid problem we obtain an accurate approximation $u_1^{H,h}$ on the composite grid. It can be shown (see [19]) that in this case performing more local defect correction steps does not change the composite grid approximation anymore.

The second example is the *two-dimensional Poisson problem* (2.1) with right hand side functions f and g such that the continuous solution is given by

$$u^\star(x, y) = \frac{1}{2}(\tanh(25(x + y - 0.125)) + 1).$$

This boundary value problem contains a high activity region near the line segment $x + y = \frac{1}{8}$. The solution $u^\star$ is shown in Figure 2.4. We take $\Omega_l = (0, \frac{1}{4}) \times (0, \frac{1}{4})$, $H = 1/16$, $h = 1/128$ and we use *piecewise quadratic interpolation* for defining artificial Dirichlet boundary values on the interface. In Figure 2.5 the continuous solution and two LDC approximations are shown. The markers in the figures correspond to values of the approximations at the grid points lying on the diagonal $y = x$. The solid line represents the continuous solution on this diagonal. In Figure 2.5.d we zoom in on the region $(0.1, 0.25) \times (0.1, 0.25)$. We observe that the approximation
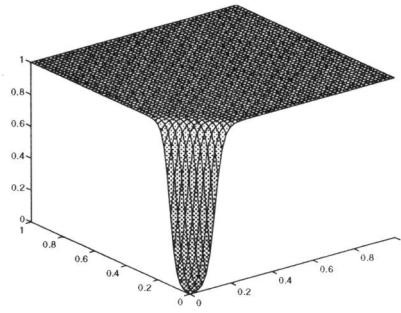
Figure 2.4   The solution of the two-dimensional Poisson problem.
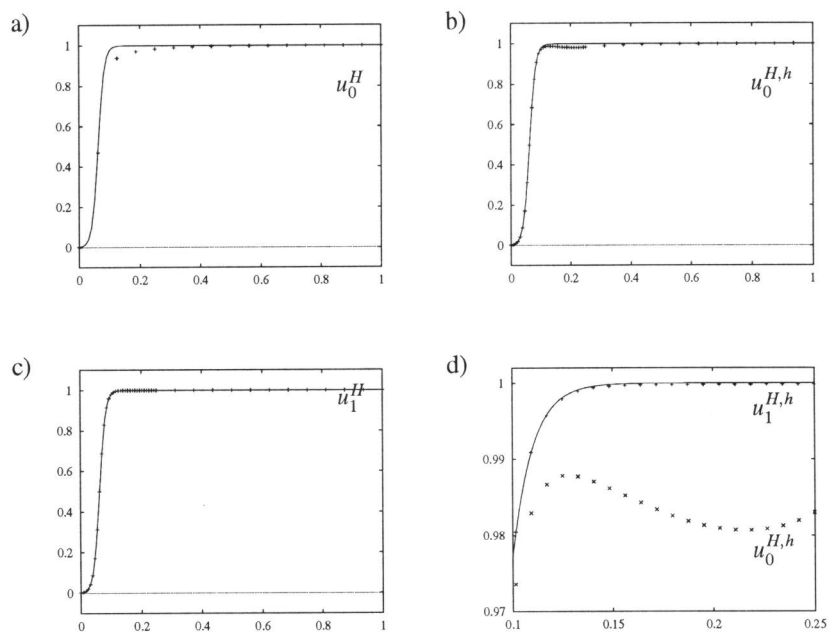
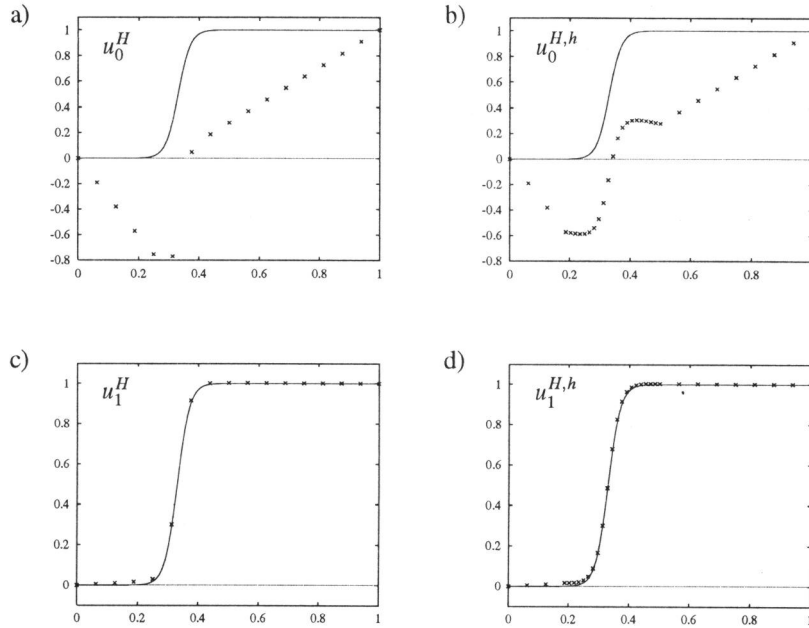**Figure 2.5**   Approximations of the continuous solution (solid line) of the two-dimensional Poisson problem resulting from the LDC method with $H = 1/16$, $\sigma = 8$, $\Omega_l = (0, 1/4) \times (0, 1/4)$. a) coarse grid approximation u_0^H; b) composite grid approximation $u_0^{H,h}$; c) composite grid approximation $u_1^{H,h}$; d) composite grid approximations $u_0^{H,h}$ ($\times$) and $u_1^{H,h}$ (+).

i	$\|u^\star\|_{\Omega^{H,h}} - u_i^{H,h}\|_\infty$
0	$2.29\ 10^{-2}$
1	$1.39\ 10^{-3}$
2	$1.35\ 10^{-3}$
3	$1.35\ 10^{-3}$

Table 2.1 Errors in the iterates of the local defect correction method for the two-dimensional Poisson problem.

$u_0^{H,h}$ is relatively inaccurate near the interface. Performing one LDC step yields a much better approximation $u_1^{H,h}$. This is also illustrated by the values in Table 2.1. These values represent the errors $\|u^\star\|_{\Omega^{H,h}} - u_i^{H,h}\|_\infty$ for several LDC approximations $u_i^{H,h}$. Here $u^\star\|_{\Omega^{H,h}}$ represents the restriction of the continuous solution $u^\star$ to $\Omega^{H,h}$. For the solution of the basic discretization (2.12) we have $\|u^\star\|_{\Omega^H} - u_0^H\|_\infty = 6.08\ 10^{-2}$. If the boundary value problem (2.1) is discretized on the uniform global fine grid Ω^h from (2.10), using central differences at all grid points $\mathbf{x} \in \Omega^h$, then the approximation u^h results. The approximation u^h satisfies $\|u^\star\|_{\Omega^h} - u^h\|_\infty = 1.44\ 10^{-3}$. Thus the accuracy of the approximation $u_1^{H,h}$ which results after one LDC step is comparable with the accuracy of the global fine grid approximation u^h. Clearly the number of grid points involved in the LDC approach ($\approx 1.2\ 10^3$) is much less than the number of grid points involved in the global fine grid approach ($\approx 1.6\ 10^4$).

For the examples above, one LDC step suffices to obtain a composite grid approximation with an accuracy which is comparable with the accuracy of the corresponding global fine grid approximation. We have observed that in many other cases one or two LDC iterations are sufficient.

2.2.3 Generalizations

In Subsection 2.2.1 we have introduced the LDC method for the two-dimensional Poisson problem (2.1) and the model composite grid $\Omega^{H,h}$. However, the LDC method is not restricted to this model setting. The method can be used for approximating the solution of a general linear second order elliptic boundary value problem on a 'general' composite grid, composed of a global coarse grid covering the domain of definition and a local fine grid covering a region of local refinement. The region of local refinement is assumed to be an open and connected subregion of the domain, which contains at least one point of the global coarse grid. Further it is assumed that the intersection of a coarse grid cell[1] with the region of local refinement is either empty, or the whole coarse grid cell, or the half of the coarse grid cell above or below a diagonal of the coarse grid cell. Examples of a global coarse grid and admissible regions of local refinement are shown in Figure 2.6. Also the composite grid may be composed of a global coarse grid and two or more local fine grids, covering disjoint subregions of the domain. If the composite grid is composed of a global coarse grid and $m > 1$ local fine grids, then m local discrete problems have to be solved in each LDC step. Since these local problems are independent of each other, they can be solved *in parallel*. In

---

[1] Here a coarse grid cell is the interior of a square of size H generated by four grid points of the global coarse grid.
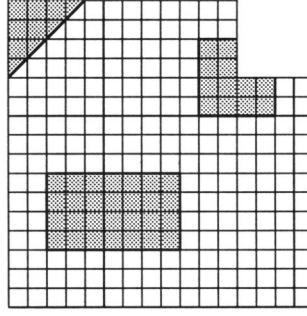
Figure 2.6 Global coarse grid with admissible regions of local refinement.

each LDC step the global discrete problem has to be solved before the local discrete problems, since the right hand sides of the local problems depend on the solution of the global discrete problem (cf. (2.16f)). The application of LDC to nonlinear boundary value problems is considered in Chapter 5. Finally it is noted that the local defect correction iteration can be generalized for three space dimensions in a straightforward way.

The generalizations above concern the boundary value problem and the composite grid. In the remainder of this subsection we consider three important generalizations of the local defect correction process (2.16) itself: local defect correction with overlap, local defect correction with inexact solution of the systems of equations, and local defect correction for coupling global and local discretizations of a boundary value problem.

First we discuss *local defect correction with overlap*. In the LDC method (2.16) the right hand side of the basic discretization is updated at all grid points of the local coarse grid Ω_l^H (cf. (2.16d)). This LDC method is a special case of the local defect correction method introduced by Hackbusch in [30]. There a second local region $\omega_l \subseteq \Omega_l$ is introduced. The right hand side of the basic discretization is updated only at grid points of the local coarse grid $\omega_l^H := \Omega^H \cap \omega_l$. Hence, this method is given by (2.16) with (2.16d) replaced by

$$w^H(\mathbf{x}) := \begin{cases} u_{l,i-1}^h(\mathbf{x}) & \mathbf{x} \in \Omega_l^H \\ u_{i-1}^H(\mathbf{x}) & \mathbf{x} \in \Omega^H \backslash \Omega_l^H \end{cases},$$

$$\bar{f}^H(\mathbf{x}) := \begin{cases} f^H(\mathbf{x}) + (L^H w^H - f^H)(\mathbf{x}) & \mathbf{x} \in \omega_l^H \\ f^H(\mathbf{x}) & \mathbf{x} \in \Omega^H \backslash \omega_l^H \end{cases}.$$

The *overlap parameter d* is defined as the distance between the interfaces $\partial \omega_l \cap \Omega$ and $\Gamma = \partial \Omega_l \cap \Omega$. It is assumed that d is a multiple of the coarse grid size H. If $d = 0$, i.e. $\omega_l^H = \Omega_l^H$ (*no overlap*), then this method is the same as the LDC method (2.16). If $d > 0$, then the method differs from (2.16) and it is called *local defect correction with overlap*.

Remark 2.7 In [30] it is shown by Hackbusch that the local defect correction process with overlap converges with a contraction number of order H^κ, $\kappa > 0$, provided that H is sufficiently small

and that $d > 0$ independent of H holds. The constant $\kappa > 0$ depends on the consistency order of the global and local discretizations and on the order of the interpolation on the interface. We consider the convergence behaviour of the local defect correction method *without* overlap in Section 3.2.   □

Remark 2.8 In [19] we have considered the difference between the continuous solution of a linear elliptic boundary value problem and the approximation resulting after only *one* iteration step of the local defect correction method with overlap. There it is shown that for *convection dominated* problems an overlap parameter $d > 0$ should be used.   □

In each iteration step of the LDC method (2.16) a system of linear equations associated with the global coarse grid and a system of linear equations associated with the local fine grid have to be solved. Since these linear systems result from discretizing a boundary value problem they are *sparse*. These linear systems can be solved using a direct method. In order to exploit the sparsity one has to adapt these methods (see e.g. [12],[27]). However, in many cases the use of *iterative methods* for solving these sparse linear systems *approximately* will be more efficient. Using an iterative method, the sparsity of the system matrix can be better exploited.

Remark 2.9 The iterative methods for solving sparse linear systems are usually divided in three classes: the *basic iterative methods* (e.g., Jacobi, Gauss-Seidel, SOR, SSOR), the *Krylov subspace methods* (e.g., CG, GMRES, BiCG) and the *multigrid methods*. For an overview and a detailed analysis of the basic iterative methods we refer to Varga [65], Young [69], and Hackbusch [33]. For an overview of the Krylov subspace methods we refer to Freund et al. [26] and Sleijpen and Van der Vorst [54]. For an introduction to multigrid methods we refer to Hackbusch [31], Stüben and Trottenberg [61] and Wesseling [67].   □

In this thesis we will not discuss the problem of choosing a suitable iterative method for solving the discrete problems on the uniform subgrids. We note that guidelines for this choice are given in [3].

Remark 2.10 It is well-known that the rate of convergence of basic iterative methods and conjugate gradient methods for solving systems of linear equations decreases if the number of unknowns increases. The number of unknowns in the discrete problems on the uniform subgrids is relatively small, since the *global* grid Ω^H has a *coarse* grid size and the local grid Ω_l^h, which has a (much) *smaller* grid size, covers only a *part of the domain*.   □

If an iterative method is used for approximately solving the discrete problems on the uniform subgrids in the LDC method (2.16), then we obtain an *outer iteration* (the LDC iteration) and two *inner iterations* (one related to the uniform global coarse grid Ω^H and one related to the uniform local fine grid Ω_l^h). The *LDC method with inexact solution of the subproblems* is presented schematically in Figure 2.7. In the i-th LDC step, $i \geq 1$, the approximations $\tilde{u}_{i-1}^H$ and $\tilde{u}_{l,i-1}^h$ can be used as initial approximations for the iterative methods for solving the global and the local discrete problems, respectively. We note that for solving the global discrete problems and the local discrete problems, different iterative solvers may be used. In the following example we consider the dependence of the LDC results on the accuracy with which the discrete subproblems are solved.
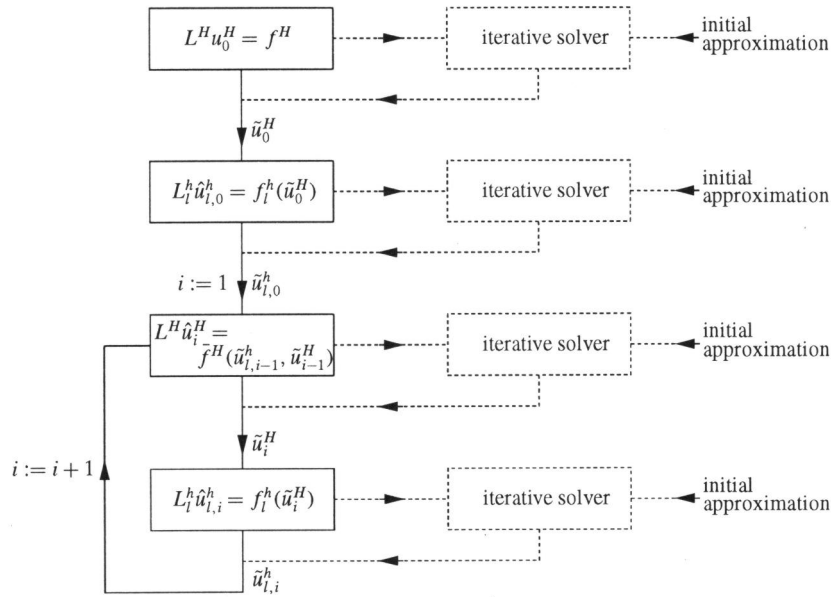
Figure 2.7 Schematic presentation of LDC with inexact solution of the subproblems.

Example 2.11 We consider the two-dimensional Poisson problem and its discretization as in Subsection 2.2.2. For solving the discrete problem on the uniform subgrids, a preconditioned conjugate gradient method with SSOR preconditioner is used (see e.g. [3]). As a general notation for the systems of linear equations appearing in the LDC method we use $\mathbf{A}\mathbf{x} = \mathbf{b}$, where the matrix-vector notation is used. The iterative solver yields approximations $\{\mathbf{x}^k\}_{k \geq 1}$ for the exact solution $\mathbf{x}$. As a stopping criterion we use

$$\frac{\|\mathbf{A}\mathbf{x}^k - \mathbf{b}\|_\infty}{\|\mathbf{b}\|_\infty} \leq tol,$$

where tol is a prescribed tolerance for a relative defect. By varying tol we can vary the accuracy with which the discrete problem is solved. In Table 2.2 the errors $\|u^\star|_{\Omega^{H,h}} - \tilde{u}_i^{H,h}\|_\infty$ are shown for $H = 1/16$, $h = 1/128$ and several values of tol. The composite grid approximations in the LDC method with inexact solution of the subproblems are denoted by $\tilde{u}_i^{H,h}$ and $u^\star$ denotes the continuous solution of the boundary value problem. We see that for $tol = 10^{-2}$ the results are comparable with the results for the LDC method with *exact* solution of the subproblems. We note that this tolerance is required both for solving the coarse grid problem and the fine grid problem in each iteration step. If one of those problems is solved using a larger value of tol, then the results are comparable with those obtained when both problems are solved using this larger value of tol. In Table 2.3 we present for several values of H and $\sigma = H/h$ the (approximate) tolerances for which the errors in the composite grid approximations do not significantly differ for LDC with exact and LDC with inexact solution of the subproblems. We observe that this tolerance depends

i	$tol = 1$	$tol = 10^{-1}$	$tol = 10^{-2}$	$tol = 10^{-3}$	exact
0	$3.32\ 10^{-1}$	$1.88\ 10^{-2}$	$2.32\ 10^{-2}$	$2.29\ 10^{-2}$	$2.29\ 10^{-2}$
1	$1.73\ 10^{-1}$	$1.26\ 10^{-2}$	$1.47\ 10^{-3}$	$1.40\ 10^{-3}$	$1.39\ 10^{-3}$
2	$1.56\ 10^{-2}$	$5.48\ 10^{-3}$	$1.33\ 10^{-3}$	$1.35\ 10^{-3}$	$1.35\ 10^{-3}$
3	$8.42\ 10^{-2}$	$3.44\ 10^{-3}$	$1.37\ 10^{-3}$	$1.35\ 10^{-3}$	$1.35\ 10^{-3}$
4	$8.49\ 10^{-2}$	$3.49\ 10^{-3}$	$1.34\ 10^{-3}$	$1.36\ 10^{-3}$	$1.35\ 10^{-3}$
5	$4.61\ 10^{-2}$	$2.57\ 10^{-3}$	$1.36\ 10^{-3}$	$1.36\ 10^{-3}$	$1.35\ 10^{-3}$
6	$4.91\ 10^{-2}$	$2.27\ 10^{-3}$	$1.41\ 10^{-3}$	$1.35\ 10^{-3}$	$1.35\ 10^{-3}$
7	$2.68\ 10^{-2}$	$1.86\ 10^{-3}$	$1.35\ 10^{-3}$	$1.35\ 10^{-3}$	$1.35\ 10^{-3}$
8	$2.85\ 10^{-2}$	$1.54\ 10^{-3}$	$1.37\ 10^{-3}$	$1.35\ 10^{-3}$	$1.35\ 10^{-3}$

Table 2.2   The errors $\|u^\star|_{\Omega^{H,h}} - \tilde{u}_i^{H,h}\|_\infty$ for the LDC method with inexact and exact solution of the subproblems in Example 2.11.

$\sigma = 8$				$k = 4$		
$k = 4$	$k = 5$	$k = 6$	$k = 7$	$\sigma = 4$	$\sigma = 8$	$\sigma = 16$
10^{-2}	$5\ 10^{-3}$	10^{-3}	10^{-3}	10^{-2}	10^{-2}	10^{-3}

Table 2.3   Critical values for tol in the LDC method with inexact solution of the subproblems in Example 2.11; $H = 2^{-k}$.

on the parameters H and σ only slightly.   □

Remark 2.12 The values in Table 2.2 show that when the subproblems are solved with a low accuracy (e.g. $tol = 1$), significantly more LDC steps are required in order to obtain a composite grid approximation with a certain accuracy than when the subproblems are solved with a high accuracy (e.g. $tol = 10^{-2}$). Clearly there is a trade-off between the work invested in solving the subproblems and the number of outer LDC iterations. The study for the optimal investment of work in each outer iteration step is not considered in this thesis. In Chapter 3 we shall analyse the LDC method with *exact solution of the subproblems*.   □

The local defect correction process (cf. (2.14),(2.15)) can be viewed as a process for *coupling a boundary value problem discretization on a global grid and a boundary value problem discretization on a local grid* (see [19],[30]). In the model setting of Section 2.1 the region of local refinement fits properly to the global coarse grid and the coordinate systems of the global grid and the local grid are the same. Also the discretization approach on the local grid is the same as the discretization approach on the global grid (namely central differences for the Laplace operator). The coupling of global and local discretizations via local defect correction can still be applied if an arbitrary shaped region of local refinement is used, the coordinate systems of the global and local grids differ and/or the discretization approach on the local grid is of a different type than the discretization approach on the global grid (see [30]). In such a general situation the grid points of

the global grid which lie inside the local region do not belong to the local grid and the interface Γ does not coincide with grid lines of the global grid. Then 'more involved' inter grid transfer operators are needed in order to restrict grid functions on the local grid to grid points of the global coarse grid and to define artificial Dirichlet boundary values on the interface. In Figure 2.8 two grids composed of a global grid and a local grid with different coordinate systems are shown.
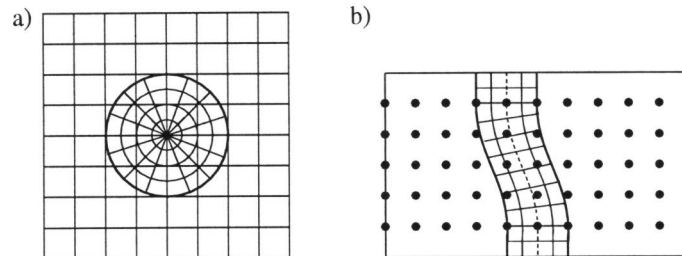
Figure 2.8   Grids composed of global and local grids with different coordinate systems.

Remark 2.13 The grid in Figure 2.8.b corresponds to an example from [30]. This example considers an elliptic boundary value problem $\frac{\partial}{\partial x}(a(x,y)\frac{\partial u}{\partial x}) + \frac{\partial}{\partial y}(a(x,y)\frac{\partial u}{\partial y}) = f$ in a rectangular domain Ω, with a coefficient a which is smooth in the regions on the left and on the right of an interface I, but discontinuous across this interface I. The local co-ordinates are adapted to the interface I.   □

2.3   THE FAST ADAPTIVE COMPOSITE GRID (FAC) METHOD

In the LDC method (2.16) the boundary value problem (2.1) is discretized on the uniform subgrids Ω^H and Ω_l^h only, not on the composite grid $\Omega^{H,h}$. This is different for the *fast adaptive composite grid* (FAC) method. The FAC method is an *iterative solution method* for an *a priori given* discretization of a boundary value problem *on a composite grid* ([46],[47],[48]). In the solution process only uniform subgrids are used.

First we consider finite difference discretizations of the model boundary value problem (2.1) on the model composite grid $\Omega^{H,h}$, including difference schemes for the grid points on the interface. Then the FAC method for solving the composite grid discretizations is described.

The composite grid is a global non-uniform grid. The composite grid is called *locally uniform* at a grid point **x**, if the northern, southern, western and eastern neighbouring grid points all have the same distance to the grid point **x**. Otherwise the composite grid is called *locally non-uniform* at the grid point **x**. Near the boundary obvious modifications are used in these definitions. Since the composite grid is composed of uniform subgrids, it is locally non-uniform only at the grid

Figure 2.9 Locally uniform (•) and locally non-uniform (○) grid points and slave points
(|); $H = 1/6$, $\sigma = 2$, $\gamma_1 = \gamma_2 = 1/2$.

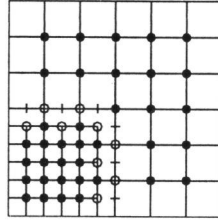points on the interface Γ and at some grid points close to the interface (see Figure 2.9). At the locally uniform grid points the standard five-point formula for the Laplace operator (either with respect to the coarse grid size H or the fine grid size h) can be used.

The locally non-uniform grid points inside Ω_l can be treated as locally uniform grid points by using the *slave points* $\mathbf{x} \in (\hat{\Omega}^h \cap \Gamma) \backslash (\hat{\Omega}^H \cap \Gamma)$ (see Figure 2.9). We use the standard five-point formula for the Laplace operator at the locally non-uniform grid points inside Ω_l. The difference stencils at these points involve the slave points. The values at the slave points are defined from the values at the composite grid points lying on the interface and the boundary data $\varphi(0, \gamma_2)$ and $\varphi(\gamma_1, 0)$ by interpolation. For example, for $(x, y) = (H + h, \gamma_2 - h)$, $H = 2h$, and piecewise linear interpolation, we use the approximation:

$$-\Delta u(x, y) \doteq H^{-2}[4u(x, y) - u(x - h, y) - u(x + h, y) - u(x, y - h)$$
$$- \frac{1}{2}u(x - h, y + h) - \frac{1}{2}u(x + h, y + h)].$$

The approach for defining values at the slave points is similar to the approach for defining the artificial Dirichlet boundary values on the interface in the LDC method in Section 2.2.1.

For the grid points on the interface two types of finite difference approximations are considered. One approach is to use *non-uniform finite differences* at the interface grid points (cf. [50, Section 3.5]). For example, using nearest neighbouring grid points, for $\mathbf{x} = (2H, \gamma_2)$, we have:

$$-\Delta u(2H, \gamma_2) \doteq H^{-2}[2u(2H, \gamma_2) - u(H, \gamma_2) - u(3H, \gamma_2)]$$
$$+ H^{-2}[2\sigma u(2H, \gamma_2) - \frac{2\sigma}{\sigma + 1}u(2H, \gamma_2 + H) - \frac{2\sigma^2}{\sigma + 1}u(2H, \gamma_2 - h)].$$

The coefficients involving the refinement factor $\sigma = H/h$ are chosen so that the order of the approximation is as high as possible (i.e., first order accurate). The approach above, in which the composite grid is considered as a truly non-uniform grid, is referred to as the *non-uniform discretization approach*. In the non-uniform discretization approach we do not use the fact that the composite grid is composed of uniform subgrids. The alternative approach is to treat the grid points on the interface as if they were grid points of the uniform global coarse grid Ω^H (see [21]). Then the standard five-point formula for the Laplace operator can be used. For example, for $\mathbf{x} = (2H, y_\Gamma)$, we obtain:

$$-\Delta u(2H, y_\Gamma) \doteq \frac{1}{H^2}(4u(2H, y_\Gamma) - u(H, y_\Gamma) - u(3H, y_\Gamma) - u(2H, y_\Gamma + H) - u(2H, y_\Gamma - H)).$$

This approach is referred to as the *uniform discretization approach*. Note that the uniform discretization approach is possible since we have $H/h \in I\!N$ and hence $\Omega^H \subset \Omega^{H,h}$. The discrete problems on the composite grid $\Omega^{H,h}$ resulting from the non-uniform discretization approach and the uniform discretization approach for the Poisson model problem (2.1) are analysed in Chapter 4.

Remark 2.14 In Section 3.2 we shall show that the discrete problem resulting from the uniform discretization approach is just the composite grid problem which is actually solved by the LDC method (2.16). $\square$

We denote the *composite grid discretization*, either resulting from the uniform discretization approach or from the non-uniform discretization approach, by

$$L^{H,h} u^{H,h} = f^{H,h} \qquad \text{on } \Omega^{H,h}, \tag{2.18}$$

which describes a system of linear equations for the unknowns $\{u^{H,h}(\mathbf{x}) \mid \mathbf{x} \in \Omega^{H,h}\}$. The Dirichlet boundary values from (2.1b) are incorporated in the grid function $f^{H,h}$. In (2.18) the finite difference operator $L^{H,h}$ is a linear mapping, $L^{H,h} : \mathcal{F}(\Omega^{H,h}) \to \mathcal{F}(\Omega^{H,h})$.

Now we describe a FAC step for solving (2.18). Let $\tilde{u}^{H,h}$ be an approximation of $u^{H,h}$. Inserting $\tilde{u}^{H,h}$ in the system $L^{H,h} u^{H,h} - f^{H,h} = 0$ yields the *composite grid defect*,

$$d^{H,h} := L^{H,h} \tilde{u}^{H,h} - f^{H,h}.$$

The correction $v^{H,h} := \tilde{u}^{H,h} - u^{H,h}$ satisfies

$$L^{H,h} v^{H,h} = d^{H,h}. \tag{2.19}$$

In the FAC method approximations of the correction $v^{H,h}$ are computed on the uniform subgrids. First, equation (2.19) is approximated on the uniform global coarse grid. The finite difference operator $L^{H,h}$ is approximated by the operator L^H from (2.12). The composite grid defect is restricted to the uniform global coarse grid via a linear surjection $\hat{r} : \mathcal{F}(\Omega^{H,h}) \to \mathcal{F}(\Omega^H)$, called a *restriction*. Then the following system of equations results:

$$L^H v^H = \hat{r} d^{H,h} \qquad \text{on } \Omega^H,$$

with v^H an approximation of $v^{H,h}$. Next an approximation of $v^{H,h}$ is computed on the uniform local fine grid. The finite difference operator $L^{H,h}$ inside Ω_l is approximated by the operator L_l^h from (2.13). The artificial Dirichlet boundary values on the interface are defined from the values $v^H(\mathbf{x})$, $\mathbf{x} \in \Omega^H \cap \Gamma$ by interpolation. When interpolating between an interface grid point and a point of the boundary $\partial\Omega$, a *zero value* at the boundary point is used. The system of linear equations which approximates the system (2.19) inside Ω_l is denoted by:

$$L_l^h v_l^h = d_l^h(v^H) \qquad \text{on } \Omega_l^h,$$

where the right hand side depends on the values $v^H(\mathbf{x})$, $\mathbf{x} \in \Omega^H \cap \Gamma$, and on the values $d^{H,h}(\mathbf{x})$, $\mathbf{x} \in \Omega_l^h$. The dependence on the global coarse grid approximation v^H is denoted explicitly. The corrections v_l^h and v^H are used to define a new approximation of $u^{H,h}$,

$$\bar{u}^{H,h}(\mathbf{x}) := \begin{cases} \tilde{u}^{H,h}(\mathbf{x}) - v_l^h(\mathbf{x}) & \mathbf{x} \in \Omega_l^h \\ \tilde{u}^{H,h}(\mathbf{x}) - v^H(\mathbf{x}) & \mathbf{x} \in \Omega^{H,h} \setminus \Omega_l^h \end{cases}.$$

In the *fast adaptive composite grid* method the steps described above are performed iteratively.

FAC algorithm

Initial approximation $u_0^{H,h}$ given

Iteration, $i = 1, 2, \ldots$:

Compute the composite grid defect

$$d^{H,h} := L^{H,h} u_{i-1}^{H,h} - f^{H,h}. \tag{2.20a}$$

Solve the global discrete problem

$$L^H v^H = \hat{r} d^{H,h} \quad \text{on } \Omega^H. \tag{2.20b}$$

Solve the local discrete problem

$$L_l^h v_l^h = d_l^h(v^H) \quad \text{on } \Omega_l^h. \tag{2.20c}$$

Define the composite grid approximation

$$u_i^{H,h}(\mathbf{x}) := \begin{cases} u_{i-1}^{H,h}(\mathbf{x}) - v_l^h(\mathbf{x}) & \mathbf{x} \in \Omega_l^h \\ u_{i-1}^{H,h}(\mathbf{x}) - v^H(\mathbf{x}) & \mathbf{x} \in \Omega^{H,h} \backslash \Omega_l^h \end{cases}. \tag{2.20d}$$

Like the LDC method, the FAC method is not restricted to the two-dimensional Poisson model problem and the model composite grid $\Omega^{H,h}$. The method can be applied to composite grid discretizations of general second-order linear elliptic boundary value problems on a 'general' composite grid as in Subsection 2.2.3. The discrete problems on the uniform grids may be solved approximately using an iterative solution method. In [48] the FAC method (2.20) is used as a starting point for deriving more general multilevel adaptive methods.

Remark 2.15 The fast adaptive composite grid method is an iterative method for solving discrete problems resulting from discretizing a boundary value problem on a composite grid. In [46] and [47] a convergence analysis of the fast adaptive composite grid method is presented in the setting of variationally posed discretizations. The numerical results reported in [36],[37],[53],[63] show that the rate of convergence of the method is very good and that the method is applicable to a wide variety of problems not covered by the theory in [46] and [47]. In [48],[49] the theory for the variational case is extended to the non-variational case of composite grid problems resulting from finite volume element discretization. Here we have presented the fast adaptive composite grid method for solving composite grid problems resulting from *finite difference discretization*. In [22] we show that the convergence rate of the FAC method (2.20) depends strongly on the choice for the restriction $\hat{r} : \mathcal{F}(\Omega^{H,h}) \to \mathcal{F}(\Omega^H)$. Based on theoretical insights, (quasi-)optimal restrictions $\hat{r}$ for the FAC method are derived in [22]. □

2.4 THE MULTI-LEVEL ADAPTIVE TECHNIQUE (MLAT)

Multigrid methods are very efficient methods for solving sparse linear systems resulting from discretizing boundary value problems. These methods iteratively solve a system of linear equations on a given grid, by constant interaction with a hierarchy of coarser grids, taking advantage of the relation between different discretizations of the same continuous problem (see e.g. [8],[31],[67]). The basic principle is that high frequency components of the error can be reduced very efficiently by basic iterative methods (the so-called *smoothing* of the error), while the lower frequencies can be approximated on the coarser grids (the so-called *coarse grid correction*). The multigrid algorithm in *full approximation storage* (FAS) form can be modified for approximating the solution of a boundary value problem on a composite grid [7]. We describe this modified method for the model problem from Section 2.1.

Let $\tilde{u}^{H,h}$ be a composite grid approximation of the solution of boundary value problem (2.1). By interpolating between the values $\tilde{u}^{H,h}(\mathbf{x})$, $\mathbf{x} \in \Omega^{H,h} \cap \Gamma$ and the boundary values $\varphi(\gamma_1, 0)$ and $\varphi(0, \gamma_2)$, artificial Dirichlet boundary values are defined on the interface. These values are used to define the local fine grid problem (cf. (2.13))

$$L_l^h u_l^h = f_l^h(\tilde{u}^{H,h}) \qquad \text{on } \Omega_l^h. \tag{2.21}$$

The right hand side in (2.21) depends on the composite grid approximation $\tilde{u}^{H,h}$. A *smoothing process* is performed with respect to this system of linear equations. Several steps of some basic iterative method (see Remark 2.9) are carried out with a starting approximation derived from $\tilde{u}^{H,h}$. This yields an approximation $\tilde{u}_l^h$ of u_l^h. Inserting $\tilde{u}_l^h$ in the system $L_l^h u_l^h = f_l^h(\tilde{u}^{H,h})$ yields the *local fine grid defect*,

$$d_l^h := L_l^h \tilde{u}_l^h - f_l^h(\tilde{u}^{H,h}).$$

In the coarse grid correction step, the system of linear equations

$$L^H \bar{u}^H = \bar{f}^H \qquad \text{on } \Omega^H, \tag{2.22}$$

with L^H from (2.12) is solved. Outside the local region, the grid function $\bar{f}^H$ is equal to the right hand side of the basic discretization (2.12),

$$\bar{f}^H(\mathbf{x}) = f^H(\mathbf{x}) \quad \mathbf{x} \in \Omega^H \backslash \Omega_l^H.$$

Inside the local region the values of the grid function $\bar{f}^H$ are given by

$$\bar{f}^H(\mathbf{x}) := (L^H w^H)(\mathbf{x}) - (\tilde{r}_l d_l^h)(\mathbf{x}), \quad \mathbf{x} \in \Omega_l^H,$$

with

$$w^H(\mathbf{x}) := \begin{cases} (\hat{r}_l \tilde{u}_l^h)(\mathbf{x}) & \mathbf{x} \in \Omega_l^H \\ \tilde{u}^{H,h}(\mathbf{x}) & \mathbf{x} \in \Omega^H \backslash \Omega_l^H \end{cases}.$$

The linear surjection $\hat{r}_l : \mathcal{F}(\Omega_l^h) \to \mathcal{F}(\Omega_l^H)$ is used to restrict local fine grid *approximations* of the solution of the boundary value problem (2.1) to the local coarse grid Ω_l^H. The linear surjection $\tilde{r}_l :$

$\mathcal{F}(\Omega_l^h) \rightarrow \mathcal{F}(\Omega_l^H)$ is used to restrict local fine grid *defects* to the local coarse grid Ω_l^H. The global coarse grid approximation $\bar{u}^H$ from (2.22) is used to correct the local fine grid approximation $\tilde{u}_l^h$,

$$\bar{u}_l^h := \tilde{u}_l^h + \tilde{p}v^H,$$

with

$$v^H(\mathbf{x}) := \begin{cases} \bar{u}^H(\mathbf{x}) - (\hat{r}_l \tilde{u}_l^h)(\mathbf{x}) & \mathbf{x} \in \Omega_l^H \\ \bar{u}^H(\mathbf{x}) - \tilde{u}^{H,h}(\mathbf{x}) & \mathbf{x} \in \Omega^H \cap \Gamma \\ 0 & \mathbf{x} \in \Omega^H \backslash (\Omega_l^H \cup (\Omega^H \cap \Gamma)) \end{cases}.$$

The operator $\tilde{p} : \mathcal{F}(\Omega^H) \rightarrow \mathcal{F}(\Omega_l^h)$ is used to transfer global coarse grid corrections to the local fine grid. The new composite grid approximation is defined by

$$\bar{u}^{H,h}(\mathbf{x}) := \begin{cases} \bar{u}_l^h(\mathbf{x}) & \mathbf{x} \in \Omega_l^h \\ \bar{u}^H(\mathbf{x}) & \mathbf{x} \in \Omega^{H,h} \backslash \Omega_l^h \end{cases}.$$

In the *multi-level adaptive technique* (MLAT) the steps described above are performed iteratively.

MLAT algorithm

Initial approximation $u_0^{H,h}$ given.

Iteration, $i = 1, 2, \ldots$:

Find an approximate solution $\tilde{u}_{l,i}^h$ of the local problem

$$L_l^h \hat{u}_{l,i}^h = f_l^h(u_{i-1}^{H,h}) \quad \text{on } \Omega_l^h. \tag{2.23a}$$

Compute the local fine grid defect

$$d_l^h := L_l^h \tilde{u}_{l,i}^h - f_l^h(u_{i-1}^{H,h}). \tag{2.23b}$$

Compute the global coarse grid right hand side

$$w^H(\mathbf{x}) := \begin{cases} (\hat{r}_l \tilde{u}_{l,i}^h)(\mathbf{x}) & \mathbf{x} \in \Omega_l^H \\ u_{i-1}^{H,h}(\mathbf{x}) & \mathbf{x} \in \Omega^H \backslash \Omega_l^H \end{cases},$$

$$\bar{f}^H(\mathbf{x}) := \begin{cases} (L^H w^H)(\mathbf{x}) - (\tilde{r}_l d_l^h)(\mathbf{x}) & \mathbf{x} \in \Omega_l^H \\ f^H(\mathbf{x}) & \mathbf{x} \in \Omega^H \backslash \Omega_l^H \end{cases}. \tag{2.23c}$$

Solve the global problem

$$L^H u_i^H = \bar{f}^H \quad \text{on } \Omega^H. \tag{2.23d}$$

Correct the local approximation

$$v^H(\mathbf{x}) := \begin{cases} u_i^H(\mathbf{x}) - (\hat{r}_l \tilde{u}_{l,i}^h)(\mathbf{x}) & \mathbf{x} \in \Omega_l^H \\ u_i^H(\mathbf{x}) - u_{i-1}^{H,h}(\mathbf{x}) & \mathbf{x} \in \Omega^H \cap \Gamma \\ 0 & \mathbf{x} \in \Omega^H \backslash (\Omega_l^H \cup (\Omega^H \cap \Gamma)) \end{cases},$$

$$u_{l,i}^h := \tilde{u}_{l,i}^h + \tilde{p}v^H. \tag{2.23e}$$

Define the composite grid approximation

$$u_i^{H,h}(\mathbf{x}) := \left\{ \begin{array}{ll} u_{l,i}^h(\mathbf{x}) & \mathbf{x} \in \Omega_l^h \\ u_i^H(\mathbf{x}) & \mathbf{x} \in \Omega^{H,h} \backslash \Omega_l^h \end{array} \right. . \qquad (2.23f)$$

Like for the LDC method (2.16), we do not use a discretization of the boundary value problem (2.1) on the composite grid $\Omega^{H,h}$ in the MLAT method. Also, the MLAT method can be applied to general second-order linear elliptic boundary value problems and 'general' composite grids as in Subsection 2.2.3. The MLAT method (2.23) is a special case of the multi-level adaptive technique introduced by Brandt [7],[9] for solving boundary value problems on (adaptively refined) composite grids.

2.5   COMPARISON OF THE METHODS

It is clear that local defect correction, the fast adaptive composite grid method and the multi-level adaptive technique are closely related. This is also noted in the literature (see e.g. [31, Section 15.2], [46], [47]), but nowhere the differences and similarities are clearly explained. In [39] multi-level versions of local defect correction and the fast adaptive composite grid method are compared for two typical linear elliptic problems by means of numerical experiments. By presenting the methods in one framework, resulting in LDC (2.16), FAC (2.20) and MLAT (2.23), we can give a theoretical comparison of the methods. Below we use results which are derived in Chapter 3.

In the LDC method (2.16) approximations of the solution of the boundary value problem (2.1) are computed by solving discretizations of the boundary value problem on the uniform subgrids Ω^H and Ω_l^h. In Section 3.2 the discretization of the boundary value problem (2.1) on the composite grid which is actually solved by the LDC method is derived. Characteristic for this composite grid discretization related to the LDC method is that grid points on the interface Γ are treated as if they were grid points of the global coarse grid Ω^H. We note that this composite grid discretization is an *implicit result* of the LDC method. The FAC method (2.20), on the other hand, is a method for approximately solving an *a priori given* discretization of the boundary value problem (2.1) on the composite grid $\Omega^{H,h}$. If the FAC method, with the initial approximation from (2.16a-c) and with $\hat{r} : \mathcal{F}(\Omega^{H,h}) \rightarrow \mathcal{F}(\Omega^H)$ satisfying

$$(\hat{r}w)(\mathbf{x}) = w(\mathbf{x}), \qquad \mathbf{x} \in \Omega^H \backslash \Omega_l^H,$$

is applied to the composite grid discretization which is related to the LDC method, then the FAC method and the LDC method yield the same iterates. This relation between the FAC method and the LDC method is shown in Section 3.4. The close connection between the FAC method and the LDC method is valid for general linear elliptic boundary value problems and 'general' composite grids as described in Subsection 2.2.3.

As stated above, the LDC iteration is related to a composite grid discretization. Since the FAC method can be applied to any system of linear equations resulting from discretizing the boundary value problem on the composite grid, the FAC method is a more general method than the

LDC method for solving boundary value problems on composite grids. On the other hand, the LDC method (2.16) is a special case of a process for coupling a global discretization and local discretizations via local defect correction. In this process more general combinations of a global grid and several local grids are allowed than those combinations which constitute a composite grid. For example, the regions of local refinement may be arbitrarily shaped and the coordinate systems for the local grids may differ from the coordinate system for the global grid. The form of the non-uniform grid composed of the global grid and the local grids is not essential for the local defect correction method, since the boundary value problem is not discretized on this non-uniform grid. We conclude that from this point of view the local defect correction approach is more general than the fast adaptive composite grid approach.

Like for the LDC method (2.16), the composite grid discretization which is actually solved by the MLAT method (2.23) is an implicit result of the iterative process. In Section 3.3 it is shown that the composite grid discretization related to the MLAT method depends on $\hat{r}_l$ in (2.23), i.e. on the way in which local fine grid approximations are restricted to the local coarse grid Ω_l^H in the MLAT algorithm. If $\hat{r}_l : \mathcal{F}(\Omega_l^h) \to \mathcal{F}(\Omega_l^H)$ is defined by

$$\hat{r}_l w := w_{|\Omega_l^H}, \quad w \in \mathcal{F}(\Omega_l^h),$$

then the composite grid discretization related to the MLAT method is the same as the composite grid discretization related to the LDC method. The difference between MLAT (2.23) and LDC (2.16) is that in the LDC method the discrete problems on Ω_l^h are solved exactly, whereas in the MLAT method the discrete problems on Ω_l^h are solved approximately by one step of a two-grid method (see Remark 3.16).

In the LDC method and in the FAC method *large values of the refinement factor $\sigma = H/h$ are* allowed. The MLAT method (2.23), however, is *based on multigrid principles*. The relaxation sweeps on the local fine grid are intended to smooth the error, while solving the global coarse grid problem is meant to reduce the smooth components of the error. Therefore, the refinement factor $\sigma = H/h$ in the MLAT method (2.23) should *not be large* (e.g., $\sigma = 2$).

3

ANALYSIS OF ITERATIVE
METHODS ON COMPOSITE
GRIDS

In this chapter we analyse the LDC method (2.16), the FAC method (2.20) and the MLAT method (2.23) introduced in Chapter 2. In Section 3.1 we extend the notation for the model composite grid $\Omega^{H,h}$ from Section 2.1 and we specify the right hand sides of the global and local discrete problems which occur in the iterative methods. Both for the LDC method and the MLAT method the composite grid discretization which is actually solved by the method is not a priori given, but it is an implicit result of the iterative process. In Section 3.2 we derive the composite grid discretization which is actually solved by the LDC method. Also we give an expression for the iteration matrix of the LDC method. The fast convergence of the LDC method is illustrated by numerical results. In Section 3.3 the composite grid discretization which is actually solved by the MLAT method is derived and the differences between the composite grid discretizations related to LDC and MLAT are discussed. In Section 3.4 we derive an expression for the iteration matrix of the FAC method applied to the composite grid discretization related to the LDC method. It is shown that, under certain reasonable assumptions, the iterates in the fast adaptive composite grid method are the same as the iterates in the local defect correction method. Parts of this chapter are also presented in [20].

3.1 PRELIMINARIES

In Chapter 2 the local defect correction method (LDC (2.16)), the fast adaptive composite grid method (FAC (2.20)) and the multi-level adaptive technique (MLAT (2.23)) have been introduced with a minimum of notation. For the mathematical analysis in this chapter a more detailed description of the methods is needed.

First we introduce notation for the model composite grid $\Omega^{H,h}$ from Section 2.1. The *coarse interface grid* Γ^H and the *fine interface grid* Γ^h are defined by

$$\Gamma^H := \Omega^H \cap \Gamma, \tag{3.1}$$

$$\Gamma^h := \Omega^h \cap \Gamma, \tag{3.2}$$
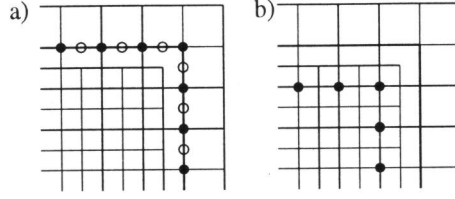
Figure 3.1 a) Grid points of Γ^H (●) and slave points (○). b) Grid points of $\tilde{\Gamma}^H$ (●).
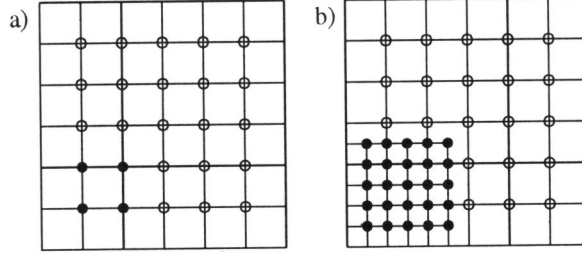
Figure 3.2 Decompositions of Ω^H and $\Omega^{H,h}$. a) Grid points of Ω_l^H (●) and Ω_c^H (○). b) Grid points of Ω_l^h (●) and Ω_c^H (○).

with Ω^H from (2.2), Ω^h from (2.10) and Γ from (2.6). Note that $\Gamma^H \subset \Gamma^h$ and $\Gamma^H \subset \Omega^{H,h}$. The points $\mathbf{x} \in \Gamma^h \backslash \Gamma^H$ are called the *slave points* (see Figure 3.1.a).

The restriction of a grid function $w : W \to I\!R$ to the coarse interface grid $\Gamma^H \subset W$ is denoted by $w_{|_\Gamma}$. This notation will be used throughout this thesis instead of the notation $w_{|_{\Gamma^H}}$ in Definition 2.3.

The set of grid points of Ω_l^H which lie at a distance H of Γ is denoted by $\tilde{\Gamma}^H$ (see Figure 3.1.b),

$$\tilde{\Gamma}^H := \{\mathbf{x} \in \Omega_l^H \mid \min_{\mathbf{y} \in \Gamma} \|\mathbf{x} - \mathbf{y}\|_2 = H\}, \tag{3.3}$$

where $\|.\|_2$ denotes the Euclidean norm.

The part of the global coarse grid Ω^H which is complementary to the local coarse grid Ω_l^H is denoted by Ω_c^H,

$$\Omega_c^H := \Omega^H \backslash \Omega_l^H. \tag{3.4}$$

The global coarse grid Ω^H and the composite grid $\Omega^{H,h}$ can be decomposed as,

$$\Omega^H = \Omega_l^H \cup \Omega_c^H,$$
$$\Omega^{H,h} = \Omega_l^h \cup \Omega_c^H,$$

see Figure 3.2.

Next we rewrite the right hand sides of the local fine grid problems in LDC, FAC and MLAT. The local fine grid problems (2.16b),(2.16f) in LDC are rewritten as

$$L_l^h u_{l,i}^h = f_l^h - L_\Gamma^h p u_i^H |_\Gamma, \quad i \geq 0. \tag{3.5}$$

In (3.5) $u_i^H|_\Gamma \in \mathcal{F}(\Gamma^H)$ represents the grid function $u_i^H \in \mathcal{F}(\Omega^H)$ restricted to the coarse interface grid Γ^H, $p : \mathcal{F}(\Gamma^H) \to \mathcal{F}(\Gamma^h)$ is a linear injection, called a *prolongation*, and $L_\Gamma^h : \mathcal{F}(\Gamma^h) \to \mathcal{F}(\Omega_l^h)$ is a linear mapping. We recall that the local fine grid problems in the LDC method result from discretizing the boundary value problem (2.1) on the local fine grid Ω_l^h, using artificial Dirichlet boundary values on the interface. The artificial Dirichlet boundary values result from the values $\{u_i^H(\mathbf{x}) \mid \mathbf{x} \in \Gamma^H\}$, $\varphi(\gamma_1, 0)$ and $\varphi(0, \gamma_2)$, by interpolation. The term $L_\Gamma^h p u_i^H|_\Gamma$ in (3.5) represents the incorporation of the artificial Dirichlet boundary values in the discrete problem. We define the grid function $f_l^h \in \mathcal{F}(\Omega_l^h)$ and the prolongation p in such a way that the term $L_\Gamma^h p u_i^H|_\Gamma$ does not depend on the boundary values $\varphi(\gamma_1, 0)$ and $\varphi(0, \gamma_2)$.

Example 3.1 We consider the Poisson problem (2.1), the five-point formula for the Laplace operator, $\sigma = 2$ and piecewise linear interpolation on the interface. When interpolating between a grid point $\mathbf{x} \in \Gamma^H$ and a point on the boundary $\partial\Omega$, *zero values* are used at the boundary point. For example, at $\mathbf{x} = (h, \gamma_2 - h)$ we obtain:

$$f_l^h(\mathbf{x}) := f(h, \gamma_2 - h) + \frac{1}{2} h^{-2} \varphi(0, \gamma_2),$$

$$(-L_\Gamma^h p u_i^H|_\Gamma)(\mathbf{x}) := \frac{1}{2} h^{-2} u_i^H((H, \gamma_2)).$$

The boundary value $\varphi(0, \gamma_2)$ is incorporated in the term f_l^h.   □

The local fine grid problems (2.23a) in MLAT and (2.20c) in FAC are rewritten as

$$L_l^h \hat{u}_{l,i}^h = f_l^h - L_\Gamma^h p u_{i-1}^{H,h}|_\Gamma, \quad i \geq 1, \tag{3.6}$$

$$L_l^h v_l^h = R_l d^{H,h} - L_\Gamma^h p v^H|_\Gamma, \tag{3.7}$$

respectively. The notation in (3.6) and (3.7) is the same as in (3.5). In (3.7) the *trivial injection* $R_l : \mathcal{F}(\Omega^{H,h}) \to \mathcal{F}(\Omega_l^h)$ is defined by

$$R_l w := w|_{\Omega_l^h}, \quad w \in \mathcal{F}(\Omega^{H,h}), \tag{3.8}$$

and $d^{H,h} \in \mathcal{F}(\Omega^{H,h})$ is the composite grid defect from (2.20a).

Now we rewrite the right hand sides of the global coarse grid problems in LDC and in MLAT. We define the finite difference operators $L_l^H : \mathcal{F}(\Omega_l^H) \to \mathcal{F}(\Omega_l^H)$ and $L_\Gamma^H : \mathcal{F}(\Gamma^H) \to \mathcal{F}(\Omega_l^H)$ via the relation

$$(L_l^H w^H|_{\Omega_l^H})(\mathbf{x}) + (L_\Gamma^H w^H|_\Gamma)(\mathbf{x}) = (L^H w^H)(\mathbf{x}), \quad \mathbf{x} \in \Omega_l^H, \ w^H \in \mathcal{F}(\Omega^H). \tag{3.9}$$

The *trivial injection* $r_l : \mathcal{F}(\Omega_l^h) \to \mathcal{F}(\Omega_l^H)$ is defined by

$$r_l w := w|_{\Omega_l^H}, \quad w \in \mathcal{F}(\Omega_l^h). \tag{3.10}$$

The global coarse grid problems (2.16e) in the LDC method are rewritten as

$$L^H u_i^H = \begin{bmatrix} L_l^H r_l u_{l,i-1}^h + L_\Gamma^H u_{i-1}^H|_\Gamma \\ f^H|_{\Omega_c^H} \end{bmatrix}, \quad i \geq 1. \tag{3.11}$$

The global coarse grid problems (2.23d) in MLAT are rewritten as

$$L^H u_i^H = \begin{bmatrix} L_l^H \hat{r}_l \tilde{u}_{l,i}^h + L_\Gamma^H u_{i-1}^{H,h}|_\Gamma - \tilde{r}_l d_l^h \\ f^H|_{\Omega_c^H} \end{bmatrix}, \quad i \geq 1. \tag{3.12}$$

On the right hand side of (3.11) and (3.12) a block partitioning corresponding to the direct sum $\mathcal{F}(\Omega^H) = \mathcal{F}(\Omega_l^H) \oplus \mathcal{F}(\Omega_c^H)$ is used.

The operators L_l^H and L_Γ^H represent L^H *inside* the subregion Ω_l. We introduce the operators $L_c^H : \mathcal{F}(\Omega_c^H) \to \mathcal{F}(\Omega_c^H)$ and $L_{\tilde{\Gamma}}^H : \mathcal{F}(\tilde{\Gamma}^H) \to \mathcal{F}(\Omega_c^H)$ which represent L^H *outside* Ω_l:

$$(L_c^H w^H|_{\Omega_c^H})(\mathbf{x}) + (L_{\tilde{\Gamma}}^H w^H|_{\tilde{\Gamma}^H})(\mathbf{x}) = (L^H w^H)(\mathbf{x}), \quad \mathbf{x} \in \Omega_c^H, \ w^H \in \mathcal{F}(\Omega^H). \tag{3.13}$$

The analysis in this chapter is not restricted to the two-dimensional Poisson model problem from Section 2.1. In the remainder of this chapter we assume that the finite difference operators L^H, L_l^H, L_Γ^H, L_c^H, $L_{\tilde{\Gamma}}^H$ and L_l^h, L_Γ^h result from discretizing a linear second-order elliptic boundary value problem

$$Lu = f \qquad \text{in } \Omega = (0, 1) \times (0, 1), \tag{3.14a}$$

$$u = \varphi \qquad \text{on } \partial\Omega. \tag{3.14b}$$

on the uniform global coarse grid Ω^H and the uniform local fine grid Ω_l^h. We assume that the discretization process on the uniform grids uses neighbouring grid points only, so the largest possible difference formula involves nine grid points. The operators $L^H : \mathcal{F}(\Omega^H) \to \mathcal{F}(\Omega^H)$, $L_l^H : \mathcal{F}(\Omega_l^H) \to \mathcal{F}(\Omega_l^H)$ and $L_l^h : \mathcal{F}(\Omega_l^h) \to \mathcal{F}(\Omega_l^h)$ are assumed to be *nonsingular*. So any system of linear equations corresponding to L^H, L_l^H or L_l^h has a unique solution.

The analysis and results in this chapter can be generalized in a straightforward way to 'general' composite grids with more than one region of local refinement as described in Subsection 2.2.3. The model composite grid $\Omega^{H,h}$ is considered only for notational convenience.

3.2   LDC AS ITERATIVE SOLUTION METHOD

In each step of the LDC method (2.16) approximations of the continuous solution of the boundary value problem (3.14) are computed both on the global coarse grid Ω^H and on the local fine grid Ω_l^h. These approximations u_i^H and $u_{l,i}^h$ are used to define an approximation $u_i^{H,h}$ on the composite grid $\Omega^{H,h}$,

$$u_i^{H,h} := \begin{bmatrix} u_{l,i}^h \\ u_i^H|_{\Omega_c^H} \end{bmatrix},$$

where a block partitioning corresponding to $\mathcal{F}(\Omega^{H,h}) = \mathcal{F}(\Omega_l^h) \oplus \mathcal{F}(\Omega_c^H)$ is used. So two iterates, $(u_i^H, u_{l,i}^h)$ and $u_i^{H,h}$, occur in each LDC step. Below we discuss the fixed points of the LDC method. In the following lemma a block partitioning corresponding to $\mathcal{F}(\Omega^H) = \mathcal{F}(\Omega_l^H) \oplus \mathcal{F}(\Omega_c^H)$ is used.

Lemma 3.2 (u^H, u_l^h) *is a fixed point of the LDC method (2.16) if and only if* (u^H, u_l^h) *satisfies the coupled system*

$$L^H u^H - \begin{bmatrix} L_l^H r_l u_l^h + L_\Gamma^H u^H|_\Gamma \\ \emptyset \end{bmatrix} = \begin{bmatrix} \emptyset \\ f^H|_{\Omega_c^H} \end{bmatrix} \qquad on \ \Omega^H, \qquad (3.15a)$$

$$L_l^h u_l^h + L_\Gamma^h p u^H|_\Gamma = f_l^h \qquad on \ \Omega_l^h. \qquad (3.15b)$$

Proof. It follows from (3.5),(3.11) that the LDC iterates $(u_i^H, u_{l,i}^h)$, $i = 1, 2, \ldots$, satisfy

$$L^H u_i^H = \begin{bmatrix} L_l^H r_l u_{l,i-1}^h + L_\Gamma^H u_{i-1}^H|_\Gamma \\ f^H|_{\Omega_c^H} \end{bmatrix},$$

$$L_l^h u_{l,i}^h = f_l^h - L_\Gamma^h p u_i^H|_\Gamma.$$

Now the lemma follows immediately since L^H and L_l^h are nonsingular. ∎

Lemma 3.3 *If* (u^H, u_l^h) *satisfies the coupled system (3.15), then*

$$u^H|_{\Omega_l^H} = u_l^h|_{\Omega_l^H} \qquad (3.16)$$

holds.

Proof. From (3.15a) and (3.9) we obtain

$$(L^H u^H)(\mathbf{x}) - (L_l^H r_l u_l^h)(\mathbf{x}) - (L_\Gamma^H u^H|_\Gamma)(\mathbf{x}) = 0, \qquad \mathbf{x} \in \Omega_l^H,$$

$$(L^H u^H)(\mathbf{x}) - (L_l^H u^H|_{\Omega_l^H})(\mathbf{x}) - (L_\Gamma^H u^H|_\Gamma)(\mathbf{x}) = 0, \qquad \mathbf{x} \in \Omega_l^H.$$

Thus

$$L_l^H(u^H|_{\Omega_l^H} - r_l u_l^h) = 0.$$

Since L_l^H is nonsingular and r_l is the trivial injection (3.10), this equation is equivalent with (3.16). ∎

Below we show that the coupled system (3.15) is related to a system of linear equations resulting from finite difference discretization of the boundary value problem (3.14) on the composite grid $\Omega^{H,h}$. We use the *trivial injections* $r_{\bar{\Gamma}} : \mathcal{F}(\Omega_l^h) \to \mathcal{F}(\bar{\Gamma}^H)$ and $r_\Gamma : \mathcal{F}(\Omega_c^H) \to \mathcal{F}(\Gamma^H)$, defined by

$$r_{\bar{\Gamma}} w := w|_{\bar{\Gamma}^H}, \qquad w \in \mathcal{F}(\Omega_l^h), \qquad (3.17a)$$

$$r_\Gamma w := w|_{\Gamma^H}, \qquad w \in \mathcal{F}(\Omega_c^H). \qquad (3.17b)$$

Lemma 3.4 *If (u^H, u_l^h) satisfies the coupled system (3.15), then the composite grid function*

$$u^{H,h} := \begin{bmatrix} u_l^h \\ u^H|_{\Omega_c^H} \end{bmatrix}$$

satisfies

$$L^{H,h} u^{H,h} = f^{H,h} \tag{3.18a}$$

with

$$L^{H,h} := \begin{bmatrix} L_l^h & L_\Gamma^h \, pr_\Gamma \\ L_{\bar\Gamma}^H r_{\bar\Gamma} & L_c^H \end{bmatrix}, \tag{3.18b}$$

$$f^{H,h} := \begin{bmatrix} f_l^h \\ f^H|_{\Omega_c^H} \end{bmatrix}. \tag{3.18c}$$

Proof. Since (u^H, u_l^h) satisfies (3.15), it follows from (3.15b) and (3.17b) that

$$L_l^h u_l^h + L_\Gamma^h \, pr_\Gamma u^H|_{\Omega_c^H} = f_l^h,$$

and from (3.13), (3.15a) and (3.17a) that

$$L_c^H u^H|_{\Omega_c^H} + L_{\bar\Gamma}^H r_{\bar\Gamma} u^H|_{\Omega_c^H} = f^H|_{\Omega_c^H}.$$

Now (3.18) follows by the definition of $u^{H,h}$. ∎

Lemma 3.5 *If $u^{H,h}$ satisfies the composite grid problem (3.18), then (u^H, u_l^h) defined by*

$$u^H := u^{H,h}|_{\Omega^H}, \tag{3.19a}$$

$$u_l^h := u^{H,h}|_{\Omega_l^h}, \tag{3.19b}$$

satisfies the coupled system (3.15).

Proof. Since $u^{H,h}$ satisfies $L^{H,h} u^{H,h} = f^{H,h}$ we obtain from (3.18)

$$L_l^h u^{H,h}|_{\Omega_l^h} + L_\Gamma^h \, pr_\Gamma u^{H,h}|_{\Omega_c^H} = f_l^h,$$

$$L_c^H u^{H,h}|_{\Omega_c^H} + L_{\bar\Gamma}^H r_{\bar\Gamma} u^{H,h}|_{\Omega_l^h} = f^H|_{\Omega_c^H}.$$

Using the definitions (3.17) and (3.19) we obtain

$$L_l^h u_l^h + L_\Gamma^h \, p u^H|_\Gamma = f_l^h,$$

$$L_c^H u^H|_{\Omega_c^H} + L_{\bar\Gamma}^H u^H|_{\tilde\Gamma^H} = f^H|_{\Omega_c^H},$$

$$L_l^H u^H|_{\Omega_l^H} + L_\Gamma^H u^H|_\Gamma = L_l^H u_l^h|_{\Omega_l^H} + L_\Gamma^H u^H|_\Gamma.$$

Now it follows from (3.9) and (3.13) that (u^H, u_l^h) satisfies (3.15). ∎

Due to Lemma 3.2 and Lemma 3.3 any fixed point (u^H, u_l^h) of the LDC method has a unique representation on the composite grid,

$$u^{H,h} := \begin{bmatrix} u_l^h \\ u^H|_{\Omega_c^H} \end{bmatrix}, \tag{3.20}$$

which is called *composite grid fixed point* of the LDC method.

Theorem 3.6 *The composite grid fixed points of the LDC method (2.16) are the solutions of the composite grid problem (3.18).*

Proof. Follows from a combination of the results of Lemma 3.2, Lemma 3.4 and Lemma 3.5. ∎

We note that

$$(L^{H,h}w)|_{\Omega_c^H} = (L^H w|_{\Omega^H})|_{\Omega_c^H}, \quad w \in \mathcal{F}(\Omega^{H,h}), \tag{3.21}$$

(cf. (3.9),(3.18b)), and that $\Gamma^H \subset \Omega_c^H$. So, in the discretization process related to (3.18), the *interface grid points* $\mathbf{x} \in \Gamma^H$ are treated as if they were *grid points of the uniform global coarse grid* Ω^H. For example, for the two-dimensional Poisson problem (2.1) the five-point formula for the Laplace operator is used at the interface grid points $\mathbf{x} \in \Gamma^H$.

Corollary 3.7 *If the finite difference operator $L^{H,h}$ in (3.18) is nonsingular, then the LDC iteration (2.16) has a unique fixed point.*

In the remainder of this chapter we assume that $L^{H,h}$ in (3.18b) is nonsingular.

Remark 3.8 In certain cases the nonsingularity of $L^{H,h}$ can be concluded from properties of L^H and L_l^h. For example, suppose that for a certain ordering of the grid points in Ω^H and Ω_l^h the matrices $\mathbf{L}^H$ and $\mathbf{L}_l^h$, corresponding to L^H and L_l^h have positive diagonal elements and non-positive off-diagonal elements and that they are irreducibly diagonally dominant (see Section 4.2). Note that this condition is often satisfied in a finite difference setting, for example for the Poisson model problem from Chapter 2. If we use *piecewise linear interpolation* on the interface, then it is easy to verify that the matrix $\mathbf{L}^{H,h}$ (for a certain ordering of the grid points in $\Omega^{H,h}$) has positive diagonal elements and non-positive off-diagonal elements and that $\mathbf{L}^{H,h}$ is irreducibly diagonally dominant. Hence $\mathbf{L}^{H,h}$ and $L^{H,h}$ are nonsingular (see Section 4.2). In case of *piecewise quadratic interpolation* things are more complicated. In Section 4.4 the nonsingularity of $L^{H,h}$ is proved for the Poisson model problem. If both L_l^h and L^H are nonsingular then, in general, this does not imply that $L^{H,h}$ is nonsingular. A counter-example is given in ([30, Example 3.3.1]). □

Now that we have derived the system of linear equations on the composite grid for the fixed points of the LDC method, we can consider the iterative behaviour of the method. We introduce the *extension operators* $R^T : \mathcal{F}(\Omega^H) \to \mathcal{F}(\Omega^{H,h})$ and $R_l^T : \mathcal{F}(\Omega_l^h) \to \mathcal{F}(\Omega^{H,h})$, defined by

$$(R^T w)(\mathbf{x}) := \begin{cases} 0 & \mathbf{x} \in \Omega_l^h \backslash \Omega_l^H \\ w(\mathbf{x}) & \mathbf{x} \in \Omega^H \end{cases}, \quad w \in \mathcal{F}(\Omega^H), \tag{3.22}$$

$$(R_l^T w)(\mathbf{x}) := \begin{cases} w(\mathbf{x}) & \mathbf{x} \in \Omega_l^h \\ 0 & \mathbf{x} \in \Omega_c^H \end{cases}, \quad w \in \mathcal{F}(\Omega_l^h). \tag{3.23}$$

The transpose of the extension operator $R_l{}^T$ is the trivial injection R_l in (3.8). The transpose $R : \mathcal{F}(\Omega^{H,h}) \to \mathcal{F}(\Omega^H)$ of the extension operator R^T is the trivial injection defined by

$$Rw := w_{|\Omega^H}, \quad w \in \mathcal{F}(\Omega^{H,h}). \tag{3.24}$$

Below we use block partitioning corresponding to the direct sums $\mathcal{F}(\Omega^H) = \mathcal{F}(\Omega_l^H) \oplus \mathcal{F}(\Omega_c^H)$ and $\mathcal{F}(\Omega^{H,h}) = \mathcal{F}(\Omega_l^h) \oplus \mathcal{F}(\Omega_c^H)$ (see Figure 3.2). Then the trivial injections R and R_l are of the form

$$R = \begin{bmatrix} r_l & \emptyset \\ \emptyset & I \end{bmatrix},$$

$$R_l{}^T = \begin{bmatrix} I & \emptyset \end{bmatrix},$$

with r_l the trivial injection from (3.10).

Theorem 3.9 *The iterates $u_i^{H,h}$ ($i \geq 1$) from the LDC method (2.16) satisfy*

$$u_i^{H,h} - u^{H,h} = M(u_{i-1}^{H,h} - u^{H,h}), \tag{3.25a}$$

with

$$M := (I - P_2)(I - P_1), \tag{3.25b}$$

$$P_1 := R^T(L^H)^{-1}RL^{H,h}, \tag{3.25c}$$

$$P_2 := R_l{}^T(L_l^h)^{-1}R_l L^{H,h}, \tag{3.25d}$$

L^H, L_l^h *from (2.16) and* $L^{H,h}, u^{H,h}$ *from (3.18).*

Proof. Recall that $u^{H,h}$ is given by

$$u^{H,h} = \begin{bmatrix} I \\ \emptyset \end{bmatrix} u_l^h + \begin{bmatrix} \emptyset & \emptyset \\ \emptyset & I \end{bmatrix} u^H,$$

with (u^H, u_l^h) satisfying

$$L^H u^H = \begin{pmatrix} L_l^H r_l u_l^h + L_\Gamma^H u^H|_\Gamma \\ f^H|_{\Omega_c^H} \end{pmatrix},$$

$$L_l^h u_l^h = f_l^h - L_\Gamma^h p u^H|_\Gamma.$$

The LDC iterates $u_i^{H,h}$, $i \geq 1$, are given by

$$u_i^{H,h} = \begin{bmatrix} I \\ \emptyset \end{bmatrix} u_{l,i}^h + \begin{bmatrix} \emptyset & \emptyset \\ \emptyset & I \end{bmatrix} u_i^H,$$

with $(u_i^H, u_{l,i}^h)$ satisfying

$$L^H u_i^H = \begin{pmatrix} L_l^H r_l u_{l,i-1}^h + L_\Gamma^H u_{i-1}^H|_\Gamma \\ f^H|_{\Omega_c^H} \end{pmatrix},$$

$$L_l^h u_{l,i}^h = f_l^h - L_\Gamma^h p u_i^H|_\Gamma.$$

Hence we have

$$u_i^{H,h} - u^{H,h} = \begin{bmatrix} I \\ \varnothing \end{bmatrix} (u_{l,i}^h - u_l^h) + \begin{bmatrix} \varnothing & \varnothing \\ \varnothing & I \end{bmatrix} (u_i^H - u^H), \qquad (*1)$$

with

$$\begin{aligned} u_{l,i}^h - u_l^h &= -(L_l^h)^{-1} L_\Gamma^h p(u_i^H|_\Gamma - u^H|_\Gamma) \\ &= -(L_l^h)^{-1} L_\Gamma^h p r_\Gamma \begin{bmatrix} \varnothing & I \end{bmatrix} (u_i^H - u^H) \end{aligned} \qquad (*2)$$

and

$$u_i^H - u^H = (L^H)^{-1} \begin{bmatrix} L_l^H r_l(u_{l,i-1}^h - u_l^h) + L_\Gamma^H(u_{i-1}^H|_\Gamma - u^H|_\Gamma) \\ \varnothing \end{bmatrix}. \qquad (*3)$$

Using (3.9) and (3.21) in $(*3)$ we obtain

$$\begin{aligned} u_i^H - u^H &= (L^H)^{-1} \begin{bmatrix} I & \varnothing \\ \varnothing & \varnothing \end{bmatrix} L^H \begin{bmatrix} r_l & \varnothing \\ \varnothing & I \end{bmatrix} (u_{i-1}^{H,h} - u^{H,h}) \\ &= (L^H)^{-1} \left(L^H \begin{bmatrix} r_l & \varnothing \\ \varnothing & I \end{bmatrix} - \begin{bmatrix} \varnothing & \varnothing \\ \varnothing & I \end{bmatrix} L^H \begin{bmatrix} r_l & \varnothing \\ \varnothing & I \end{bmatrix} \right) (u_{i-1}^{H,h} - u^{H,h}) \\ &= \left(\begin{bmatrix} r_l & \varnothing \\ \varnothing & I \end{bmatrix} - (L^H)^{-1} \begin{bmatrix} \varnothing & \varnothing \\ \varnothing & I \end{bmatrix} L^{H,h} \right) (u_{i-1}^{H,h} - u^{H,h}). \end{aligned}$$

Since $L^{H,h}(u_{i-1}^{H,h} - u^{H,h})$ is of the form $\begin{bmatrix} \varnothing \\ \star \end{bmatrix}$, we obtain

$$u_i^H - u^H = \left(\begin{bmatrix} r_l & \varnothing \\ \varnothing & I \end{bmatrix} - (L^H)^{-1} \begin{bmatrix} r_l & \varnothing \\ \varnothing & I \end{bmatrix} L^{H,h} \right) (u_{i-1}^{H,h} - u^{H,h}). \qquad (*4)$$

Combining $(*1)$, $(*2)$ and $(*4)$ yields

$$\begin{aligned} u_i^{H,h} - u^{H,h} &= - \begin{bmatrix} I \\ \varnothing \end{bmatrix} (L_l^h)^{-1} L_\Gamma^h p r_\Gamma \begin{bmatrix} \varnothing & I \end{bmatrix} (u_i^H - u^H) + \begin{bmatrix} \varnothing & \varnothing \\ \varnothing & I \end{bmatrix} (u_i^H - u^H) \\ &= \left(- \begin{bmatrix} I \\ \varnothing \end{bmatrix} (L_l^h)^{-1} L_\Gamma^h p r_\Gamma \begin{bmatrix} \varnothing & I \end{bmatrix} \begin{bmatrix} r_l & \varnothing \\ \varnothing & I \end{bmatrix} + \begin{bmatrix} \varnothing & \varnothing \\ \varnothing & I \end{bmatrix} \begin{bmatrix} r_l & \varnothing \\ \varnothing & I \end{bmatrix} \right. \\ &\quad \left. - \begin{bmatrix} \varnothing & \varnothing \\ \varnothing & I \end{bmatrix} (L^H)^{-1} \begin{bmatrix} r_l & \varnothing \\ \varnothing & I \end{bmatrix} L^{H,h} \right) \end{aligned}$$

$$+ \begin{bmatrix} I \\ \emptyset \end{bmatrix} (L_l^h)^{-1} L_\Gamma^h pr_\Gamma \begin{bmatrix} \emptyset & I \end{bmatrix} (L^H)^{-1} \begin{bmatrix} r_l & \emptyset \\ \emptyset & I \end{bmatrix} L^{H,h} \Bigg) (u_{i-1}^{H,h} - u^{H,h})$$

$$= \Bigg(\begin{bmatrix} \emptyset & -(L_l^h)^{-1} L_\Gamma^h pr_\Gamma \\ \emptyset & \emptyset \end{bmatrix} + \begin{bmatrix} \emptyset & \emptyset \\ \emptyset & I \end{bmatrix} - \begin{bmatrix} \emptyset & \emptyset \\ \emptyset & I \end{bmatrix} R^T (L^H)^{-1} R L^{H,h}$$

$$+ \begin{bmatrix} \emptyset & -(L_l^h)^{-1} L_\Gamma^h pr_\Gamma \\ \emptyset & \emptyset \end{bmatrix} R^T (L^H)^{-1} R L^{H,h} \Bigg) (u_{i-1}^{H,h} - u^{H,h})$$

$$= \begin{bmatrix} \emptyset & -(L_l^h)^{-1} L_\Gamma^h pr_\Gamma \\ \emptyset & I \end{bmatrix} (I - P_1)(u_{i-1}^{H,h} - u^{H,h}).$$

Since

$$\begin{bmatrix} \emptyset & -(L_l^h)^{-1} L_\Gamma^h pr_\Gamma \\ \emptyset & I \end{bmatrix} = I - \begin{bmatrix} I & (L_l^h)^{-1} L_\Gamma^h pr_\Gamma \\ \emptyset & \emptyset \end{bmatrix}$$

$$= I - \begin{bmatrix} I \\ \emptyset \end{bmatrix} (L_l^h)^{-1} \begin{bmatrix} L_l^h & L_\Gamma^h pr_\Gamma \end{bmatrix}$$

$$= I - R_l{}^T (L_l^h)^{-1} R_l L^{H,h}$$

$$= I - P_2,$$

we obtain (3.25). ∎

Remark 3.10 There is a certain freedom with respect to the choice for the restriction operator R in (3.24). The result of Theorem 3.9 holds for any restriction operator $R : \mathcal{F}(\Omega^{H,h}) \to \mathcal{F}(\Omega^H)$ which has the form

$$R = \begin{bmatrix} \hat{r}_l & \emptyset \\ \emptyset & I \end{bmatrix},$$

with $\hat{r}_l : \mathcal{F}(\Omega_l^h) \to \mathcal{F}(\Omega_l^H)$ a linear surjection. This follows since $(I - P_2)$ is of the form

$$\begin{bmatrix} \emptyset & \star \\ \emptyset & \star \end{bmatrix},$$

and thus $(I - P_2)R^T$ is independent of the choice of $\hat{r}_l$, and $L^{H,h}(u_{i-1}^{H,h} - u^{H,h})$ is of the form

$$\begin{bmatrix} \emptyset \\ \star \end{bmatrix},$$

and hence $R L^{H,h}(u_{i-1}^{H,h} - u^{H,h})$ is independent of $\hat{r}_l$. □

Remark 3.11 In case of $m > 1$ regions of local refinement, the iteration matrix of the local defect correction method would be of the form

$$\bar{M} = (I - \bar{P}_2 - \bar{P}_3 \ldots - \bar{P}_{m+1})(I - \bar{P}_1),$$

with $\bar{P}_1$ similar to P_1 in (3.25c) and $\bar{P}_2, \bar{P}_3, \ldots, \bar{P}_{m+1}$ similar to P_2 in (3.25d). □

Lemma 3.12 *The operator P_2 from (3.25d) satisfies*

$$(P_2)^2 = P_2. \qquad (3.26)$$

Proof.

$$
\begin{aligned}
(P_2)^2 &= R_l{}^T (L_l^h)^{-1} R_l L^{H,h} R_l{}^T (L_l^h)^{-1} R_l L^{H,h} \\
&= R_l{}^T (L_l^h)^{-1} \begin{bmatrix} I & \emptyset \end{bmatrix} \begin{bmatrix} L_l^h & L_\Gamma^h pr_\Gamma \\ L_{\bar\Gamma}^H & L_c^H \end{bmatrix} \begin{bmatrix} I \\ \emptyset \end{bmatrix} (L_l^h)^{-1} R_l L^{H,h} \\
&= R_l{}^T (L_l^h)^{-1} L_l^h (L_l^h)^{-1} R_l L^{H,h} \\
&= P_2.
\end{aligned}
$$

∎

For the approximation $u_0^{H,h}$, resulting from the starting procedure in the LDC method, we have the following result.

Lemma 3.13 *The initial approximation $u_0^{H,h}$ in the LDC iteration (2.16) satisfies*

$$u_0^{H,h} - u^{H,h} = (I - P_2)(R^T (L^H)^{-1} f^H - u^{H,h}), \qquad (3.27)$$

with P_2 from (3.25d), R^T from (3.22), L^H, f^H from (2.16) and $u^{H,h}$ from (3.18).

Proof. As in the proof of Theorem 3.9 we can derive

$$
\begin{aligned}
u_0^{H,h} - u^{H,h} &= \begin{bmatrix} I \\ \emptyset \end{bmatrix} (u_{l,0}^h - u_l^h) + \begin{bmatrix} \emptyset & \emptyset \\ \emptyset & I \end{bmatrix} (u_0^H - u^H), \\
u_{l,0}^h - u_l^h &= -(L_l^h)^{-1} L_\Gamma^h pr_\Gamma \begin{bmatrix} \emptyset & I \end{bmatrix} (u_0^H - u^H).
\end{aligned}
$$

Since $L^H u_0^H = f^H$ we have $u_0^H - u^H = (L^H)^{-1} f^H - u^H$. Hence,

$$
\begin{aligned}
u_0^{H,h} - u^{H,h} &= -\begin{bmatrix} I \\ \emptyset \end{bmatrix} (L_l^h)^{-1} L_\Gamma^h pr_\Gamma \begin{bmatrix} \emptyset & I \end{bmatrix} ((L^H)^{-1} f^H - u^H) \\
&\quad + \begin{bmatrix} \emptyset & \emptyset \\ \emptyset & I \end{bmatrix} ((L^H)^{-1} f^H - u^H) \\
&= -\begin{bmatrix} I \\ \emptyset \end{bmatrix} (L_l^h)^{-1} L_\Gamma^h pr_\Gamma \begin{bmatrix} \emptyset & I \end{bmatrix} (R^T (L^H)^{-1} f^H - u^{H,h}) \\
&\quad + \begin{bmatrix} \emptyset & \emptyset \\ \emptyset & I \end{bmatrix} (R^T (L^H)^{-1} f^H - u^{H,h}) \\
&= \begin{bmatrix} \emptyset & -(L_l^h)^{-1} L_\Gamma^h pr_\Gamma \\ \emptyset & I \end{bmatrix} (R^T (L^H)^{-1} f^H - u^{H,h}).
\end{aligned}
$$

Now (3.27) follows immediately since

$$
\begin{bmatrix} \emptyset & -(L_l^h)^{-1} L_\Gamma^h pr_\Gamma \\ \emptyset & I \end{bmatrix} = (I - P_2),
$$

as shown in the proof of Theorem 3.9.   ■

Combination of the results in Theorem 3.9, Lemma 3.12 and Lemma 3.13, yields the following expression for the LDC iterates.

Corollary 3.14 *The iterates $u_i^{H,h}$ ($i \geq 1$) of the LDC method (2.16) satisfy*

$$u_i^{H,h} - u^{H,h} = ((I - P_2)(I - P_1)(I - P_2))^i (R^T (L^H)^{-1} f^H - u^{H,h}). \qquad (3.28)$$

From Theorem 3.6 and Corollary 3.14 we conclude that the LDC method in (2.16) is a linear iterative method for solving the system of linear equations (3.18) and that the rate of convergence of the LDC method is determined by the operator

$$\tilde{M} = (I - P_2)(I - P_1)(I - P_2). \qquad (3.29)$$

From the definition of the LDC method it is clear that this method can be viewed as a Schwarz domain decomposition method (see e.g. [16]). In mathematical terms this is made precise by the expression for the error propagation operator M in (3.25b). The LDC method (2.16) is a *multiplicative* Schwarz method based on *two overlapping subregions*.

Using the expression for the error propagation operator $\tilde{M}$, we can show a close relation between the LDC method and the FAC method. This relation will be discussed in Section 3.4.

Unfortunately, we have not been able to derive satisfactory bounds for the norm or spectral radius of $\tilde{M}$. With respect to this we note that almost all convergence analyses of related methods (e.g., FAC applied to a FVE discretization as in [48]) use a variational setting, whereas it is not clear to us how the discrete operator $L^{H,h}$ (and thus P_1 and P_2) can be put in such a variational setting. Another way to develop convergence theory for domain decomposition methods is based on the maximum principle (e.g., [15],[41]. However, since in the LDC method the global coarse grid problem is updated in a local region, instead of on an interior boundary, it is not clear to us how maximum principle arguments can be applied in this case. So a satisfactory convergence analysis of the LDC method (2.16), i.e. local defect correction without overlap (see Section 2.2.3), is still lacking, although we have been able to show that the rate of convergence is determined by the operator $\tilde{M}$ (i.e. we need bounds for the norm or spectral radius of $\tilde{M}$). In Example 3.15 we illustrate the fast convergence of the LDC method numerically.

Example 3.15 Consider the boundary value problems:

Case 1. The Poisson problem

$$-\Delta u = f \quad \text{in } \Omega = (0, 1) \times (0, 1),$$
$$u = g \quad \text{on } \partial\Omega.$$

We choose f, g such that the solution $u^\star$ is the same as in Subsection 2.2.2 (cf. (2.4)). Note that the choice of f and g has no influence on the convergence behaviour of the method.

Case 2. The elliptic problem with variable coefficients

$$-(2 + \sin(\frac{\pi x}{3}))u_{xx} - e^{xy}u_{yy} + \cos(\frac{\pi x}{5})u_x + (1 + x)e^y u_y = f \quad \text{in } \Omega,$$
$$u = g \quad \text{on } \partial\Omega.$$

Case 1	$H = 1/20$			$\sigma = 2$		
	$\sigma = 2$	$\sigma = 4$	$\sigma = 8$	$H = 1/20$	$H = 1/40$	$H = 1/80$
linear	$2.2\ 10^{-2}$	$2.9\ 10^{-2}$	$3.1\ 10^{-2}$	$2.2\ 10^{-2}$	$1.5\ 10^{-2}$	$1.1\ 10^{-2}$
quadratic	$1.9\ 10^{-2}$	$2.2\ 10^{-2}$	$2.3\ 10^{-2}$	$1.9\ 10^{-2}$	$1.0\ 10^{-2}$	$0.7\ 10^{-2}$
Case 2	$H = 1/20$			$\sigma = 2$		
	$\sigma = 2$	$\sigma = 4$	$\sigma = 8$	$H = 1/20$	$H = 1/40$	$H = 1/80$
linear	$2.3\ 10^{-2}$	$3.1\ 10^{-2}$	$3.3\ 10^{-2}$	$2.3\ 10^{-2}$	$2.7\ 10^{-2}$	$2.0\ 10^{-2}$
quadratic	$2.7\ 10^{-2}$	$3.8\ 10^{-2}$	$4.1\ 10^{-2}$	$2.7\ 10^{-2}$	$2.9\ 10^{-2}$	$1.7\ 10^{-2}$

Table 3.1 Average error reduction factors ρ.

We choose f, g such that the solution $u^\star$ is the same as for Case 1.

We take $\Omega_l = (0, 1/4) \times (0, 1/4)$. Both on the uniform global coarse grid and on the uniform local fine grid we use a standard discretization. We take central difference approximations both for the second order and for the first order derivatives. We consider both piecewise linear interpolation and piecewise quadratic interpolation on the interface. In Table 3.1 we give the average error reduction per iteration in the first four iterations:

$$\rho := \frac{1}{4} \sum_{i=1}^{4} \frac{\|u_i^{H,h} - u^{H,h}\|_\infty}{\|u_{i-1}^{H,h} - u^{H,h}\|_\infty}.$$

We see that, both for Case 1 and for Case 2, the rate of convergence is high and more or less independent of the parameters H and $\sigma = H/h$. The error reduction factors for piecewise linear and piecewise quadratic interpolation are comparable. So for these (and related) test problems we observe a satisfactory convergence behaviour of the LDC method. $\square$

3.3 MLAT AS ITERATIVE SOLUTION METHOD

In this section we discuss the fixed points of the MLAT method (2.23). In the i-th MLAT step the local problem

$$L_l^h \hat{u}_{l,i}^h = f_l^h - L_\Gamma^h p u_{i-1}^{H,h}|_\Gamma$$

is solved approximately. In this section we assume that the approximate solution $\tilde{u}_{l,i}^h$ results from $u_{l,i-1}^h$ by applying ν steps of a linear iterative method:

$$\tilde{u}_{l,i}^h - \hat{u}_{l,i}^h = S_l^{\ \nu}(u_{l,i-1}^h - \hat{u}_{l,i}^h).$$

In the MLAT method coarse grid corrections are transferred to the local fine grid by the operator $\tilde{p} : \mathcal{F}(\Omega^H) \to \mathcal{F}(\Omega_l^h)$. We introduce the linear injection $\tilde{p}_l : \mathcal{F}(\Omega_l^H) \to \mathcal{F}(\Omega_l^h)$, called a *prolongation*, via the relation

$$\tilde{p} = \begin{bmatrix} \tilde{p}_l & \star \end{bmatrix},$$

where a block partitioning corresponding to the direct sum $\mathcal{F}(\Omega^H) = \mathcal{F}(\Omega_l^H) \oplus \mathcal{F}(\Omega_c^H)$ is used. We define

$$M_l := (I - \tilde{p}_l (L_l^H)^{-1} \tilde{r}_l L_l^h) S_l^\nu, \tag{3.30}$$

and we assume that the *spectral radius* $\rho(M_l)$ of M_l satisfies $\rho(M_l) < 1$

Remark 3.16 In multigrid terminology M_l is called a *two-grid iteration matrix* (see e.g. [31, Section 2.4]). This matrix describes a *two-grid method* for approximately solving the local fine grid problems in MLAT. Suitable choices of the smoothing process (S_l^ν), the prolongation $\tilde{p}_l$ and the restriction $\tilde{r}_l$ yield a convergent two-grid method (see e.g. [31],[61]). Then $\rho(M_l) < 1$ holds.
□

In each step of the MLAT method (2.23) approximations of the continuous solution of the boundary value problem (3.14) are computed both on the global coarse grid Ω^H and on the local fine grid Ω_l^h.

Lemma 3.17 (u^H, u_l^h) *is a fixed point of the MLAT iteration (2.23) if and only if* (u^H, u_l^h) *satisfies the coupled system*

$$L^H u^H - \begin{bmatrix} L_l^H \hat{r}_l u_l^h + L_\Gamma^H u^H |_\Gamma \\ \emptyset \end{bmatrix} = \begin{bmatrix} \emptyset \\ f^H |_{\Omega_c^H} \end{bmatrix} \qquad on \ \Omega^H, \tag{3.31a}$$

$$L_l^h u_l^h + L_\Gamma^h p u^H |_\Gamma = f_l^h \qquad on \ \Omega_l^h. \tag{3.31b}$$

Proof. Let (u^H, u_l^h) be a fixed point of the MLAT iteration. It follows from (2.23) and (3.12) that

$$L^H u^H = \begin{bmatrix} L_l^H \hat{r}_l \tilde{u}_l^h + L_\Gamma^H u^H |_\Gamma - \tilde{r}_l L_l^h (\tilde{u}_l^h - \hat{u}_l^h) \\ f^H |_{\Omega_c^H} \end{bmatrix} \qquad (*1)$$

$$u_l^h = \tilde{u}_l^h + \tilde{p}_l (u^H |_{\Omega_l^H} - \hat{r}_l \tilde{u}_l^h). \tag{$*2$}$$

In $(*1)$ $\hat{u}_l^h$ is the solution of

$$L_l^h \hat{u}_l^h = f_l^h - L_\Gamma^h p u^H |_\Gamma, \tag{$*3$}$$

and $\tilde{u}_l^h$ is an approximation of $\hat{u}_l^h$ resulting from ν steps of a linear iterative method, with iteration matrix S_l, and initial approximation u_l^h. Thus we have

$$\tilde{u}_l^h - \hat{u}_l^h = S_l^\nu (u_l^h - \hat{u}_l^h). \tag{$*4$}$$

Using (3.9) in $(*1)$ we obtain

$$u^H |_{\Omega_l} - \hat{r}_l \tilde{u}_l^h = -(L_l^H)^{-1} \tilde{r}_l L_l^h (\tilde{u}_l^h - \hat{u}_l^h).$$

Substituting this in $(*2)$ yields

$$u_l^h - \tilde{u}_l^h = -\tilde{p}_l (L_l^H)^{-1} \tilde{r}_l L_l^h (\tilde{u}_l^h - \hat{u}_l^h). \tag{$*5$}$$

Using (∗4) and (∗5) we obtain

$$
\begin{aligned}
u_l^h - \hat{u}_l^h &= u_l^h - \tilde{u}_l^h + \tilde{u}_l^h - \hat{u}_l^h \\
&= -\tilde{p}_l(L_l^H)^{-1}\hat{r}_l L_l^h(\tilde{u}_l^h - \hat{u}_l^h) + (\tilde{u}_l^h - \hat{u}_l^h) \\
&= -\tilde{p}_l(L_l^H)^{-1}\tilde{r}_l L_l^h S_l^\nu(u_l^h - \hat{u}_l^h) + S_l^\nu(u_l^h - \hat{u}_l^h) \\
&= (I - \tilde{p}_l(L_l^H)^{-1}\tilde{r}_l L_l^h)S_l^\nu(u_l^h - \hat{u}_l^h) \\
&= M_l(u_l^h - \hat{u}_l^h).
\end{aligned}
$$

Note that $I - M_l$ is nonsingular due to $\rho(M_l) < 1$. Thus $\hat{u}_l^h = u_l^h$, and by (∗4) $\tilde{u}_l^h = \hat{u}_l^h = u_l^h$. Then (3.31) follows from (∗1) and (∗3).

Let (u^H, u_l^h) satisfy (3.31). Suppose that $u_{i-1}^H = u^H$ and $u_{l,i-1}^h = u_l^h$ in (2.23). We have to show that $u_i^H = u^H$ and $u_{l,i}^h = u_l^h$.

Since u_l^h satisfies $L_l^h u_l^h = f_l^h - L_\Gamma^h p u^H|_\Gamma$, we have $\hat{u}_{l,i}^h = u_l^h$. Since $\tilde{u}_{l,i}^h - \hat{u}_{l,i}^h = S_l^\nu(u_{l,i-1}^h - \hat{u}_{l,i}^h)$ and $u_{l,i-1}^h = \hat{u}_{l,i}^h = u_l^h$, we have $\tilde{u}_{l,i}^h = u_l^h$. Hence from (3.12) we obtain

$$
L^H u_i^H = \begin{pmatrix} L_l^H \hat{r}_l u_l^h + L_\Gamma^H u^H|_\Gamma \\ f^H|_{\Omega_c^H} \end{pmatrix}, \qquad (\ast 6)
$$

and thus $u_i^H = u^H$.

From (3.9), (∗6) and $u_i^H = u^H$ we obtain

$$
L_l^H u_i^H|_{\Omega_l^H} = L_l^H \hat{r}_l u_l^h.
$$

Since L_l^H is nonsingular this is equivalent with $u_i^H|_{\Omega_l^H} = \hat{r}_l u_l^h$. Now the correction v^H in (2.23e) satisfies

$$
\begin{aligned}
v^H(\mathbf{x}) &= u_i^H(\mathbf{x}) - (\hat{r}_l \tilde{u}_{l,i}^h)(\mathbf{x}) = u_i^H(\mathbf{x}) - (\hat{r}_l u_l^h)(\mathbf{x}) = 0 & \mathbf{x} \in \Omega_l^H \\
v^H(\mathbf{x}) &= u_i^H(\mathbf{x}) - u_{i-1}^{H,h}(\mathbf{x}) = u^H(\mathbf{x}) - u^H(\mathbf{x}) = 0 & \mathbf{x} \in \Gamma^H \\
v^H(\mathbf{x}) &= 0 & \mathbf{x} \in \Omega_c^H
\end{aligned}.
$$

Thus $u_{l,i}^h = \tilde{u}_{l,i}^h = u_l^h$. ∎

The coupled system (3.31) is similar to the coupled system (3.15) which describes the fixed points of the LDC iteration.

Corollary 3.18 *If $\hat{r}_l$ is the trivial injection from (3.10), then the LDC method (2.16) and the MLAT method (2.23) have the same fixed points.*

Lemma 3.19 *If (u^H, u_l^h) satisfies the coupled system (3.31), then*

$$
u^H|_{\Omega_l^H} = (\hat{r}_l u_l^h)|_{\Omega_l^H} \tag{3.32}
$$

holds.

Proof. Similar to the proof of Lemma 3.3.   ■

Below we show that the coupled system (3.31) is related to a system of linear equations resulting from finite difference discretization of the boundary value problem (3.14) on the composite grid $\Omega^{H,h}$. We use the restriction $\hat{r}_{\bar{\Gamma}} : \mathcal{F}(\Omega_l^h) \rightarrow \mathcal{F}(\tilde{\Gamma}^H)$, defined by

$$(\hat{r}_{\bar{\Gamma}} w)_{|\tilde{\Gamma}^H} = (\hat{r}_l w)_{|\tilde{\Gamma}^H}, \quad w \in \mathcal{F}(\Omega_l^h). \tag{3.33}$$

Lemma 3.20 *If* (u^H, u_l^h) *satisfies the coupled system (3.31), then the composite grid function*

$$u^{H,h} := \begin{bmatrix} u_l^h \\ u^H_{|\Omega_c^H} \end{bmatrix}$$

satisfies

$$\hat{L}^{H,h} u^{H,h} = f^{H,h} \tag{3.34a}$$

with

$$\hat{L}^{H,h} := \begin{bmatrix} L_l^h & L_{\Gamma}^h pr_{\Gamma} \\ L_{\bar{\Gamma}}^H \hat{r}_{\bar{\Gamma}} & L_c^H \end{bmatrix}, \tag{3.34b}$$

and $f^{H,h}$ *from (3.18c).*

Proof. Similar to the proof of Lemma 3.4 with $r_{\bar{\Gamma}}$ replaced by $\hat{r}_{\bar{\Gamma}}$.   ■

Lemma 3.21 *If* $u^{H,h}$ *satisfies the composite grid problem (3.34), then* (u^H, u_l^h) *defined by*

$$u^H := u^{H,h}_{|\Omega^H},$$
$$u_l^h := u^{H,h}_{|\Omega_l^h},$$

satisfies the coupled system (3.31).

Proof. Similar to the proof of Lemma 3.4 with $r_{\bar{\Gamma}}$ replaced by $\hat{r}_{\bar{\Gamma}}$.   ■

We define the *composite grid fixed points* of MLAT by

$$u^{H,h} := \begin{bmatrix} u_l^h \\ u^H_{|\Omega_c^H} \end{bmatrix} \tag{3.35}$$

where (u^H, u_l^h) is a fixed point of the MLAT method (2.23).

Theorem 3.22 *The composite grid fixed points of the MLAT method (2.23) are the solutions of the composite grid problem (3.34).*

Proof. Follows from a combination of Lemma 3.17, Lemma 3.20 and Lemma 3.21.   ■

Corollary 3.23 *If the finite difference operator $\hat{L}^{H,h}$ from (3.34b) is nonsingular, then the MLAT iteration (2.23) has a unique fixed point.*

If $\hat{r}_l$ is the *trivial injection* from (3.10), then the composite grid problem (3.34) is the same as the composite grid problem in Theorem 3.6. The discretization approach which yields this composite grid problem is described in Section 3.2. The interface grid points are treated as if they were grid points of the uniform global coarse grid Ω^H. If $\hat{r}_l$ is a *weighted restriction*, then the interface grid points are discretized in a different way. An example is given below.

Example 3.24 It suffices to consider the one-dimensional Poisson equation $-u_{xx} = f$. We take $\Omega_l = (y, z)$ and $\sigma = 2$, and we use central differences on the uniform subgrids. If $\hat{r}_l$ is the *trivial injection* from (3.10), then we have

$$(\hat{L}^{H,h}u)(y) := \frac{1}{H^2}(2u(y) - u(y - H) - u(y + H)).$$

If $\hat{r}_l$ is the *weighted restriction* defined by

$$(\hat{r}_l w_l^h)(x) := \frac{1}{4}(w_l^h(x - h) + 2w_l^h(x) + w_l^h(x + h)), \quad x \in \Omega_l^H,$$

(cf. ([31, Section 2.3]), then the difference approximation at y reads

$$(\hat{L}^{H,h}u)(y) := \frac{1}{H^2}(2u(y) - u(y - H) - \frac{1}{4}u(y + h) - \frac{1}{2}u(y + H) - \frac{1}{4}u(y + 3h)).$$

$\square$

Remark 3.25 In [7],[9] it is suggested that the converged solution of the multi-level adaptive technique satisfies the composite grid discretization (3.18), independently of the choice of $\hat{r}_l$. As we have seen in this section, the converged solution of the multi-level adaptive technique satisfies the composite grid discretization (3.34), which depends on $\hat{r}_l$. So *even for linear problems* the approximations in MLAT method depend on the choice for $\hat{r}_l$. Contrary to this, the approximations in the Full Approximation Scheme (FAS) for linear problems, which is used as starting point for deriving MLAT, do not depend on the choice for the restriction operator used to transfer fine grid approximations to the coarse grid [8, Section 8.1]. $\square$

In the MLAT method (2.23) the local fine grid problems are solved approximately by a two-grid method (cf. Remark 3.16). If we consider MLAT with exact solution of the local fine grid problems (2.23a), then the local fine grid defect in (2.23b) is equal to 0 at all grid points of the local fine grid and the correction of the local approximation in (2.23e) can be omitted. Then the right hand sides of the global and local problems are defined in the same way as in an LDC step, i.e. by local defect correction and artificial Dirichlet values on the interface. If $\hat{r}_l = r_l$ in the MLAT step, then the only difference between an MLAT step and an LDC step is the order in which the global coarse grid problem and the local fine grid problem are solved.

3.4   COMPARISON OF LDC AND FAC

As we have seen in Section 2.3 the FAC method is an iterative solution method for an a priori given composite grid discretization. In Section 3.2 we have derived the composite grid discretization (3.18) which is actually solved by the LDC method. In order to compare the LDC method and the FAC method, we apply the FAC method to the composite grid discretization (3.18).

In the FAC method a restriction $\hat{r} : \mathcal{F}(\Omega^{H,h}) \to \mathcal{F}(\Omega^H)$ is used. We assume that $\hat{r}$ has the form

$$\hat{r} = \left[\begin{array}{cc} \hat{r}_l & \emptyset \\ \emptyset & I \end{array} \right]. \tag{3.36}$$

Here and in the remainder of this section block partitionings corresponding to $\mathcal{F}(\Omega^{H,h}) = \mathcal{F}(\Omega_l^h) \oplus \mathcal{F}(\Omega_c^H)$ and $\mathcal{F}(\Omega^H) = \mathcal{F}(\Omega_l^H) \oplus \mathcal{F}(\Omega_c^H)$ are used (see Figure 3.2). By (3.36) we have that outside the region Ω_l composite grid defects $d^{H,h}$ from (2.20a) are restricted to the global coarse grid Ω^H in a trivial way. Inside the region Ω_l a linear surjection $\hat{r}_l : \mathcal{F}(\Omega_l^h) \to \mathcal{F}(\Omega_l^H)$ is used.

Theorem 3.26 *The iterates $u_i^{H,h}$ $(i \geq 1)$ from the FAC iteration (2.20) applied to the composite grid problem (3.18) satisfy*

$$u_i^{H,h} - u^{H,h} = \hat{M}(u_{i-1}^{H,h} - u^{H,h}), \tag{3.37a}$$

with

$$\hat{M} := (I - P_2)(I - \hat{P}_1), \tag{3.37b}$$

$$\hat{P}_1 := \hat{r}^T (L^H)^{-1} \hat{r} L^{H,h}, \tag{3.37c}$$

$$P_2 := R_l^T (L_l^h)^{-1} R_l L^{H,h}, \tag{3.37d}$$

R_l from (3.8), $\hat{r}$ from (3.36), L^H, L_l^h from (2.20) and $L^{H,h}, u^{H,h}$ from (3.18).

Proof. It follows from (2.20) and (3.7) that the FAC iterates $u_i^{H,h}$ satisfy

$$u_i^{H,h} - u^{H,h} = u_{i-1}^{H,h} - u^{H,h} - \left[\begin{array}{c} I \\ \emptyset \end{array} \right] v_l^h - \left[\begin{array}{cc} \emptyset & \emptyset \\ \emptyset & I \end{array} \right] v^H,$$

with

$$v^H = (L^H)^{-1} \hat{r}(L^{H,h} u_{i-1}^{H,h} - f^{H,h}),$$
$$v_l^h = (L_l^h)^{-1} R_l(L^{H,h} u_{i-1}^{H,h} - f^{H,h}) - (L_l^h)^{-1} L_\Gamma^h p v^H|_\Gamma.$$

Thus we obtain

$$u_i^{H,h} - u^{H,h} = u_{i-1}^{H,h} - u^{H,h} - R_l^T (L_l^h)^{-1} R_l(L^{H,h} u_{i-1}^{H,h} - f^{H,h})$$
$$+ \left[\begin{array}{c} I \\ \emptyset \end{array} \right] (L_l^h)^{-1} L_\Gamma^h p v^H|_\Gamma - \left[\begin{array}{cc} \emptyset & \emptyset \\ \emptyset & I \end{array} \right] v^H$$

$$= u_{i-1}^{H,h} - u^{H,h} - R_l^T(L_l^h)^{-1}R_l L^{H,h}(u_{i-1}^{H,h} - u^{H,h})$$

$$- \left(\begin{bmatrix} \emptyset & \emptyset \\ \emptyset & I \end{bmatrix} - \begin{bmatrix} I \\ \emptyset \end{bmatrix} (L_l^h)^{-1}L_\Gamma^h pr_\Gamma \begin{bmatrix} \emptyset & I \end{bmatrix} \right) (L^H)^{-1}\hat{r}(L^{H,h}u_{i-1}^{H,h} - f^{H,h})$$

$$= (I - P_2)(u_{i-1}^{H,h} - u^{H,h}) - \begin{bmatrix} \emptyset & -(L_l^h)^{-1}L_\Gamma^h pr_\Gamma \\ \emptyset & I \end{bmatrix} \hat{r}^T(L^H)^{-1}\hat{r}L^{H,h}(u_{i-1}^{H,h} - u^{H,h})$$

$$= (I - P_2)(u_{i-1}^{H,h} - u^{H,h}) - (I - P_2)\hat{P}_1(u_{i-1}^{H,h} - u^{H,h})$$

$$= (I - P_2)(I - \hat{P}_1)(u_{i-1}^{H,h} - u^{H,h}),$$

where we have used

$$\begin{bmatrix} \emptyset & -(L_l^h)^{-1}L_\Gamma^h pr_\Gamma \\ \emptyset & I \end{bmatrix} = (I - P_2),$$

as shown in the proof of Theorem 3.9. ∎

In Remark 3.10 we have seen that in the expression for the error propagation operator of the LDC method there is a certain freedom with respect to the choice for the restriction operator R. By combining the results of Theorem 3.9, Remark 3.10 and Lemma 3.13, we obtain *for the LDC iterates $u_i^{H,h}$*:

$$u_i^{H,h} - u^{H,h} = \hat{M}^i(I - P_2)(R^T(L^H)^{-1}f^H - u^{H,h}), \qquad i \geq 1, \tag{3.38}$$

with $\hat{M}$ from (3.37b).

Remark 3.27 In the expression for the iteration matrix of the FAC method there is no freedom with respect to the choice for the restriction operator $\hat{r}$. This is due to the fact that for an arbitrarily chosen initial approximation $u_0^{H,h}$ in the FAC method, the term $L^{H,h}(u_0^{H,h} - u^{H,h})$ is *not* of the form

$$\begin{bmatrix} \emptyset \\ \star \end{bmatrix}.$$

For $i \geq 2$ the terms $L^{H,h}(u_i^{H,h} - u^{H,h})$ are of this form (see [22]). □

In the FAC method the initial approximation $u_0^{H,h}$ has to be specified. A possible choice for $u_0^{H,h}$ is the approximation resulting from the starting procedure in the LDC method (2.16a-c). With this initial approximation, the FAC iterates satisfy

$$u_i^{H,h} - u^{H,h} = \hat{M}^i(I - P_2)(R^T(L^H)^{-1}f^H - u^{H,h}), \tag{3.39}$$

which is obtained by combining the results of Theorem 3.26 and Lemma 3.13. It follows from (3.38) and (3.39) that the iterates generated by the LDC method are the same as the iterates generated by the FAC method described above. In this FAC method the initial approximation resulting from the LDC starting procedure is used and composite grid defects are restricted to the global coarse grid in a trivial way outside Ω_l (cf. (3.36)).

Corollary 3.28 *If the FAC method (2.20) with the initial approximation resulting from (2.16a-c) and $\hat{r}$ as in (3.36), is applied to the composite grid discretization (3.18), then the FAC iterates on the composite grid are identical to the composite grid iterates in the LDC method (2.16).*

Remark 3.29 The difference between the FAC method for solving (3.18) and the LDC method for solving (3.18) is, in *multigrid terminology* (see e.g. [8, Chapter 8]), the difference between a *correction scheme* version and a *full approximation scheme* version of an iterative solution method for (3.18). □

Remark 3.30 In [22] we have shown that if the FAC method is applied to the composite grid discretization (3.18), it is optimal to use a restriction $\hat{r}$ of the form (3.36). The fast convergence of the FAC method with an optimal restriction operator is illustrated by numerical results. If the FAC method is applied to the discrete equations resulting from a non-uniform discretization approach (see Section 2.3), it is *not* optimal to use a restriction operator of the form (3.36). In [22] quasi-optimal restriction operators for the FAC method applied to non-uniform composite grid problems are derived. □

4

FINITE DIFFERENCE DISCRETIZATION METHODS ON COMPOSITE GRIDS

In this chapter we discuss three finite difference approaches for the discretization of elliptic boundary value problems on a composite grid. The three discretization approaches are identical at all composite grid points which do not lie on the interface; they differ at the interface grid points.

The first approach is related to the LDC method. The composite grid problem resulting from this approach is the discrete problem which is actually solved by the LDC method (cf. Section 3.2). The composite grid problem which results from the second approach is the discrete problem which is actually solved by the MLAT method, with a reasonable choice for the restriction operator $\hat{r}_l$ (cf. Section 3.3). Both these approaches use the fact that interface grid points belong to a global uniform grid underlying the composite grid. The third approach does not use this fact; non-uniform finite differences are used at the interface grid points.

In Section 4.3 we consider a simple two-point boundary value problem. We discuss elementary properties of the discrete Green's functions and the local discretization errors corresponding to the three discretization approaches. Most of these properties, which play an important role in the analysis of the global discretization error, can be generalized to the two-dimensional case.

In Section 4.4 we derive a discretization error bound for the finite difference approach related to the LDC method applied to the two-dimensional Poisson model problem of Section 2.1. We show the sharpness of the bound via numerical results. The discretization error bound is derived for the model composite grid $\Omega^{H,h}$ from Section 2.1. The bound is valid without restrictions on H, h and H/h. We note that, as far as we know, this is the first result for discretization error estimation on composite grids in which the grid sizes H and h are essentially independent.

Section 4.2 is of a preparatory nature. Some basic linear algebra concepts are introduced, such as monotone matrices, M-matrices and the Schur complement.

Parts of this chapter are also presented in [21].

4.1 INTRODUCTION

In Chapter 3 we have derived the systems of linear equations which are actually solved by the LDC method and the MLAT method (cf. (3.18) and (3.34), respectively). These systems of linear equations result from finite difference discretization of the boundary value problem (3.14) on the composite grid $\Omega^{H,h}$. At the grid points of $\Omega^{H,h}$ which do not lie on the interface Γ, *standard uniform finite differences* are used. A prolongation $p : \mathcal{F}(\Gamma^H) \to \mathcal{F}(\Gamma^h)$ is used for eliminating the values at the slave points (cf. the term $L_\Gamma^h pr_\Gamma$ in (3.18b) and in (3.34b)). In this chapter we consider only *piecewise linear interpolation* and *piecewise quadratic interpolation* on the interface. In the discretization method related to the LDC method, *standard uniform finite differences* are used at the interface grid points: the interface grid points are treated as if they were grid points of the uniform global coarse grid Ω^H. Note that this is possible since $\Gamma^H \subset \Omega^H \subset \Omega^{H,h}$. The difference stencils at the interface grid points in the discretization method related to MLAT depend on the restriction $\hat{r}_l : \mathcal{F}(\Omega_l^h) \to \mathcal{F}(\Omega_l^H)$ in (2.23). These difference stencils are combinations of standard uniform finite difference stencils and the restriction $\hat{r}_l$ (see Example 3.24).

Both in the discretization method related to LDC and in the discretization method related to MLAT, one makes use of the fact that interface grid points belong to the uniform coarse grid $\Omega^H \subset \Omega^{H,h}$. Alternatively one can consider the composite grid as a truly non-uniform grid. Then *non-uniform finite differences* are used at the interface grid points.

In Section 4.3 we consider the three finite difference discretization methods mentioned above for the one-dimensional Poisson problem. We show some interesting properties of the finite difference operators and we derive sharp bounds for the global discretization errors. The one-dimensional case is of interest for several reasons. The analysis of finite difference discretization methods on composite grids is much more transparent for the one-dimensional case than for the two-dimensional case and the essential results can be generalized to the more interesting two-dimensional case, which is considered in Section 4.4. Even for the one-dimensional Poisson problem, the discretization error bound for the discretization approach related to MLAT with $\hat{r}_l$ not equal to the trivial injection, is significantly worse than the discretization error bound for the discretization approach related to the LDC method.

In the previous chapters we mainly used grid functions and operators in our notation. In this chapter it is more convenient to use the matrix-vector notation. We recall from Definition 2.5 that for a given ordering of the points in the grid V the vector representation of a grid function $v \in \mathcal{F}(V)$ is denoted by **v**. In a similar way, for given orderings of the points in the grids V and W, a linear mapping $L : \mathcal{F}(V) \to \mathcal{F}(W)$ can be represented by a *matrix* $\mathbf{L} \in I\!\!R^{m \times n}$, with m, n the number of grid points in W, V respectively.

4.2 SOME BASIC NOTIONS

In this chapter we frequently use the notion of M-matrices. We recall some standard definitions and properties here (see e.g. [23, Chapter 5], [32, Section 4.3]).

Let $\mathbf{A}$ be a matrix with index set I. The elements of the matrix are denoted by $a_{ij}, i, j \in I$.

We write

$$\mathbf{A} \geq \mathbf{B} \quad \text{if } a_{ij} \geq b_{ij} \quad \text{for all } i, j \in I,$$

and define analogously $\mathbf{A} \leq \mathbf{B}$, $\mathbf{A} > \mathbf{B}$, $\mathbf{A} < \mathbf{B}$.

Definition 4.1 The matrix $\mathbf{A}$ is called *monotone* if $\mathbf{A}$ is nonsingular and $\mathbf{A}^{-1} \geq 0$.

The index $i \in I$ is said to be *directly connected* with $j \in I$ if $a_{ij} \neq 0$. We say that $i \in I$ is *connected* with $j \in I$ if there exists a chain of direct connections

$$i = i_0, i_1, i_2, \ldots, i_l = j \text{ with } a_{i_{k-1} i_k} \neq 0 \quad (1 \leq k \leq l).$$

Definition 4.2 The matrix $\mathbf{A}$ is called *irreducible* if every $i \in I$ is connected with every $j \in I$.

Definition 4.3 The matrix $\mathbf{A}$ is called *diagonally dominant* if

$$\sum_{j \neq i} |a_{ij}| \; < \; |a_{ii}| \quad \text{for all } i \in I.$$

Definition 4.4 The matrix $\mathbf{A}$ is called *irreducibly diagonally dominant* if $\mathbf{A}$ is irreducible and

$$\sum_{j \neq i} |a_{ij}| \; \leq \; |a_{ii}| \quad \text{for all } i \in I,$$

with strict inequality for at least one $i \in I$.

Definition 4.5 The matrix $\mathbf{A}$ is called an *M-matrix* if

$$a_{ii} > 0 \;\; \text{for all } i \in I, \;\; a_{ij} \leq 0 \;\; \text{for all } i \neq j, \tag{4.1a}$$

$$\mathbf{A} \text{ nonsingular and } \mathbf{A}^{-1} \geq 0. \tag{4.1b}$$

Lemma 4.6 *Assume that $\mathbf{A}$ satisfies (4.1a) and that one of the following properties holds:*

i) $\mathbf{A}$ *is diagonally dominant.*
ii) $\mathbf{A}$ *is irreducibly diagonally dominant.*

Then $\mathbf{A}$ is an M-matrix.

Proof. Criterion 4.3.10 in [32].   ∎

Lemma 4.7 *Assume that $\mathbf{A}$ satisfies $a_{ij} \leq 0$ for all $i \neq j$ and that there exists a vector $\mathbf{v} \geq 0$ with $\mathbf{Av} > 0$. Then $\mathbf{A}$ is an M-matrix.*

Proof. Theorem 5.1 in [23].   ∎

In Section 4.4 we use the notion of the *Schur complement*. We recall some standard definitions and properties here (see e.g. [23, Chapter 1]).

Let $\mathbf{A}$ be partitioned as

$$\mathbf{A} = \left[\begin{array}{cc} \mathbf{A}_{11} & \mathbf{A}_{12} \\ \mathbf{A}_{21} & \mathbf{A}_{22} \end{array} \right] \tag{4.2}$$

with $\mathbf{A}_{11}$ nonsingular.

Definition 4.8 The *Schur complement* $\mathbf{S}$ (of the block $\mathbf{A}_{11}$ in $\mathbf{A}$) is defined by

$$\mathbf{S} := \mathbf{A}_{22} - \mathbf{A}_{21}\mathbf{A}_{11}^{-1}\mathbf{A}_{12}.$$

Lemma 4.9 *Let* $\mathbf{A}$ *in (4.2) be square. Then* $\mathbf{A}$ *is nonsingular if and only if the Schur complement* $\mathbf{S}$ *is nonsingular. In this case*

$$\mathbf{S}^{-1} = \left[\begin{array}{cc} \mathbf{0} & \mathbf{I} \end{array} \right] \mathbf{A}^{-1} \left[\begin{array}{c} \mathbf{0} \\ \mathbf{I} \end{array} \right]$$

holds.

Proof. Theorem 1.23 in [23]. ■

In Section 4.3 and Section 4.4 we consider systems of linear equations,

$$\mathbf{A}\mathbf{u} = \mathbf{f}, \tag{4.3}$$

resulting from finite difference discretization of a boundary value problem on a composite grid $\Omega^{H,h}$. Here and in the remainder of this chapter the super scripts ^{H,h} are omitted if this does not lead to confusion.

By $\mathbf{u}^\star$ we denote the vector representation of $u^\star|_{\Omega^{H,h}}$, where $u^\star$ is the continuous solution of the boundary value problem. The *local discretization error vector* $\mathbf{d}$ is defined by

$$\mathbf{d} := \mathbf{f} - \mathbf{A}\mathbf{u}^\star.$$

If $\mathbf{A}$ is nonsingular, then the *global discretization error vector* $\mathbf{u} - \mathbf{u}^\star$ satisfies

$$\mathbf{u} - \mathbf{u}^\star = \mathbf{A}^{-1}\mathbf{d}.$$

Let $\mathbf{e_x}$ be the composite grid basis vector related to the grid point $\mathbf{x} \in \Omega^{H,h}$, i.e.

$$\mathbf{e_x}(\mathbf{y}) := \left\{ \begin{array}{ll} 1 & \mathbf{y} = \mathbf{x} \\ 0 & \mathbf{y} \neq \mathbf{x} \end{array} \right. .$$

If $\mathbf{A}$ is nonsingular, then $\mathbf{A}^{-1}\mathbf{e_x}$ is called the *discrete Green's function* corresponding to the grid point $\mathbf{x}$.

4.3 ONE-DIMENSIONAL MODEL PROBLEM

The analysis of finite difference approaches for the discretization of linear elliptic boundary value problems on composite grids is rather technical in the two-dimensional case. For the one-dimensional case the analysis is much more transparent. Moreover, the results obtained for the one-dimensional case can be generalized to the two-dimensional case. Therefore first we consider the Poisson problem:

$$-u_{xx}(x) = f(x), \quad 0 < x < 1,$$
$$u(0) = u(1) = 0. \tag{4.4}$$

We define the one-dimensional composite grid $\Omega^{H,h}$ by

$$\Omega^{H,h} := \Omega_l^h \cup \Omega_c^H,$$
$$\Omega_l^h := \{ih \mid 1 \le i \le n\}, \quad \text{with } n := \gamma/h - 1,$$
$$\Omega_c^H := \{\gamma + iH \mid 0 \le i \le m - 1\}, \quad \text{with } m := (1 - \gamma)/H.$$

We assume that $\gamma/H \in I\!N$ and $H/h \in I\!N$. The composite grid is locally non-uniform at the interface grid point γ (see Figure 4.1). We define $\sigma := H/h$. We are particularly interested in values $\sigma \gg 1$. We use the *lexicographical ordering* of the grid points in $\Omega^{H,h}$.

We use the standard central difference approximations

$$-u_{xx}(x) \doteq h^{-2}[-u(x-h) + 2u(x) - u(x+h)], \qquad \text{at } x \in \Omega_l^h, \tag{4.5a}$$
$$-u_{xx}(x) \doteq H^{-2}[-u(x-H) + 2u(x) - u(x+H)], \qquad \text{at } x \in \Omega_c^H \backslash \{\gamma\}. \tag{4.5b}$$

For the approximation of $-u_{xx}$ at the interface grid point γ we introduce the following three approaches:

$$(Lu)(\gamma) := H^{-2}[-u(\gamma - H) + 2u(\gamma) - u(\gamma + H)], \tag{4.6a}$$

$$(\hat{L}u)(\gamma) := H^{-2}[-\{\frac{1}{\sigma}u(\gamma - H) + \sum_{i=1}^{\sigma-1} \frac{\sigma - i}{\sigma^2}(u(\gamma - H - ih) + u(\gamma - H + ih))\}$$
$$+ 2u(\gamma) - u(\gamma + H)], \tag{4.6b}$$

$$(\tilde{L}u)(\gamma) := H^{-2}[-\frac{2\sigma^2}{\sigma + 1}u(\gamma - h) + 2\sigma u(\gamma) - \frac{2\sigma}{\sigma + 1}u(\gamma + H)]. \tag{4.6c}$$

The system of linear equations resulting from the finite difference approach (4.5), (4.6a) is denoted by $\mathbf{Lu} = \mathbf{f}$. The right hand side of the differential equation in (4.4) is discretized as usual, i.e. $\mathbf{f}(x) := f(x)$ for all $x \in \Omega^{H,h}$. In this approach the interface grid point γ is treated as a uniform coarse grid point. We note that this approach is related to the LDC method (see Section 3.2). The system of linear equations resulting from the finite difference approach (4.5), (4.6b) is denoted
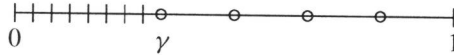

Figure 4.1 One-dimensional composite grid $\Omega^{H,h}$, $H = 1/6$, $h = 1/24$.

by $\hat{\mathbf{L}}\hat{\mathbf{u}} = \mathbf{f}$. This approach is related to the MLAT method (see Section 3.3), with the restriction operator $\hat{r}_l : \mathcal{F}(\Omega_l^h) \to \mathcal{F}(\Omega_l^H)$ defined by

$$(\hat{r}_l w)(x) := \frac{1}{\sigma} w(x) + \sum_{i=1}^{\sigma-1} \frac{\sigma - i}{\sigma^2}(w(x - ih) + w(x + ih)), \quad x \in \Omega_l^H, \quad w \in \mathcal{F}(\Omega_l^h). \quad (4.7)$$

Here we use the notation $\Omega_l^H := \{iH \mid 1 \leq i \leq N\}$, with $N := \gamma/H - 1$.

Remark 4.10 The restriction operator $\hat{r}_l$ is a *weighted restriction operator*. This restriction operator is closely related to the *piecewise linear interpolation operator*. If the piecewise linear interpolation operator $\Omega_l^H \to \Omega_l^h$ is denoted by $\hat{p}_l$, then we have $\hat{r}_l^\star = \hat{p}_l$, where $\hat{r}_l^\star$ is the adjoint with respect to the scalar products

$$(v, w)_H = H \sum_{x \in \Omega_l^H} v(x)w(x), \quad v, w \in \mathcal{F}(\Omega_l^H),$$

$$(v, w)_h = h \sum_{x \in \Omega_l^h} v(x)w(x), \quad v, w \in \mathcal{F}(\Omega_l^h).$$

In a multigrid setting (like in MLAT) the piecewise linear interpolation operator $\hat{p}_l$ and the weighted restriction operator $\hat{r}_l$ are often used.   □

The system of linear equations resulting from the finite difference approach (4.5), (4.6c) is denoted by $\tilde{\mathbf{L}}\tilde{\mathbf{u}} = \mathbf{f}$. In this approach a non-uniform finite difference scheme using nearest neighbouring grid points is applied at the interface grid point γ.

Remark 4.11 The matrix $\tilde{\mathbf{L}}$ has band width 3. The matrices $\mathbf{L}$ and $\hat{\mathbf{L}}$ have band width $\sigma + 2$. So for $\sigma \gg 1$ the band width of $\tilde{\mathbf{L}}$ is much smaller than the band width of $\mathbf{L}$ and $\hat{\mathbf{L}}$.   □

The three discretization approaches differ only at the interface grid point γ (cf. (4.6)). Hence the *local discretization error vectors* $\mathbf{d}$, $\hat{\mathbf{d}}$ and $\tilde{\mathbf{d}}$, differ only in the component corresponding to the grid point γ. For $u^\star \in C^4([0, 1])$ we obtain:

$$\mathbf{d}(\gamma) = -\frac{1}{12}H^2 u^{\star(4)}(\xi), \quad \xi \in (\gamma - H, \gamma + H), \quad (4.8a)$$

$$\hat{\mathbf{d}}(\gamma) = -\frac{1}{12}H^2 u^{\star(4)}(\xi) - \frac{1}{12}\frac{\sigma^2 - 1}{\sigma^2}u^{\star(2)}(\gamma - H) + \mathcal{O}(Hh), \quad \xi \in (\gamma - H, \gamma + H), (4.8b)$$

$$\tilde{\mathbf{d}}(\gamma) = \frac{1}{3(\sigma + 1)}H(\frac{1}{\sigma}u^{\star(3)}(\xi) - \sigma u^{\star(3)}(\eta)), \quad \xi \in (\gamma - h, \gamma), \quad \eta \in (\gamma, \gamma + H). \quad (4.8c)$$

The results are obtained using suitable Taylor expansions. The constant in the $\mathcal{O}(.)$ term on the right hand side of (4.8b) is independent of σ. The finite difference approximation in (4.6a) is second-order accurate in the coarse grid size H. The approximation in (4.6c) is first-order accurate in H for $\sigma > 1$. From (4.8b) we have that, for σ fixed, $\lim_{H\downarrow 0} \hat{\mathbf{d}}(\gamma) = -\frac{1}{12}\frac{\sigma^2-1}{\sigma^2}u^{\star(2)}(\gamma)$. So the finite difference approximation in (4.8b) is *not consistent* for $\sigma > 1$.

In the following we show some interesting properties of the discrete Green's functions related to the grid points γ and $\gamma - h$. As we have seen in (4.8) the components of the local discretization error vectors differ at the interface grid point γ. For two-dimensional problems, interpolation at the interface is required. As we shall see in Section 4.4 relatively large components of the local discretization error vector occur at certain fine grid points at a distance h of the interface. Below we show that the various discretizations for the one-dimensional case result in significantly different discrete Green's functions related to the grid point $\gamma - h$.

First we consider the discretization $\mathbf{L}\mathbf{u} = \mathbf{f}$.

Theorem 4.12 *The finite difference matrix* $\mathbf{L}$ *satisfies:*

    i) $\mathbf{L}$ *is monotone and* $\|\mathbf{L}^{-1}\|_\infty \leq 1/8$,

    ii) $\|\mathbf{L}^{-1}\mathbf{e}_\gamma\|_\infty = \gamma(1 - \gamma)H$,

    iii) $\|\mathbf{L}^{-1}\mathbf{e}_{\gamma-h}\|_\infty = (\gamma - h)(1 - \gamma + H)\frac{h^2}{H}$.

Proof. *i)* It follows easily from Lemma 4.6.*ii* that $\mathbf{L}$ is an M-matrix. Let $\mathbf{g}$ be the composite grid vector related to the function $g(x) := x(1 - x)/2$. It is easy to see that

$$\mathbf{L}\mathbf{g} = (1, 1, \ldots, 1)^T.$$

Then we obtain

$$\|\mathbf{L}^{-1}\|_\infty = \|\mathbf{L}^{-1}(1, 1, \ldots, 1)^T\|_\infty \leq \max_{0<x<1} x(1 - x)/2 = 1/8.$$

ii) We introduce the function $\tilde{g}$, which is continuous on $[0, 1]$, linear on the intervals $(0, \gamma - h)$, $(\gamma - h, \gamma)$, $(\gamma, 1)$ and has values

$$\tilde{g}(0) = \tilde{g}(1) = 0,$$
$$\tilde{g}(\gamma - h) = (\gamma - h)(1 - \gamma)H,$$
$$\tilde{g}(\gamma) = \gamma(1 - \gamma)H.$$

A simple computation yields that

$$\mathbf{L}\tilde{\mathbf{g}} = \mathbf{e}_\gamma,$$

with $\tilde{\mathbf{g}}$ the composite grid vector related to the function $\tilde{g}$. Now the result follows using that $\tilde{g}$ is positive and attains its maximum value at γ.

iii) Similar as for *ii)*, but with the function $\tilde{g}$ satisfying

$$\tilde{g}(0) = \tilde{g}(1) = 0,$$
$$\tilde{g}(\gamma - h) = (\gamma - h)(1 - \gamma + H)\frac{h^2}{H},$$
$$\tilde{g}(\gamma) = (\gamma - H)(1 - \gamma)\frac{h^2}{H}.$$

                                                                 ■

We see that for H fixed the norm of the discrete Green's function related to $\gamma - h$ decreases proportional to h^2 for $h \downarrow 0$. This behaviour is similar to the case of a discrete Green's function corresponding to a *grid point next to the boundary* in a global uniform grid with grid size h. The

situation is very different for the discrete Green's function related to the interface point γ. For this Green's function we have a damping proportional to H, i.e. similar to the case of a discrete Green's function corresponding to an *interior point* of a global uniform grid with grid size H.

For the discretization $\hat{\mathbf{L}}\hat{\mathbf{u}} = \mathbf{f}$ the results are the same as in Theorem 4.12.

Theorem 4.13 *The finite difference matrix* $\hat{\mathbf{L}}$ *satisfies:*

    i) $\hat{\mathbf{L}}$ *is monotone and* $\|\hat{\mathbf{L}}^{-1}\|_\infty \leq 1/8$,

    ii) $\|\hat{\mathbf{L}}^{-1}\mathbf{e}_\gamma\|_\infty = \gamma(1-\gamma)H$,

    iii) $\|\hat{\mathbf{L}}^{-1}\mathbf{e}_{\gamma-h}\|_\infty = (\gamma-h)(1-\gamma+H)\frac{h^2}{H}$.

Proof. *i)* It follows easily from Lemma 4.6.*ii* that $\hat{\mathbf{L}}$ is an M-matrix. For $\mathbf{g}$ the composite grid vector related to $g(x) := x(1-x)/2$ we obtain

$$\hat{\mathbf{L}}\mathbf{g} = (1, 1, \ldots, 1)^T + \frac{\sigma^2-1}{12\sigma^2}\mathbf{e}_\gamma.$$

Since $\hat{\mathbf{L}}^{-1} \geq 0$ and $\frac{\sigma^2-1}{12\sigma^2} \geq 0$ we obtain

$$\|\hat{\mathbf{L}}^{-1}\|_\infty = \|\hat{\mathbf{L}}^{-1}(1, 1, \ldots, 1)^T\|_\infty \leq \max_{0<x<1} x(1-x)/2 = 1/8.$$

ii), *iii)* Similar to the proof of Theorem 4.12. ∎

For the discretization $\tilde{\mathbf{L}}\tilde{\mathbf{u}} = \mathbf{f}$ the norm of the discrete Green's function related to $\gamma - h$ behaves differently.

Theorem 4.14 *The finite difference matrix* $\tilde{\mathbf{L}}$ *satisfies:*

    i) $\tilde{\mathbf{L}}$ *is monotone and* $\|\tilde{\mathbf{L}}^{-1}\|_\infty \leq 1/8$,

    ii) $\|\tilde{\mathbf{L}}^{-1}\mathbf{e}_\gamma\|_\infty = \frac{\sigma+1}{2\sigma}\gamma(1-\gamma)H$,

    iii) $\|\tilde{\mathbf{L}}^{-1}\mathbf{e}_{\gamma-h}\|_\infty = (\gamma-h)(1-\gamma+h)h$.

Proof. Similar to the proof of Theorem 4.12. In the proof of *ii)* and *iii)* the values of the function $\tilde{g}$ at $\gamma - h$ and γ are given by

$$\tilde{g}(\gamma-h) = (\gamma-h)(1-\gamma+h)h \qquad \tilde{g}(\gamma-h) = \frac{\sigma+1}{2\sigma}(1-\gamma)(\gamma-h)H$$
$$\text{and}$$
$$\tilde{g}(\gamma) = (\gamma-h)(1-\gamma)h \qquad \tilde{g}(\gamma) = \frac{\sigma+1}{2\sigma}\gamma(1-\gamma)H$$

respectively. ∎

The result for the discrete Green's function related to γ is very similar to the result in Theorem 4.12. There is a significant difference between the results for the discrete Green's functions related to $\gamma - h$ in Theorem 4.14 and Theorem 4.12. For H fixed we have a discrete Green's function of size $\mathcal{O}(h^2)$ for $\mathbf{L}$ (and $\hat{\mathbf{L}}$), whereas we have a discrete Green's function of size $\mathcal{O}(h)$ for $\tilde{\mathbf{L}}$. In Section 4.4 we shall see that similar results hold for the two-dimensional case.

Using standard techniques and the results in (4.8), Theorem 4.12, Theorem 4.13 and Theorem 4.14 we can derive *sharp bounds for the global discretization errors*:

$$\|\mathbf{u} - \mathbf{u}^\star\|_\infty \le C_1 h^2 + C_2 H^2 + C_3 H^3, \tag{4.9a}$$

$$\|\hat{\mathbf{u}} - \mathbf{u}^\star\|_\infty \le C_1 h^2 + C_2 H^2 + C_3 H^3 + \hat{C}_3 H + \bar{C}_3 H^2 h, \tag{4.9b}$$

$$\|\tilde{\mathbf{u}} - \mathbf{u}^\star\|_\infty \le C_1 h^2 + C_2 H^2 + \tilde{C}_3 H^2. \tag{4.9c}$$

The constants C_1 and C_2 depend on $\max\{|u^{\star(4)}(x)| \mid x \in (0, \gamma)\}$ and $\max\{|u^{\star(4)}(x)| \mid x \in (\gamma, 1)\}$ respectively. The constant C_3 depends on $\max\{|u^{\star(4)}(x)| \mid x \in (\gamma - H, \gamma + H)\}$, $\hat{C}_3$ depends on $|u^{\star(2)}(\gamma - H)|$, $\bar{C}_3$ depends on $\max\{|u^{\star(4)}(x)| \mid x \in (\gamma - 2H, \gamma)\}$, and $\tilde{C}_3$ depends on $\max\{|u^{\star(3)}(x)| \mid x \in (\gamma - h, \gamma + H)\}$.

The bound for the global discretization error in (4.9b) contains two additional terms compared to the bound in (4.9a). One of these terms is an $\mathcal{O}(H)$ term. So the discretization approach in (4.6b) is less favourable than the discretization approach in (4.6a).

Remark 4.15 We recall that the discretization approach in (4.6b) is related to the MLAT method with the weighted restriction operator $\hat{r}_l$ from (4.7). If in the MLAT method the trivial injection is used for $\hat{r}_l$, then the discrete problem resulting from MLAT is the same as the discrete problem resulting from the LDC method (cf. Corollary 3.18). Then the discretization error estimate (4.9a) holds for the discrete problem resulting from the MLAT method. Hence from a discretization point of view, one should use the *trivial injection* for $\hat{r}_l$ in MLAT. □

The difference between $\mathbf{L}$ and $\tilde{\mathbf{L}}$ as discussed below Theorem 4.14 has only little influence on the global discretization error. This is due to the fact that in the one-dimensional case no interpolation on the interface is required. Hence the local discretization error at $\gamma - h$ is $\mathcal{O}(h^2)$. In the two-dimensional case interpolation on the interface is required and relatively large components of the local discretization error occur at certain fine grid points at a distance h of the interface. Then a difference between the discrete Green's functions related to these grid points for $\mathbf{L}$ and $\tilde{\mathbf{L}}$ results in a significant difference between the global discretization errors (see Example 4.25 and Example 4.27).

Remark 4.16 Results similar to those in Theorem 4.12, Theorem 4.13 and Theorem 4.14 can be obtained if a composite grid with two interface grid points or a composite grid with two or more disjoint regions of local refinement is considered. □

4.4   THE TWO-DIMENSIONAL CASE

In Section 4.3 we have considered three approaches for the discretization of a one-dimensional Poisson problem on a composite grid. We have seen that the discretization approach which is related to the LDC method has some favourable properties. The difference stencils which are used in this method are all very simple since the interface grid points are treated as if they were grid points of the uniform coarse grid (cf. (4.6a)). The local discretization error at the interface grid points is $\mathcal{O}(H^2)$ (cf. (4.8a)) and possibly large (local discretization) error components related
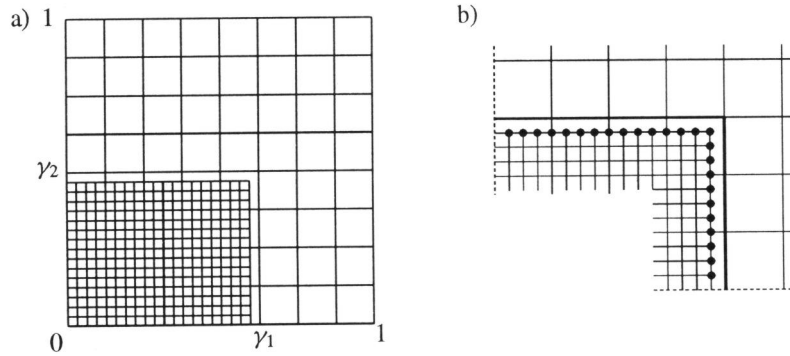
Figure 4.2   a) Composite grid $\Omega^{H,h}$, $H = 1/8$, $h = 1/32$. b) The interface Γ and grid points of $\tilde{\Gamma}^h$ ($\bullet$).

to fine grid points near the interface are damped strongly by the inverse matrix $\mathbf{L}^{-1}$ (cf. Theorem 4.12.*iii*).

In this section we analyse the finite difference discretization approach which is related to the LDC method for two-dimensional elliptic boundary value problems. We shall derive a sharp bound for the global discretization error for a model problem and discuss some generalizations. In this section we consider the model composite grid $\Omega^{H,h}$ from Section 2.1. We are particularly interested in estimates expressing the dependence of the discretization error on both the coarse grid size H and the fine grid size h.

4.4.1   Model Problem

We consider the two-dimensional Poisson problem on the unit square,

$$-\Delta u = f \qquad \text{in } \Omega := (0, 1) \times (0, 1), \tag{4.10a}$$

$$u = 0 \qquad \text{on } \partial\Omega, \tag{4.10b}$$

and the model composite grid $\Omega^{H,h}$ from Section 2.1. This composite grid is composed of a uniform grid with grid size H covering Ω and a uniform grid with grid size h covering the subregion $\Omega_l = (0, \gamma_1) \times (0, \gamma_2)$. We only consider coarse grid sizes H such that $1/H \in I\!N$, $\gamma_1/H \in I\!N$, $\gamma_2/H \in I\!N$ and fine grid sizes h such that $h = H/\sigma$, $\sigma \in I\!N$. We recall the composite grid notation from Section 2.1 and Section 3.1, and we introduce some more notation to be used in Subsection 4.4.2:

$$\hat{\Omega}^H = \{(x, y) \in I\!R^2 \mid x/H \in I\!N,\ y/H \in I\!N\},\ \Omega^H := \hat{\Omega}^H \cap \Omega,$$

$$\hat{\Omega}^h = \{(x, y) \in I\!R^2 \mid x/h \in I\!N,\ y/h \in I\!N\},\ \Omega^h := \hat{\Omega}^h \cap \Omega,$$

$$\Omega_l^h := \hat{\Omega}^h \cap \Omega_l,\ \Omega^{H,h} := \Omega^H \cup \Omega_l^h,$$

$$\Omega_c^H = \hat{\Omega}^H \cap (\Omega \backslash \Omega_l),$$

$$\Gamma := \partial\Omega_l \backslash \partial\Omega,$$

$$\Gamma^H := \Omega^H \cap \Gamma, \ \Gamma^h := \Omega^h \cap \Gamma,$$

$$\Gamma_{ver} = \{(x, y) \in I\!R^2 \mid x = \gamma_1, 0 < y \leq \gamma_2\},$$

$$\Gamma_{hor} = \{(x, y) \in I\!R^2 \mid y = \gamma_2, 0 < x \leq \gamma_1\},$$

$$\Gamma_{ver}^H := \Omega^H \cap \Gamma_{ver}, \ \Gamma_{ver}^h := \Omega^h \cap \Gamma_{ver},$$

$$\Gamma_{hor}^H := \Omega^{H} \cap \Gamma_{hor}, \ \Gamma_{hor}^h := \Omega^h \cap \Gamma_{hor},$$

$$\tilde{\Gamma}^h := \{\mathbf{x} \in \Omega_l^h \mid \min_{\mathbf{y} \in \Gamma} \|\mathbf{x} - \mathbf{y}\|_2 = h\}.$$

At grid points $\mathbf{x} \in \Omega_c^H$ and $\mathbf{x} \in \Omega_l^h \setminus \tilde{\Gamma}^h$ we use the five-point formula for the Laplace operator:

$$-\Delta u(\mathbf{x}) \doteq H^{-2}(4u(\mathbf{x}) - u(\mathbf{x} + (H, 0)) - u(\mathbf{x} - (H, 0))$$
$$- u(\mathbf{x} + (0, H)) - u(\mathbf{x} - (0, H))) \tag{4.11a}$$

and

$$-\Delta u(\mathbf{x}) \doteq h^{-2}(4u(\mathbf{x}) - u(\mathbf{x} + (h, 0)) - u(\mathbf{x} - (h, 0))$$
$$- u(\mathbf{x} + (0, h)) - u(\mathbf{x} - (0, h))), \tag{4.11b}$$

respectively. So the *interface grid points are treated as if they were grid points of the uniform coarse grid* Ω^H. At grid points $\mathbf{x} \in \tilde{\Gamma}^h$ we use the following discretization. We assume a given interpolation operator $p : \mathcal{F}(\Gamma^H) \to \mathcal{F}(\Gamma^h)$. Now at $\mathbf{x}$ we discretize by applying the five-point formula from (4.11b); values corresponding to *slave points* $\mathbf{y} \in \Gamma^h \setminus \Gamma^H$ are eliminated using p. Obvious modifications are used at grid points close to the boundary $\partial\Omega$.

The discretization above is fully determined if p is given. We consider both a *piecewise linear interpolation* and a *piecewise quadratic interpolation*. The piecewise linear interpolation is denoted by $p^{(1)}$. The piecewise quadratic interpolation is denoted by $p^{(2)}$. In the remainder the notation p refers to both $p^{(1)}$ and $p^{(2)}$. If $w \in \mathcal{F}(\Gamma^H)$ is given, then at $\mathbf{y} \in \Gamma^h \setminus \Gamma^H$ we use an interpolated value $(pw)(\mathbf{y})$ as shown in Figure 4.3. If $\mathbf{x}$ has distance H to the boundary $\partial\Omega$, then we use the Dirichlet boundary values in the interpolation. For example, for $\mathbf{y} = (ih, \gamma_2), 0 < i < \sigma$, the linear interpolation is defined by

$$(p^{(1)}w)(\mathbf{y}) = (1 - \frac{i}{\sigma})u((0, \gamma_2)) + \frac{i}{\sigma}w((H, \gamma_2)) = \frac{i}{\sigma}w((H, \gamma_2)),$$

since we consider homogeneous Dirichlet boundary conditions.

We note that in case of *quadratic interpolation* there is some freedom: one may apply a shift of the interpolation points by a factor H (in Figure 4.3: use $\mathbf{x} - (2H, 0)$, $\mathbf{x} - (H, 0)$, $\mathbf{x}$ as interpolation points). To avoid technical complications in the proofs of Lemma 4.17 and Theorem 4.18, we assume that in case of quadratic interpolation on the line segment $[(H, \gamma_2), (2H, \gamma_2)]$, the points $(H, \gamma_2), (2H, \gamma_2), (3H, \gamma_2)$ are used. In case of quadratic interpolation on the line segment $[(\gamma_1, H), (\gamma_1, 2H)]$ we assume that the points $(\gamma_1, H), (\gamma_1, 2H), (\gamma_1, 3H)$ are used. Then

$\mathbf{x} \in \Gamma_{hor}^H, \; \mathbf{y} \in \Gamma_{hor}^h \setminus \Gamma_{hor}^H$

$\circ : \; w$ values

$- \cdot - - : p^{(1)}w$

$\underline{\qquad} : p^{(2)}w$

$\mathbf{x} - (H, 0) \quad \mathbf{y} \quad \mathbf{x} \qquad \mathbf{x} + (H, 0)$
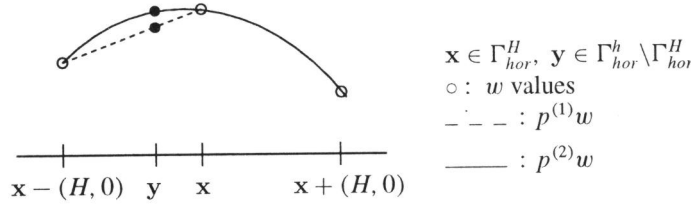
Figure 4.3 Piecewise linear and piecewise quadratic interpolation on the interface.

both for piecewise linear and piecewise quadratic interpolation we have $(pv_{|\Gamma^H})(\mathbf{x}) \leq v(\mathbf{x})$ for $\mathbf{x} \in \Gamma^h$, if v is a positive constant function.

The system of linear equations resulting from the finite difference approach described above is denoted by

$$\mathbf{L}\mathbf{u} = \mathbf{f}, \tag{4.12}$$

for some given ordering of the grid points of $\Omega^{H,h}$. The right hand side of the differential equation in (4.10) is discretized as usual, i.e. $\mathbf{f}(\mathbf{x}) := f(\mathbf{x})$ for all $\mathbf{x} \in \Omega^{H,h}$.

4.4.2 Global Discretization Error Bound

In this subsection we use block partitioning corresponding to $\mathcal{F}(\Omega^{H,h}) = \mathcal{F}(\Omega_l^h) \oplus \mathcal{F}(\Omega_c^H)$. First the grid points of Ω_l^h are ordered and then the grid points of Ω_c^H. For the composite grid matrix in (4.12) we write

$$\mathbf{L} = \begin{bmatrix} \mathbf{L}_{11} & -\mathbf{L}_{12}pr_\Gamma \\ -\mathbf{L}_{21} & \mathbf{L}_{22} \end{bmatrix}. \tag{4.13}$$

The matrix $\mathbf{L}_{11}$ results from standard central difference discretization of the boundary value problem

$$-\Delta u = f \quad \text{in } \Omega_l := (0, \gamma_1) \times (0, \gamma_2),$$
$$u = 0 \quad \text{on } \partial\Omega_l,$$

on the uniform grid Ω_l^h. Hence $\mathbf{L}_{11}$ is an M-matrix. The operator $p : \mathcal{F}(\Gamma^H) \to \mathcal{F}(\Gamma^h)$ is defined by piecewise linear ($p^{(1)}$) or piecewise quadratic ($p^{(2)}$) interpolation and r_Γ is the trivial injection from (3.17b). For ease of notation, the matrix corresponding to the operator $pr_\Gamma : \mathcal{F}(\Omega_c^H) \to \mathcal{F}(\Gamma^h)$ is denoted by pr_Γ too. The matrix $[\mathbf{L}_{11} \; -\mathbf{L}_{12}]$ corresponds to the standard five-point stencil for the Laplace operator on the local fine grid Ω_l^h and $[-\mathbf{L}_{21} \; \mathbf{L}_{22}]$ corresponds to the standard five-point stencil for the Laplace operator on the coarse grid Ω_c^H.

For a grid $V \subset \Omega^{H,h}$ we denote by $\mathbb{1}_V$ the composite grid vector with the components related to the grid points of V equal to 1 and the other components equal to 0. In this section both the grid function representation and the vector representation of discrete approximations is used. Vectors are printed in bold. In the proofs in this subsection we use the difference star notation (cf. e.g. [32]).

In the analysis in this subsection we use three main arguments: a stability result (cf. Theorem 4.19), a strong damping of errors on $\tilde{\Gamma}^h$ (cf. Theorem 4.20) and local discretization error estimates (cf. (4.16)). First we show the existence of a *barrier function* for $\mathbf{L}$.

Lemma 4.17 *Let* $w : \mathbb{R}^2 \to \mathbb{R}$ *be given by* $w(x, y) := x(1 - x)/2$. *Let* $\mathbf{w}$ *be the vector representation of the grid function* $w_{|\Omega^{H,h}}$. *Both for linear and quadratic interpolation, the matrix* $\mathbf{L}$ *satisfies*

$$\mathbf{L}\mathbf{w} \geq \mathbb{I}_{\Omega^{H,h}}. \tag{4.14}$$

Proof. For $\mathbf{x} \in \Omega_c^H$ we obtain

$$(\mathbf{L}\mathbf{w})(\mathbf{x}) \geq H^{-2} \begin{bmatrix} & -1 & \\ -1 & 4 & -1 \\ & -1 & \end{bmatrix}_{\mathbf{x}} w = 1.$$

Similarly, for $\mathbf{x} \in \Omega_l^h \backslash \tilde{\Gamma}^h$ we obtain

$$(\mathbf{L}\mathbf{w})(\mathbf{x}) \geq h^{-2} \begin{bmatrix} & -1 & \\ -1 & 4 & -1 \\ & -1 & \end{bmatrix}_{\mathbf{x}} w = 1.$$

Finally, we consider $\mathbf{x} \in \tilde{\Gamma}^h$. We define the set of neighbouring grid points,
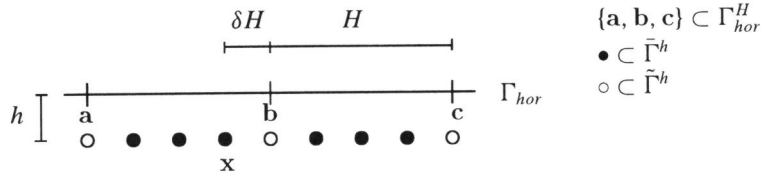
$$N_h(\mathbf{x}) := \{\mathbf{x} + (h, 0), \mathbf{x} - (h, 0), \mathbf{x} + (0, h), \mathbf{x} - (0, h)\}.$$

We introduce the grid function $\tilde{w} \in \mathcal{F}(\hat{\Omega}^h)$, given by

$$\tilde{w}(\mathbf{y}) := \begin{cases} (pw_{|\Gamma^H})(\mathbf{y}) & \text{if } \mathbf{y} \in \Gamma^h \backslash \Gamma^H \\ w(\mathbf{y}) & \text{otherwise} \end{cases}.$$

Note that both for piecewise linear and for piecewise quadratic interpolation we have $0 \leq \tilde{w}(\mathbf{y}) \leq w(\mathbf{y})$ for all $\mathbf{y} \in \hat{\Omega}^h \cap \bar{\Omega}$. Using this, we obtain for $\mathbf{x} \in \tilde{\Gamma}^h$

$$\begin{aligned}
(\mathbf{L}\mathbf{w})(\mathbf{x}) &\geq h^{-2} \begin{bmatrix} & -1 & \\ -1 & 4 & -1 \\ & -1 & \end{bmatrix}_{\mathbf{x}} \tilde{w} \\
&= h^{-2}(4\tilde{w}(\mathbf{x}) - \sum_{\mathbf{y} \in N_h(\mathbf{x})} \tilde{w}(\mathbf{y})) \\
&\geq h^{-2}(4w(\mathbf{x}) - \sum_{\mathbf{y} \in N_h(\mathbf{x})} w(\mathbf{y})) \\
&= h^{-2} \begin{bmatrix} & -1 & \\ -1 & 4 & -1 \\ & -1 & \end{bmatrix}_{\mathbf{x}} w = 1.
\end{aligned}$$

Figure 4.4   Example of $\mathbf{x} \in \bar{\Gamma}^h$.

This completes the proof.   ∎

In the following theorem we prove monotonicity of $\mathbf{L}$. For the case with piecewise linear interpolation it is easy to show that $\mathbf{L}$ is an M-matrix. The case with piecewise quadratic interpolation is rather involved. This is due to the fact that then $\mathbf{L}$ is *not* an M-matrix. We shall show that $\mathbf{L}$ can be written as the product of two M-matrices. The technique is based on ideas from [6],[42].

Theorem 4.18 *Both for piecewise linear and piecewise quadratic interpolation, the matrix* $\mathbf{L}$ *is monotone, i.e.* $\mathbf{L}$ *is nonsingular and* $\mathbf{L}^{-1} \geq 0$ *holds.*

Proof. First we consider the case with piecewise linear interpolation.
For every line segment $[\mathbf{x} - (H, 0), \mathbf{x}] =: l_{\mathbf{x}}$ on Γ_{hor} (cf. Figure 4.3) the linear interpolation $p^{(1)}$ of a grid function $u \in \mathcal{F}(\Gamma^H)$ on $l_{\mathbf{x}}$ results in

$$(p^{(1)}u)(\mathbf{y}) = \alpha_1(\mathbf{y})u(\mathbf{x} - (H, 0)) + (1 - \alpha_1(\mathbf{y}))u(\mathbf{x})$$

with $0 \leq \alpha_1(\mathbf{y}) \leq 1$ for $\mathbf{y} \in l_{\mathbf{x}} \cap \Gamma^h$.
A similar result holds on Γ_{ver}. Using this, it follows that $\mathbf{L}$ is an irreducibly diagonally dominant matrix with coefficients $(\mathbf{L})_{ii} > 0$ for all i and $(\mathbf{L})_{ij} \leq 0$ for $i \neq j$. By Lemma 4.6.*ii* we find that $\mathbf{L}$ is an M-matrix and thus $\mathbf{L}$ is monotone.
Next we consider the case with piecewise quadratic interpolation on the interface.
A special role is played by the difference stencils in which the quadratic interpolation is used. We introduce the set

$$\bar{\Gamma}^h := \{(x, y) \in \tilde{\Gamma}^h \mid (x + h, y) \notin \Gamma^H \wedge (x, y + h) \notin \Gamma^H\}.$$

As an example we take $\mathbf{x} \in \bar{\Gamma}^h$ as shown in Figure 4.4. The difference stencil at $\mathbf{x}$ is as follows:

$$[\mathbf{L}]_{\mathbf{x}}u = h^{-2}(4u(\mathbf{x}) - u(\mathbf{x} - (h, 0)) - u(\mathbf{x} + (h, 0)) - u(\mathbf{x} - (0, h))$$
$$- \alpha_3 u(\mathbf{a}) - \alpha_2 u(\mathbf{b}) - \alpha_1 u(\mathbf{c})), \qquad (*1)$$

with $\alpha_1 = \frac{1}{2}\delta(\delta - 1)$, $\alpha_2 = (1 - \delta)(1 + \delta)$, $\alpha_3 = \frac{1}{2}\delta(1 + \delta)$, $0 < \delta < 1$.
Note that $0 < \delta < 1$ implies $\alpha_1 < 0, 0 < \alpha_2 < 1, 0 < \alpha_3$. Also we have

$$\frac{-\alpha_1}{\alpha_2} = \frac{1}{2}\frac{\delta}{1 + \delta} \leq \frac{1}{4}. \qquad (*2)$$

We decompose $\mathbf{L}$ as $\mathbf{L} = \mathbf{D} + \mathbf{N} + \mathbf{P}$ such that:

$\mathbf{D}$ is a diagonal matrix and $diag(\mathbf{D}) = diag(\mathbf{L})$,

$diag(\mathbf{N}) = 0$ and the elements of N satisfy $(\mathbf{N})_{ij} \leq 0$ for all $i \neq j$,

$diag(\mathbf{P}) = 0$, and the elements of P satisfy $(\mathbf{P})_{ij} \geq 0$ for all $i \neq j$.

Now introduce $\mathbf{N}_1, \mathbf{N}_2$ with stencils $[\mathbf{N}_i]_{\mathbf{x}}$ $(i = 1, 2)$ defined as follows.
For $\mathbf{x} \notin (\Gamma^H \cup \bar{\Gamma}^h)$ we take $[\mathbf{N}_1]_{\mathbf{x}} := [\mathbf{N}]_{\mathbf{x}}$, $[\mathbf{N}_2]_{\mathbf{x}} := [\mathbf{0}]_{\mathbf{x}}$. Also at the corner point $\mathbf{x} = (\gamma_1, \gamma_2)$
we take $[\mathbf{N}_1]_{\mathbf{x}} := [\mathbf{N}]_{\mathbf{x}}$, $[\mathbf{N}_2]_{\mathbf{x}} := [\mathbf{0}]_{\mathbf{x}}$.
For $\mathbf{x} \in \Gamma^H_{hor} \backslash \{(\gamma_1, \gamma_2)\}$ we take

$$[\mathbf{N}_1]_{\mathbf{x}} := H^{-2} \begin{bmatrix} 0 & -1 & 0 \\ 0 & 0 & 0 \\ 0 & -1 & 0 \end{bmatrix}, \quad [\mathbf{N}_2]_{\mathbf{x}} := H^{-2} \begin{bmatrix} 0 & 0 & 0 \\ -1 & 0 & -1 \\ 0 & 0 & 0 \end{bmatrix}.$$

Similarly, for $\mathbf{x} \in \Gamma^H_{ver} \backslash \{(\gamma_1, \gamma_2)\}$ we take

$$[\mathbf{N}_1]_{\mathbf{x}} := H^{-2} \begin{bmatrix} 0 & 0 & 0 \\ -1 & 0 & -1 \\ 0 & 0 & 0 \end{bmatrix}, \quad [\mathbf{N}_2]_{\mathbf{x}} := H^{-2} \begin{bmatrix} 0 & -1 & 0 \\ 0 & 0 & 0 \\ 0 & -1 & 0 \end{bmatrix}.$$

Obvious modifications are used if $\mathbf{x}$ is close to the boundary $\partial\Omega$.
Finally we consider $\mathbf{x} \in \bar{\Gamma}^h$. As an example we take $\mathbf{x}$ as in Figure 4.4; then we define (cf. (∗1)):

$$[\mathbf{N}_1]_{\mathbf{x}} u := h^{-2}(-u(\mathbf{x} - (h, 0)) - u(\mathbf{x} + (h, 0)) - u(\mathbf{x} - (0, h)) - \alpha_2 u(\mathbf{b})),$$
$$[\mathbf{N}_2]_{\mathbf{x}} := [\mathbf{0}]_{\mathbf{x}}.$$

Note that $[\mathbf{N}_2]_{\mathbf{x}} \neq [\mathbf{0}]_{\mathbf{x}}$ only for $\mathbf{x} \in \Gamma^H \backslash \{(\gamma_1, \gamma_2)\}$. From the definitions of D and $\mathbf{N}_2$ it immediately follows that $(\mathbf{I} + \mathbf{D}^{-1}\mathbf{N}_2)$ is diagonally dominant and that $(\mathbf{I} + \mathbf{D}^{-1}\mathbf{N}_2)_{ij} \leq 0$ for all $i \neq j$. Thus $(\mathbf{I} + \mathbf{D}^{-1}\mathbf{N}_2)$ is an M-matrix (cf. Lemma 4.6.i).
It is easy to check that $(\mathbf{D} + \mathbf{N}_1)$ is an irreducibly diagonally dominant matrix (use $0 < \alpha_2 < 1$) with $(\mathbf{D} + \mathbf{N}_1)_{ii} > 0$ for all i and $(\mathbf{D} + \mathbf{N}_1)_{ij} \leq 0$ for all $i \neq j$. Thus $(\mathbf{D} + \mathbf{N}_1)$ is an M-matrix (cf. Lemma 4.6.ii).
From the definitions of $\mathbf{N}_1$ and $\mathbf{N}_2$ it follows that

$$\mathbf{N} \leq \mathbf{N}_1 + \mathbf{N}_2. \tag{∗3}$$

Next we consider the nonnegative matrix P. First note that $[\mathbf{P}]_{\mathbf{x}} \neq [\mathbf{0}]_{\mathbf{x}}$ only for points $\mathbf{x} \in \bar{\Gamma}^h$. Again, as a model situation, we take $\mathbf{x}$ as in Figure 4.4, in which case we have (cf. (∗1)):

$$[\mathbf{P}]_{\mathbf{x}} u = -h^{-2} \alpha_1 u(\mathbf{c}). \tag{∗4}$$

For this $\mathbf{x}$ we also have

$$[\mathbf{N}_1 \mathbf{D}^{-1} \mathbf{N}_2]_{\mathbf{x}} u = \frac{1}{4} h^{-2} \alpha_2 (u(\mathbf{a}) + u(\mathbf{c})). \tag{∗5}$$

Combination of the results in (∗2), (∗4), (∗5) and using $\mathbf{N}_1 \mathbf{D}^{-1} \mathbf{N}_2 \geq 0$ yields the inequality

$$\mathbf{P} \leq \mathbf{N}_1 \mathbf{D}^{-1} \mathbf{N}_2. \tag{∗6}$$

From (∗3), (∗6) we obtain:

$$\mathbf{L} = \mathbf{D} + \mathbf{N} + \mathbf{P} \leq \mathbf{D} + \mathbf{N}_1 + \mathbf{N}_2 + \mathbf{N}_1\mathbf{D}^{-1}\mathbf{N}_2 = (\mathbf{D} + \mathbf{N}_1)(\mathbf{I} + \mathbf{D}^{-1}\mathbf{N}_2).$$

Since both $\mathbf{D} + \mathbf{N}_1$ and $\mathbf{I} + \mathbf{D}^{-1}\mathbf{N}_2$ are M-matrices we conclude that for all $i \neq j$:

$$((\mathbf{D} + \mathbf{N}_1)^{-1}\mathbf{L})_{ij} \leq (\mathbf{I} + \mathbf{D}^{-1}\mathbf{N}_2)_{ij} \leq 0.$$

By Lemma 4.17 we have that a vector $\mathbf{v} > 0$ exists such that $\mathbf{L}\mathbf{v} > 0$. Due to $(\mathbf{D} + \mathbf{N}_1)^{-1} \geq 0$ this yields $(\mathbf{D} + \mathbf{N}_1)^{-1}\mathbf{L}\mathbf{v} > 0$. Then we obtain from Lemma 4.7 that $(\mathbf{D} + \mathbf{N}_1)^{-1}\mathbf{L}$ is an M-matrix. Thus we see that $\mathbf{L} = (\mathbf{D} + \mathbf{N}_1)((\mathbf{D} + \mathbf{N}_1)^{-1}\mathbf{L})$ is the product of two M-matrices and consequently we have that $\mathbf{L}$ is nonsingular and that $\mathbf{L}^{-1} \geq 0$.   ∎

Stability of the discretization follows from the results of Lemma 4.17 and Theorem 4.18.

Theorem 4.19 *Both for linear and quadratic interpolation we have the following stability result:*

$$\|\mathbf{L}^{-1}\|_\infty \leq \frac{1}{8}. \tag{4.15}$$

Proof. Using $\mathbf{L}^{-1} \geq 0$ (cf. Theorem 4.18) and (4.14) we obtain

$$\|\mathbf{L}^{-1}\|_\infty = \|\mathbf{L}^{-1}\mathbb{I}_{\Omega^{H,h}}\|_\infty \leq \|\mathbf{w}\|_\infty,$$

with $\mathbf{w}$ as in Lemma 4.17. Since $\max_{0<x<1} x(1-x)/2 = 1/8$ we get $\|\mathbf{w}\|_\infty \leq \frac{1}{8}$.   ∎

As in the one-dimensional case in Section 4.3, we consider a problem where the source term has non-zero values only in $\tilde{\Gamma}^h$. More precisely, we derive bounds for $\|\mathbf{L}^{-1}\mathbb{I}_{\tilde{\Gamma}^h}\|_\infty$.

Theorem 4.20 *The following inequality holds:*

$$\|\mathbf{L}^{-1}\mathbb{I}_{\tilde{\Gamma}^h}\|_\infty \leq (C_p C_\Gamma + H)\frac{h^2}{H}, \tag{4.16a}$$

with

$$C_\Gamma := 2 - \gamma_1 - \gamma_2 \leq 2 \tag{4.16b}$$

and

$$C_p := \begin{cases} 1 & \textit{for linear interpolation,} \\ \frac{5}{4} & \textit{for quadratic interpolation.} \end{cases} \tag{4.16c}$$

Proof. We define $\mathbf{v} := \mathbf{L}^{-1}\mathbb{I}_{\tilde{\Gamma}^h}$. The partitioning in (4.13) is used to obtain

$$\begin{bmatrix} \mathbf{L}_{11} & -\mathbf{L}_{12}pr_\Gamma \\ -\mathbf{L}_{21} & \mathbf{L}_{22} \end{bmatrix} \begin{bmatrix} \mathbf{v}_1 \\ \mathbf{v}_2 \end{bmatrix} = \begin{bmatrix} \mathbf{e} \\ 0 \end{bmatrix},$$

where e is the vector representation of the grid function $e \in \mathcal{F}(\Omega_l^h)$ defined by

$$e(\mathbf{x}) := \begin{cases} 1 & \mathbf{x} \in \tilde{\Gamma}^h \\ 0 & \mathbf{x} \in \Omega_l^h \backslash \tilde{\Gamma}^h \end{cases}.$$

Using the block LU-factorization of $\mathbf{L}$,

$$\mathbf{L} = \begin{bmatrix} \mathbf{I} & 0 \\ -\mathbf{L}_{21}\mathbf{L}_{11}^{-1} & \mathbf{I} \end{bmatrix} \begin{bmatrix} \mathbf{L}_{11} & -\mathbf{L}_{12}pr_\Gamma \\ 0 & \mathbf{S} \end{bmatrix},$$

with the Schur complement

$$\mathbf{S} := \mathbf{L}_{22} - \mathbf{L}_{21}\mathbf{L}_{11}^{-1}\mathbf{L}_{12}pr_\Gamma, \qquad (*1a)$$

we obtain

$$\mathbf{v}_1 = \mathbf{L}_{11}^{-1}\mathbf{L}_{12}pr_\Gamma\mathbf{v}_2 + \mathbf{L}_{11}^{-1}\mathbf{e}, \qquad (*1b)$$
$$\mathbf{v}_2 = \mathbf{S}^{-1}\mathbf{L}_{21}\mathbf{L}_{11}^{-1}\mathbf{e}. \qquad (*1c)$$

Note that we can represent $\mathbf{e}$ as

$$\mathbf{e} = h^2\mathbf{L}_{12}\mathbf{w}, \qquad (*2)$$

with $\mathbf{w}$ the vector representation of the grid function $w \in \mathcal{F}(\Gamma^h)$ defined by:

$$w(\mathbf{x}) := \begin{cases} 1/2 & \text{for } \mathbf{x} = (\gamma_1 - h, \gamma_2) \\ 1/2 & \text{for } \mathbf{x} = (\gamma_1, \gamma_2 - h) \\ 1 & \text{otherwise} \end{cases}.$$

So for $\mathbf{v}_1$ we have

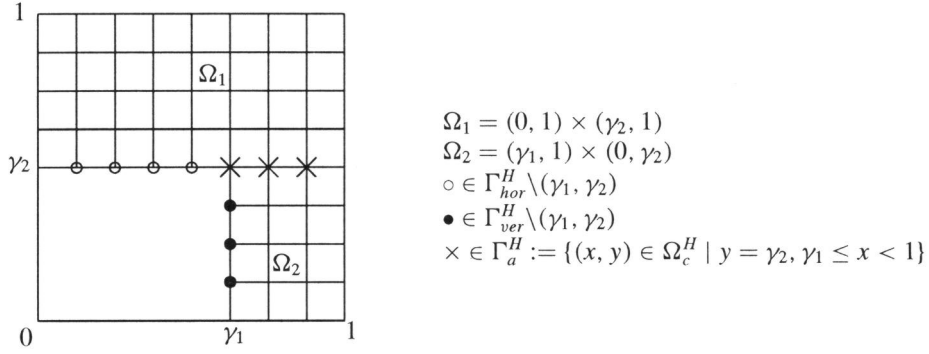$$\mathbf{L}_{11}\mathbf{v}_1 - \mathbf{L}_{12}(pr_\Gamma\mathbf{v}_2 + h^2\mathbf{w}) = 0.$$

The discrete maximum principle yields $\|\mathbf{v}_1\|_\infty \leq \|pr_\Gamma\mathbf{v}_2\|_\infty + h^2$. For piecewise linear interpolation we have $\|p^{(1)}r_\Gamma\mathbf{v}_2\|_\infty \leq \|\mathbf{v}_2\|_\infty$ and for piecewise quadratic interpolation we have $\|p^{(2)}r_\Gamma\mathbf{v}_2\|_\infty \leq \frac{5}{4}\|\mathbf{v}_2\|_\infty$. This yields

$$\|\mathbf{v}_1\|_\infty \leq C_p\|\mathbf{v}_2\|_\infty + h^2, \qquad (*3)$$

with $C_p = 1$ if $p = p^{(1)}$ and $C_p = \frac{5}{4}$ if $p = p^{(2)}$.

It remains to obtain a bound for $\|\mathbf{v}_2\|_\infty = \|\mathbf{S}^{-1}\mathbf{L}_{21}\mathbf{L}_{11}^{-1}\mathbb{I}_{\tilde{\Gamma}^h}\|_\infty$.

We introduce $\mathbf{u} := \mathbf{L}_{11}^{-1}\mathbf{e}$. From $(*2)$ we obtain that $\mathbf{L}_{11}\mathbf{u} - \mathbf{L}_{12}(h^2\mathbf{w}) = 0$ holds. The discrete maximum principle yields that $0 \leq \mathbf{u}(\mathbf{x}) \leq h^2$ for all $\mathbf{x} \in \Omega_l^h$. For the vector $\hat{\mathbf{u}} := \mathbf{L}_{21}\mathbf{u}$ only the components related to grid points on $\Gamma^H \backslash \{(\gamma_1, \gamma_2)\}$ are non-zero and we have $0 \leq \hat{\mathbf{u}}(\mathbf{x}) \leq H^{-2}h^2 = \sigma^{-2}$ for all $\mathbf{x} \in \Gamma^H \backslash \{(\gamma_1, \gamma_2)\}$. We define $e_{hor}^H \in \mathcal{F}(\Omega_c^H)$ as the grid function with value 1 at all points of $\Gamma_{hor}^H \backslash \{(\gamma_1, \gamma_2)\}$ and value 0 at all other points of Ω_c^H; $\mathbf{e}_{hor}^H$ denotes the corresponding vector. Similarly we define the vector $\mathbf{e}_{ver}^H$ (cf. Figure 4.5). Note that $\hat{\mathbf{u}} = \mathbf{L}_{21}\mathbf{L}_{11}^{-1}\mathbf{e}$ and that the

$\Omega_1 = (0, 1) \times (\gamma_2, 1)$
$\Omega_2 = (\gamma_1, 1) \times (0, \gamma_2)$
$\circ \in \Gamma^H_{hor} \setminus (\gamma_1, \gamma_2)$
$\bullet \in \Gamma^H_{ver} \setminus (\gamma_1, \gamma_2)$
$\times \in \Gamma^H_a := \{(x, y) \in \Omega^H_c \mid y = \gamma_2, \gamma_1 \leq x < 1\}$

Figure 4.5 Partitioning of Ω^H_c.

characteristic function in Ω^H_c corresponding to $\Gamma^H \setminus \{(\gamma_1, \gamma_2)\}$ is given by $e^H_{hor} + e^H_{ver}$. Hence we have the following result

$$0 \leq \mathbf{L}_{21}\mathbf{L}_{11}^{-1}\mathbf{e} \leq \sigma^{-2}(e^H_{hor} + e^H_{ver}). \qquad (*4)$$

Due to $\mathbf{S}^{-1} = \begin{bmatrix} \mathbf{0} & \mathbf{I} \end{bmatrix} \mathbf{L}^{-1} \begin{bmatrix} \mathbf{0} \\ \mathbf{I} \end{bmatrix}$ (cf. Lemma 4.9) and the monotonicity of $\mathbf{L}$ (cf. Theorem 4.18) we have $\mathbf{S}^{-1} \geq 0$. Combination with the result in $(*4)$ yields

$$\|\mathbf{v}_2\|_\infty = \|\mathbf{S}^{-1}\mathbf{L}_{21}\mathbf{L}_{11}^{-1}\mathbf{e}\|_\infty \leq \sigma^{-2}(\|\mathbf{S}^{-1}e^H_{hor}\|_\infty + \|\mathbf{S}^{-1}e^H_{ver}\|_\infty). \qquad (*5)$$

We now consider the term $\|\mathbf{S}^{-1}e^H_{hor}\|_\infty$. We use notation as explained in Figure 4.5. The piecewise linear function g is defined as

$$g(x, y) := \begin{cases} \frac{1}{1-\gamma_2}(1 - y) & \text{if } y \geq \gamma_2 \\ 1 & \text{if } y < \gamma_2 \end{cases}.$$

The vector corresponding to the grid function $g_{|\Omega^H_c}$ is denoted by $\mathbf{g}$.

Now consider $\mathbf{S}\mathbf{g} = (\mathbf{L}_{22} - \mathbf{L}_{21}\mathbf{L}_{11}^{-1}\mathbf{L}_{12}pr_\Gamma)\mathbf{g}$.
For $\mathbf{x} \in \Omega^H_c \setminus (\Gamma^H_{hor} \cup \Gamma^H_{ver} \cup \Gamma^H_a)$ we have

$$(\mathbf{S}\mathbf{g})(\mathbf{x}) = [\mathbf{L}_{22}]_{\mathbf{x}} g \geq H^{-2} \begin{bmatrix} & -1 & \\ -1 & 4 & -1 \\ & -1 & \end{bmatrix}_{\mathbf{x}} g = 0. \qquad (*6a)$$

For $\mathbf{x} \in \Gamma^H_a$ we obtain

$$(\mathbf{S}\mathbf{g})(\mathbf{x}) = [\mathbf{L}_{22}]_{\mathbf{x}} g \geq H^{-2} \begin{bmatrix} & -1 & \\ -1 & 4 & -1 \\ & -1 & \end{bmatrix}_{\mathbf{x}} g$$

$$
= -\frac{\partial^2}{\partial x^2} g|_{y=\gamma_2} - \frac{1}{H}\frac{\partial}{\partial y} g|_{\Omega_1} + \frac{1}{H}\frac{\partial}{\partial y} g|_{\Omega_2}
$$

$$
= 0 + \frac{1}{H}\frac{1}{1-\gamma_2} + 0 \geq 0. \qquad (*6b)
$$

With respect to the result on $\Gamma_{ver}^H \cup \Gamma_{hor}^H \backslash \{(\gamma_1, \gamma_2)\}$ we first note the following.
Define $\mathbf{z} := \mathbf{L}_{11}^{-1} \mathbf{L}_{12} pr_\Gamma \mathbf{g}$. Due to the assumption we made concerning the quadratic interpolation on the line segments $[(H, \gamma_2), (2H, \gamma_2)]$ and $[(\gamma_1, H), (\gamma_1, 2H)]$ and because $g \equiv 1$ on Γ we have $pr_\Gamma \mathbf{g} \leq 1$. The discrete maximum principle then yields $0 \leq \mathbf{z}(\mathbf{x}) \leq 1$ for all $\mathbf{x} \in \Omega_I^h$. Thus we get

$$
0 \leq \mathbf{L}_{21} \mathbf{L}_{11}^{-1} \mathbf{L}_{12} pr_\Gamma \mathbf{g} \leq H^{-2}(\mathbf{e}_{hor}^H + \mathbf{e}_{ver}^H).
$$

Using this we obtain for $\mathbf{x} \in \Gamma_{ver}^H \backslash \{(\gamma_1, \gamma_2)\}$:

$$
(\mathbf{Sg})(\mathbf{x}) = ((\mathbf{L}_{22} - \mathbf{L}_{21}\mathbf{L}_{11}^{-1}\mathbf{L}_{12} pr_\Gamma)\mathbf{g})(\mathbf{x}) \geq H^{-2} \begin{bmatrix} & -1 & \\ 0 & 4 & -1 \\ & -1 & \end{bmatrix}_{\mathbf{x}} g - H^{-2}
$$

$$
= -\frac{\partial^2}{\partial y^2} g|_{\Gamma_{ver}} - \frac{1}{H}\frac{\partial}{\partial x} g|_{\Omega_2} + \frac{1}{H^2} - \frac{1}{H^2} = 0. \qquad (*6c)
$$

For $\mathbf{x} \in \Gamma_{hor}^H \backslash \{(\gamma_1, \gamma_2)\}$ we obtain:

$$
(\mathbf{Sg})(\mathbf{x}) = ((\mathbf{L}_{22} - \mathbf{L}_{21}\mathbf{L}_{11}^{-1}\mathbf{L}_{12} pr_\Gamma)\mathbf{g})(\mathbf{x}) \geq H^{-2} \begin{bmatrix} & -1 & \\ -1 & 4 & -1 \\ & 0 & \end{bmatrix}_{\mathbf{x}} g - H^{-2}
$$

$$
= -\frac{\partial^2}{\partial x^2} g|_{\Gamma_{hor}} - \frac{1}{H}\frac{\partial}{\partial y} g|_{\Omega_1} + \frac{1}{H^2} - \frac{1}{H^2} = \frac{1}{H}\frac{1}{1-\gamma_2}. \qquad (*6d)
$$

Combination of $(*6a\text{-}d)$ yields

$$
\mathbf{Sg} \geq \frac{1}{H}\frac{1}{1-\gamma_2}\mathbf{e}_{hor}^H,
$$

and thus, using the monotonicity of $\mathbf{S}$, we obtain

$$
\|\mathbf{S}^{-1}\mathbf{e}_{hor}^H\|_\infty \leq H(1-\gamma_2)\|\mathbf{g}\|_\infty = H(1-\gamma_2).
$$

The term $\|\mathbf{S}^{-1}\mathbf{e}_{ver}^H\|_\infty$ can be treated similarly. Using these results in $(*5)$ we obtain

$$
\|\mathbf{v}_2\|_\infty \leq \sigma^{-2}(H(1-\gamma_2) + H(1-\gamma_1)). \qquad (*7)
$$

Using $(*7)$ in $(*3)$ completes the proof of the theorem.   ∎

We note that the result in Theorem 4.20 is very similar to the result in Theorem 4.12 for the one-dimensional case. It is well-known (cf. e.g. [5],[14]) that in case of a global uniform grid with grid size h relatively large (e.g., $\mathcal{O}(1)$) local discretization errors at grid points *close to the boundary*

may still result in acceptable (e.g., $\mathcal{O}(h^2)$) global discretization errors. In Theorem 4.20 we have a very similar effect with H fixed and $h \downarrow 0$, but now with respect to the local discretization errors at grid points of $\tilde{\Gamma}^h$ (i.e. *close to the interface*). The result of Theorem 4.20 plays an important role in the analysis of the global discretization error below.

The *local discretization error* at $\mathbf{y} \in \Omega^{H,h}$ for the discrete problem $\mathbf{Lu} = \mathbf{f}$ is denoted by $\mathbf{d}(\mathbf{y})$. As usual in a finite difference setting we assume that the solution of the boundary value problem satisfies $u^\star \in C^4(\bar{\Omega})$. Since standard finite difference stencils (related to uniform grids) are used at $\mathbf{y} \in \Omega_l^h \backslash \tilde{\Gamma}^h$ and at $\mathbf{y} \in \Omega_c^H$, we obtain

$$\max_{\mathbf{y} \in \Omega_l^h \backslash \tilde{\Gamma}^h} |\mathbf{d}(\mathbf{y})| \le C_1 h^2, \tag{4.16a}$$

$$\max_{\mathbf{y} \in \Omega_c^H} |\mathbf{d}(\mathbf{y})| \le C_2 H^2. \tag{4.16b}$$

The constants C_1 and C_2 are of the form

$$C_1 = c_1 \max\{|u^{\star(4)}(\mathbf{x})| \mid \mathbf{x} \in (0, \gamma_1 - h) \times (0, \gamma_2 - h)\}, \tag{4.17a}$$

$$C_2 = c_2 \max\{|u^{\star(4)}(\mathbf{x})| \mid \mathbf{x} \in \Omega \backslash ((0, \gamma_1 - H) \times (0, \gamma_2 - H))\}, \tag{4.17b}$$

with c_1, c_2 independent of $H, h, u^\star$.

Due to the interpolation on the interface we obtain

$$\max_{\mathbf{y} \in \tilde{\Gamma}^h} |\mathbf{d}(\mathbf{y})| \le \hat{C}_1 h^2 + C_3 \sigma^2 H^{j-1} \tag{4.16c}$$

with $j = 1$ for piecewise linear interpolation ($p^{(1)}$) and $j = 2$ for piecewise quadratic interpolation ($p^{(2)}$). The constants $\hat{C}_1$ and C_3 are of the form

$$\hat{C}_1 = c_1 \max\{|u^{\star(4)}(\mathbf{x})| \mid \mathbf{x} \in \Omega_l \backslash ((0, \gamma_1 - 2h) \times (0, \gamma_2 - 2h))\} \tag{4.17c}$$

$$C_3 = c_3 \max\{|u^{\star(1+j)}(\mathbf{x})| \mid \mathbf{x} \in \Gamma\}, \tag{4.17d}$$

with c_3 independent of $h, H, u^\star$.

Remark 4.21 At $\mathbf{y} \in \tilde{\Gamma}^h$ we obtain $\mathbf{d}(\mathbf{y}) = \mathcal{O}(1)$ for piecewise linear interpolation on the interface. So the discretization for the Poisson problem (4.10) on the composite grid $\Omega^{H,h}$ in case of linear interpolation on the interface is not consistent if we take σ fixed and $H \downarrow 0$. □

The bound in (4.16c) is not sharp for the (less interesting) case $\sigma = 1$. A composite grid makes sense only for problems in which the solution $u^\star$ varies much more rapidly in Ω_l than in $\Omega \backslash \Omega_l$. Thus we assume $C_1 \gg \hat{C}_1 + C_2 + C_3$. Clearly, then one would use a composite grid with $h \ll H$, i.e. $\sigma \gg 1$. In that case the local discretization error on $\tilde{\Gamma}^h$ can be large compared to the local discretization error on $\Omega^{H,h} \backslash \tilde{\Gamma}^h$ (cf. (4.16)). A strong damping of these large local discretization errors is a necessity to obtain an acceptable *global discretization error*.

Theorem 4.22 *For the global discretization error the following holds*

$$\|\mathbf{u} - \mathbf{u}^\star\|_\infty \le \frac{13}{8} \max\{C_1, \hat{C}_1\} h^2 + \frac{1}{8} C_2 H^2 + 3 C_3 H^j, \tag{4.18}$$

with C_i ($i = 1, 2, 3$) and $\hat{C}_1$ as in (4.17), $j = 1$ for piecewise linear interpolation and $j = 2$ for piecewise quadratic interpolation.

Proof. Using Theorems 4.18-4.22 and (4.16) we obtain

$$
\|\mathbf{u} - \mathbf{u}^\star\|_\infty \leq \frac{1}{8}C_1 h^2 + \frac{1}{8}C_2 H^2 + (C_p C_\Gamma + H)\frac{h^2}{H}(\hat{C}_1 h^2 + C_3 \sigma^2 H^{j-1})
$$
$$
= \frac{1}{8}C_1 h^2 + \hat{C}_1(C_p C_\Gamma \frac{h}{\sigma} + h^2)h^2 + \frac{1}{8}C_2 H^2 + C_3(C_p C_\Gamma + H)H^j,
$$

with C_p and C_Γ as in (4.16). Now (4.18) follows using $h \leq H \leq \frac{1}{2}$, $C_p \leq \frac{5}{4}$ and $C_\Gamma \leq 2$. ∎

The bound in (4.18) nicely separates the discretization error terms related to the high activity region, the low activity region and the interpolation on the interface. As usual in finite difference estimates, high (fourth order) derivatives are involved. We shall illustrate the sharpness of the bounds via numerical results in Subsection 4.4.3. Note that the constants on the right hand side of (4.18) do not depend on $\sigma = H/h$. Hence, despite the fact that the local discretization error depends strongly on σ (cf. (4.16c)), the discretization approach described in this section is suitable for discretizing on composite grids with large refinement factors. We note that asymptotically for $H \downarrow 0$ the bound in (4.18) for linear interpolation ($j = 1$) is worse than the bound for quadratic interpolation. In practice (where we have a given desired accuracy) it may well happen that the results for quadratic and for linear interpolation are comparable (see Example 4.26).

Remark 4.23 It follows from (4.18) that for linear interpolation the discretization is *convergent* if we take σ fixed and $H \downarrow 0$, although the discretization is *not consistent* (cf. Remark 4.21). □

Comparing our results with related results for composite grid discretizations in the literature, we note the following. In [13] an analysis of a composite grid problem resulting from finite volume element discretization is given. In this analysis weaker assumptions concerning the regularity of the solution are used than in our analysis. However, only the case with $\sigma = 2$ is treated. The finite volume type of method in [13] uses vertex centered approximations. A finite volume method for composite grids using special cell centered approximations is analysed in [38]. This analysis also uses weaker assumptions concerning the regularity of the solution. In the schemes in [38] larger values of σ are allowed. The error estimate in [38] is of the form

$$
\|\mathbf{u} - \mathbf{u}^\star\| \leq K_1 H^{m+\frac{1}{2}} + K_2 h^{m+\frac{1}{2}},
$$

with $\|.\|$ a discrete H^1-norm, $m > 0$ related to the regularity of the solution, and 'constants' K_1 and K_2 *which depend on the refinement factor* $\sigma = H/h$. The constants on the right hand side of (4.18) are independent of σ. In Section 4.4.3 we show the sharpness of the discretization error estimate (4.18) via numerical results.

Remark 4.24 Results very similar to those in Theorem 4.20 and Theorem 4.22 can be obtained if we consider a composite grid with Ω_l of the form $(\gamma_{11}, \gamma_{12}) \times (\gamma_{21}, \gamma_{22})$ with $0 < \gamma_{11} < \gamma_{12} < 1$, $0 < \gamma_{21} < \gamma_{22} < 1$. □

In the remainder of this subsection we comment on a generalization of our discretization error analysis to more general elliptic boundary value problems. In the analysis above we used three

main arguments: local discretization error estimates (as in (4.16)), a stability result (as in Theorem 4.19) and a strong damping of local discretization errors on $\tilde{\Gamma}^h$ (as in Theorem 4.20).
We consider an elliptic boundary value problem, on the unit square $\Omega = (0, 1) \times (0, 1)$, of the form

$$-a_{11}(x, y)u_{xx} - a_{22}(x, y)u_{yy} + a_1(x, y)u_x + a_2(x, y)u_y = f, \quad \text{in } \Omega, \qquad (4.19)$$

with homogeneous Dirichlet boundary conditions. The coefficient functions are smooth and satisfy the usual requirements for an elliptic problem which is not convection dominated. We use a standard finite difference discretization with central differences for the first order derivatives. This results in a composite grid matrix $\mathbf{L}$ as in (4.13).

We first discuss the case with piecewise linear interpolation. The resulting local discretization error estimates are as in (4.16), with $j = 1$. Under the following conditions:

$$a_{ii}(x, y) > \frac{H}{2}|a_i(x, y)|, \quad (x, y) \in \Omega, \ i = 1, 2,$$

the matrix $\mathbf{L}$ is an M-matrix. We cannot apply the usual technique for proving the existence of a barrier function (cf. [32], §5.1) because the composite grid discretization is *not consistent*. However, in this fairly concrete setting one can still derive concrete barrier functions. For example, in the case with $c(x, y) = d(x, y) \equiv 0$ we can take the same function as in Lemma 4.17, and for the case with $c(x, y) = \text{constant} > 0$ we can use $w(x, y) = x$ as a barrier function. If the existence of a barrier function can be proved, we have a stability result as in Theorem 4.19 (with $\frac{1}{8}$ replaced by another constant). With respect to the result in Theorem 4.20 we note the following. We refer to equations in the proof of Theorem 4.20. As in ($*2$), we can represent e as $\mathbf{e} = h^2 \mathbf{L}_{12}\mathbf{w}$, with $0 \leq \|\mathbf{w}\|_\infty \leq c_1$. The constant c_1 depends on the coefficient functions a, b, c, d, but is independent of H and h. For $\begin{pmatrix} \mathbf{v}_1 \\ \mathbf{v}_2 \end{pmatrix} = \mathbf{L}^{-1} \mathbb{I}_{\tilde{\Gamma}^h}$ we obtain (cf. ($*1$) and ($*3$))

$$\|\mathbf{v}_1\|_\infty \leq \|\mathbf{v}_2\|_\infty + c_1 h^2,$$
$$\|\mathbf{v}_2\|_\infty = h^2\|\mathbf{S}^{-1}\mathbf{L}_{21}\mathbf{L}_{11}^{-1}\mathbf{L}_{12}\mathbf{w}\|_\infty.$$

So it remains to obtain a bound for $\|\mathbf{v}_2\|_\infty$. We sketch an approach, different from the one used in the proof of Theorem 4.20, that could be applied to a more general problem as the one in (4.19). Note that $\mathbf{L}_{22}^{-1}\mathbf{L}_{21} \geq 0$ and $\mathbf{L}_{11}^{-1}\mathbf{L}_{12}\,pr_\Gamma \geq 0$, so using the discrete maximum principle we obtain

$$\|\mathbf{L}_{22}^{-1}\mathbf{L}_{21}\mathbf{L}_{11}^{-1}\mathbf{L}_{12}\,pr_\Gamma\|_\infty \leq \|\mathbf{L}_{22}^{-1}\mathbf{L}_{21}\|_\infty\|\mathbf{L}_{11}^{-1}\mathbf{L}_{12}\,pr_\Gamma\|_\infty \leq \|\mathbf{L}_{22}^{-1}\mathbf{L}_{21}\|_\infty = \|\mathbf{L}_{22}^{-1}\mathbf{L}_{21}\,\mathbb{I}_{\Omega_l^h}\|_\infty.$$

We introduce $\mathbf{u} := \mathbf{L}_{22}^{-1}\mathbf{L}_{21}\,\mathbb{I}_{\Omega_l^h}$, so u satisfies $\mathbf{L}_{22}\mathbf{u} - \mathbf{L}_{21}\,\mathbb{I}_{\Omega_l^h} = 0$. This corresponds to the discretization, on a uniform grid with size H, of the differential equation on a subdomain $\tilde{\Omega} \subset \Omega$ (see Figure 4.6). We use Dirichlet boundary conditions with values 0 on the part of $\partial\tilde{\Omega}$ which coincides with $\partial\Omega$ and values 1 on the remaining part of $\partial\tilde{\Omega}$.
Due to the maximum principle we have that $\|\mathbf{u}\|_\infty < 1$ holds. Since we restrict ourselves to diffusion problems it is reasonable to assume that even $\|\mathbf{u}\|_\infty < 1 - c_2 H$ holds with $c_2 > 0$. If the
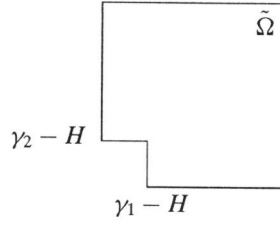
Figure 4.6 Example of the subdomain $\tilde{\Omega} \subset \Omega$.

latter inequality holds, we obtain

$$
\begin{aligned}
\|\mathbf{v}_2\|_\infty &= h^2 \|(\mathbf{I} - \mathbf{L}_{22}^{-1}\mathbf{L}_{21}\mathbf{L}_{11}^{-1}\mathbf{L}_{12}\,pr_\Gamma)^{-1}\mathbf{L}_{22}^{-1}\mathbf{L}_{21}\mathbf{L}_{11}^{-1}\mathbf{L}_{12}\mathbf{w}\|_\infty \\
&\le h^2 \sum_{k=0}^{\infty} \|\mathbf{L}_{22}^{-1}\mathbf{L}_{21}\mathbf{L}_{11}^{-1}\mathbf{L}_{12}\,pr_\Gamma\|_\infty^k \|\mathbf{L}_{22}^{-1}\mathbf{L}_{21}\mathbf{L}_{11}^{-1}\mathbf{L}_{12}\mathbf{w}\|_\infty \\
&\le h^2 \sum_{k=0}^{\infty} (1 - c_2 H)^k c_1 = \frac{c_1}{c_2}\frac{h^2}{H}.
\end{aligned}
$$

So we then have a result as in Theorem 4.20. From these observations we derive the claim that for the case with piecewise linear interpolation the analysis presented in this subsection can be extended to more general elliptic boundary value problems as in (4.19).

For the case with piecewise quadratic interpolation it is not clear (to us) how the analysis of this subsection can be extended to a more general setting. It is not clear how we can prove monotonicity of $\mathbf{L}$ (as in Theorem 4.18) if we have a problem as in (4.19) with variable coefficients. In the next subsection we present numerical results for a problem as in (4.19). There we observe that both for linear and for quadratic interpolation we have a discretization error behaviour which is very similar to the behaviour in case of the Poisson problem.

4.4.3 Numerical Results

In this subsection we show results of some numerical experiments. First, we present results related to the sharpness of the global discretization error bound proved in Theorem 4.22. Then we discuss a two-dimensional non-uniform discretization method which can be seen as a generalization of the one-dimensional method with stiffness matrix $\tilde{\mathbf{L}}$ of Section 4.3 (cf. (4.6a)). Finally, we show composite grid discretization errors for a problem with variable coefficients (Example 4.28) and for a problem with a singular solution (Example 4.29).

In Example 4.25-4.27 we will illustrate certain phenomena using numerical results for the following model problem:

$$
\begin{aligned}
-\Delta u &= f \quad \text{in } \Omega = (0, 1) \times (0, 1), \\
u &= g \quad \text{on } \partial\Omega.
\end{aligned}
\tag{4.20}
$$

We consider two cases:

Case 1: f, g such that the solution $u^\star$ is given by

$$u^\star(x, y) = x^2 + y^2. \tag{4.21}$$

Case 2: f, g such that the solution $u^\star$ is given by

$$u^\star(x, y) = \frac{1}{2}\{\tanh(25(x + y - \frac{1}{8})) + 1\}. \tag{4.22}$$

Clearly in Case 1 we have a very smooth solution and we do not need a composite grid. This example is used for theoretical considerations. The solution $u^\star$ in Case 2 is shown in Figure 2.4 in Subsection 2.2.2. The solution varies very rapidly in a small part of the domain and is relatively smooth in the remaining part of the domain. In both cases we take $\Omega_l = (0, 1/4) \times (0, 1/4)$.

Example 4.25 In the upper bound for the global discretization error as proved in Theorem 4.22 we have a term $C_3 H$ if we use piecewise linear interpolation on the interface ($j = 1$). In this example we show that the bound is sharp with respect to this $C_3 H$ term. We consider Case 1. Then for C_1, $\hat{C}_1$, C_2 in (4.18) we have $C_1 = \hat{C}_1 = C_2 = 0$. In Table 4.1 we show values of the global discretization error $\|\mathbf{u} - \mathbf{u}^\star\|_\infty$ for several values of H and $\sigma = H/h$. We clearly observe the linear dependence on H. Further there is no significant dependence of the errors on the refinement factor σ.   □

Example 4.26 We consider Case 2 and use piecewise quadratic interpolation on the interface. For this composite grid problem Theorem 4.22 yields a discretization error bound of the form $D_1 h^2 + D_2 H^2$ with $D_1 \gg D_2$. Based on this bound we expect the following. If we take H fixed then decreasing h (i.e. increasing σ) should result in h^2 convergence until a certain threshold value σ_{max} is reached. This convergence behaviour can be observed in the rows of Table 4.2. For $H = 1/8$ we see a threshold value $\sigma_{max} \approx 16$. Also note that in Table 4.2 there is only little variation in the values if we take h fixed and vary σ. For example, along the diagonal from $(H, \sigma) = (1/128, 1)$ to $(H, \sigma) = (1/8, 16)$ (i.e. $h = 1/128$) all values are about $1.4 \, 10^{-3}$. This means that the global discretization error corresponding to the composite grid problem with $H = 1/8$, $h = 1/128$ is approximately of the same size as the global discretization error corresponding to the standard discrete problem on the global uniform grid with $h = 1/128$. So in a sense the quality

$\sigma = 2$			
$H = 1/16$	$H = 1/32$	$H = 1/64$	$H = 1/128$
$1.08 \, 10^{-3}$	$4.47 \, 10^{-4}$	$2.01 \, 10^{-4}$	$9.60 \, 10^{-5}$
$H = 1/16$			
$\sigma = 2$	$\sigma = 4$	$\sigma = 8$	$\sigma = 16$
$1.08 \, 10^{-3}$	$1.26 \, 10^{-3}$	$1.35 \, 10^{-3}$	$1.42 \, 10^{-3}$

Table 4.1   Global discretization errors; Case 1; piecewise linear interpolation.

H	1	2	4	8	16	32	σ
1/8	$2.55 \ 10^{-1}$	$6.02 \ 10^{-2}$	$2.29 \ 10^{-2}$	$5.39 \ 10^{-3}$	$1.49 \ 10^{-3}$	$1.54 \ 10^{-3}$	
1/16	$6.08 \ 10^{-2}$	$2.29 \ 10^{-2}$	$5.54 \ 10^{-3}$	$1.35 \ 10^{-3}$	$8.03 \ 10^{-4}$		
1/32	$2.30 \ 10^{-2}$	$5.61 \ 10^{-3}$	$1.41 \ 10^{-3}$	$3.33 \ 10^{-4}$			
1/64	$5.63 \ 10^{-3}$	$1.43 \ 10^{-3}$	$3.51 \ 10^{-4}$				
1/128	$1.44 \ 10^{-3}$	$3.55 \ 10^{-4}$					
1/256	$3.57 \ 10^{-3}$						

Table 4.2 Global discretization errors; Case 2; piecewise quadratic interpolation.

of the discrete solutions of these two problems is the same. Note that in this particular example the global uniform grid with $h = 1/128$ contains about $1.6 \ 10^4$ grid points, whereas the composite grid contains about $1.1 \ 10^3$ grid points.

When we repeat this experiment, but now with linear interpolation instead of quadratic interpolation on the interface, we obtain discretization errors which are very close to the discretization errors shown in Table 4.2 (differences less than a few percent). For the values of H and h considered in this example the error in the high activity region and the low activity region (corresponding to the first and second term on the right hand side of (4.18)) dominate the linear interpolation error on the interface (corresponding to the third term on the right hand side of (4.18)). $\square$

We now discuss an obvious two-dimensional generalization of the one-dimensional approach in (4.6c). We use the same finite difference approximations as in Subsection 4.4.1 at all grid points of $\Omega^{H,h}\backslash\Gamma^H$. Again, we use piecewise linear ($j = 1$) or piecewise quadratic ($j = 2$) interpolation. On Γ^H we do not use uniform finite differences as in (4.11a), but non-uniform finite differences of the same type as in (4.6c). For example, at $\mathbf{x} \in \Gamma_{ver}^H$ we use:

$$-\Delta u \doteq H^{-2}(-\frac{2\sigma^2}{\sigma+1}u(\mathbf{x}-(h,0)) + 2\sigma u(\mathbf{x}) - \frac{2\sigma}{\sigma+1}u(\mathbf{x}+(H,0)))$$
$$+ H^{-2}(-u(\mathbf{x}-(0,H)) + 2u(\mathbf{x}) - u(\mathbf{x}+(0,H))). \tag{4.23}$$

This results in a composite grid problem denoted by $\tilde{\mathbf{L}}\tilde{\mathbf{u}} = \mathbf{f}$. The local discretization errors are as in (4.16) but now with an $\mathcal{O}(H)$ error at points $\mathbf{x} \in \Gamma^H$ (cf. (4.8c)). In Section 4.3 we noticed that in the one-dimensional case the local discretization error on $\tilde{\Gamma}^h$ is reduced only by a factor h (cf. Theorem 4.14). Numerical results show that in the two-dimensional case we also have $\|\tilde{\mathbf{L}}^{-1}\mathbb{I}_{\tilde{\Gamma}^h}\|_\infty \approx c \ h$. So for the local discretization errors on $\tilde{\Gamma}^h$ of size $\hat{C}_1 h^2 + C_3 \sigma^2 H^{j-1}$ (cf. (4.16c)) we have a damping factor $c \ h = cH/\sigma$, instead of the damping factor cH/σ^2 as in Theorem 4.20. This then implies a global discretization error estimate of the form

$$\|\tilde{\mathbf{u}} - \mathbf{u}^\star\|_\infty \leq K_1 h^2 + \frac{1}{8}K_2 H^2 + K_3 c\sigma H^j, \tag{4.24}$$

with K_i constants which are similar to the constants C_i in (4.18). Clearly, due to the factor σ the bound in (4.24) is less favourable than the result in Theorem 4.22.

$\sigma = 2$			
$H = 1/16$	$H = 1/32$	$H = 1/64$	$H = 1/128$
$1.48 \ 10^{-3}$	$6.82 \ 10^{-4}$	$3.25 \ 10^{-4}$	$1.60 \ 10^{-4}$
$H = 1/16$			
$\sigma = 2$	$\sigma = 4$	$\sigma = 8$	$\sigma = 16$
$1.48 \ 10^{-3}$	$2.54 \ 10^{-3}$	$3.84 \ 10^{-3}$	$5.30 \ 10^{-3}$

Table 4.3   Global discretization errors; Case 1; linear interpolation; stiffness matrix $\tilde{\mathbf{L}}$.

Example 4.27 This example is similar to Example 4.25 but now with the stiffness matrix $\tilde{\mathbf{L}}$ instead of the stiffness matrix $\mathbf{L}$. We use piecewise linear interpolation on the interface and we consider Case 1. Then the bound in (4.24) is of the form $C_3 c \sigma H$, so we expect an increasing discretization error if σ is increased. A dependence of the global discretization error on σ is observed in Table 4.3, too. Apparently this dependence is not linear in σ. Probably this is due to the fact that the local discretization errors on $\tilde{\Gamma}^h$, i.e. $\mathbf{d}(\mathbf{y})$ with $\mathbf{y} \in \tilde{\Gamma}^h$, show an oscillating behaviour and approximating $\mathbf{d}(\mathbf{y})$ by $\max_{\mathbf{x} \in \tilde{\Gamma}^h} |\mathbf{d}(\mathbf{x})|$ for all $\mathbf{y} \in \tilde{\Gamma}^h$ (as is done to obtain (4.24)) is too pessimistic.   □

The discretization error analysis in Subsection 4.4.2 applies to the Poisson equation with a solution $u^\star \in C^4(\bar{\Omega})$. In the following experiments we apply the composite grid finite difference method of Subsection 4.4.1 to other problems. In Example 4.28 we consider a problem in which the differential operator has variable coefficients, and with data such that the solution $u^\star$ is still in $C^4(\bar{\Omega})$. In Example 4.29 we consider a Poisson equation with a singular solution ($u^\star \notin C(\bar{\Omega})$).

Example 4.28 We consider an elliptic boundary value problem as in (4.19), i.e. with variable coefficients. We consider the problem:

$$-(2 + \sin(\tfrac{\pi x}{3}))u_{xx} - e^{xy}u_{yy} + \cos(\tfrac{\pi x}{5})u_x + (1 + x)e^y u_y = f \quad \text{in } \Omega,$$
$$u = g \quad \text{on } \partial\Omega,$$

with Ω the unit square. We take the data f, g such that the solution $u^\star$ is as in (4.22). We use a standard discretization with central differences for the first order derivatives. The resulting discretization errors with $H = 1/16$ are shown in Table 4.4. Note that the results are very similar to the results for the Poisson equation in Example 4.26. As in Table 4.2, we observe an $O(h^2)$ behaviour until a certain threshold value σ_{max} is reached. We also see that for linear and quadratic

σ	1	2	4	8	16	32
linear	$6.66 \ 10^{-2}$	$2.43 \ 10^{-2}$	$5.87 \ 10^{-3}$	$1.45 \ 10^{-3}$	$9.91 \ 10^{-4}$	$1.02 \ 10^{-3}$
quadratic	$6.66 \ 10^{-2}$	$2.43 \ 10^{-2}$	$5.87 \ 10^{-3}$	$1.46 \ 10^{-3}$	$9.25 \ 10^{-4}$	$9.51 \ 10^{-4}$

Table 4.4   Global discretization errors; $H = 1/16$; Example 4.28.

h	1/16	1/32	1/64	1/128	1/256	1/512
$\|u - u^\star\|_\infty$	$7.14\ 10^{-2}$	$2.85\ 10^{-2}$	$9.74\ 10^{-3}$	$3.05\ 10^{-3}$	$9.08\ 10^{-4}$	$2.63\ 10^{-4}$

Table 4.5   Global discretization errors on uniform grids; Example 4.29.

σ	1	2	4	8	16	32
linear	$7.14\ 10^{-2}$	$2.90\ 10^{-2}$	$1.04\ 10^{-2}$	$4.27\ 10^{-3}$	$4.01\ 10^{-3}$	$3.93\ 10^{-3}$
quadratic	$7.14\ 10^{-2}$	$2.86\ 10^{-2}$	$9.80\ 10^{-3}$	$3.11\ 10^{-3}$	$1.15\ 10^{-3}$	$1.06\ 10^{-3}$

Table 4.6   Global discretization errors on composite grids; $H = 1/16$; Example 4.29.

interpolation we have approximately the same threshold value for σ. Apparently, for $H = 1/16$ the error in the low activity region (corresponding to the term $\sim C_2 H^2$ in (4.18)) dominates the linear interpolation error on Γ (corresponding to the term $\sim C_3 H$ in (4.18)).   □

Example 4.29 We consider a problem with a singular solution (as in [30], [39]):

$$-\Delta u = f \quad \text{in } \Omega = (0, 1) \times (0, 1),$$
$$u = g \quad \text{on } \partial\Omega,$$

with f, g such that the solution is given by $u^\star(x, y) = \log(\sqrt{x^2 + y^2})$.

Due to the singularity at the origin it is not reasonable to compare discretization errors on certain (uniform or composite) grids by using the maximum norm on different grids. We use a uniform coarse grid on Ω with size $H = 1/16$, denoted by $\Omega^{1/16}$. On this grid and on finer grids we always measure discretization errors using the maximum norm over $\Omega^{1/16}$. When we use a global uniform grid with size h, denoted by Ω^h, and the standard central difference discretization for the Laplace operator, we obtain discretization errors as in Table 4.5. In Table 4.6 we show the values $\|u - u^\star\|_\infty$ for the composite grid discretization of Subsection 4.4.1, with $H = 1/16$. From these results we see that for piecewise linear (quadratic) interpolation we obtain fine grid accuracy until the threshold value $\sigma = 8$ ($\sigma = 16$) is reached.   □

COMPOSITE GRID METHODS FOR NONLINEAR BOUNDARY VALUE PROBLEMS

In the previous chapters we have considered only linear boundary value problems. In this chapter we consider the problem of solving nonlinear boundary value problems using composite grids. Discretization of a nonlinear boundary value problem results in a system of nonlinear equations. In Section 5.1 we briefly recall Newton's method for solving such a system of nonlinear equations.

The coupling of global coarse grid and local fine grid discretizations of a boundary value problem as in Section 2.2, can be applied to nonlinear boundary value problems too. Then systems of nonlinear equations on the uniform subgrids have to be solved. In the nonlinear LDC method an outer local defect correction iteration is combined with inner Newton iterations for solving these systems. The nonlinear LDC method is discussed in Section 5.2 for the model composite grid $\Omega^{H,h}$ from Section 2.1. Sufficient conditions are given for the nonlinear LDC method to be well-defined. By this we mean that all systems of nonlinear equations occurring in the method are locally uniquely solvable. It is shown that the nonlinear LDC method is closely related to a system of nonlinear equations resulting from discretizing the boundary value problem on the composite grid $\Omega^{H,h}$.

In Section 5.3 a combination of Newton's method and the fast adaptive composite (FAC) grid method from Section 2.3 for solving the composite grid discretization related to the nonlinear LDC method is described. In this so-called Newton-FAC method an outer Newton iteration on the composite grid $\Omega^{H,h}$ is performed. In each step of the Newton method the linear Jacobian system on the composite grid $\Omega^{H,h}$ is solved by the FAC method.

5.1 INTRODUCTION

In Chapter 2 and Chapter 3 we have discussed iterative methods for solving *linear* elliptic boundary value problems on composite grids. In this chapter we shall consider the numerical solution of *nonlinear* boundary value problems on composite grids. As in Chapter 2 and Chapter 3 we use a model boundary value problem on the unit square. The nonlinear counterpart of the linear second-order elliptic boundary value problem (3.14) is denoted by

$$N(u) = 0 \qquad \text{in } \Omega = (0, 1) \times (0, 1), \tag{5.1a}$$

$$u = g \qquad \text{on } \partial\Omega. \tag{5.1b}$$

We use the model composite grid $\Omega^{H,h}$ introduced in Section 2.1. The composite grid notation in this chapter is the same as in chapters 2 and 3.

After discretization of a nonlinear boundary value problem a system of nonlinear algebraic equations results. Usually such a system of nonlinear equations is solved by Newton's method or one of its variants (see e.g. [52, Section 7.1],[2, Chapter 8]). Here we briefly recall Newton's method; for a thorough discussion of this type of methods we refer to [52]. We consider the system of nonlinear algebraic equations,

$$
\begin{aligned}
f_1(u_1, u_2, \ldots, u_n) &= 0, \\
f_2(u_1, u_2, \ldots, u_n) &= 0, \\
&\vdots \\
f_n(u_1, u_2, \ldots, u_n) &= 0,
\end{aligned}
\tag{5.2}
$$

with $f_i : I\!\!R^n \to I\!\!R, i = 1, \ldots, n$. We assume that the system (5.2) has at least one solution. The system (5.2) is written in matrix-vector notation as $\mathbf{f}(\mathbf{u}) = \mathbf{0}$, with $\mathbf{u} \in I\!\!R^n, \mathbf{f} : I\!\!R^n \to I\!\!R^n$. Given an initial guess $\mathbf{u}_0$, a sequence of approximations $\mathbf{u}_1, \mathbf{u}_2, \ldots, \mathbf{u}_m, \ldots$, to a solution $\mathbf{u}^\star$ of (5.2) is generated by

$$\mathbf{u}_{m+1} := \mathbf{u}_m + \mathbf{v}_m \tag{5.3}$$

with $\mathbf{v}_m$ the solution of the system of linear equations

$$\frac{\partial \mathbf{f}}{\partial \mathbf{u}}(\mathbf{u}_m)\mathbf{v}_m = -\mathbf{f}(\mathbf{u}_m). \tag{5.4}$$

In (5.4) $\frac{\partial \mathbf{f}}{\partial \mathbf{u}}(\mathbf{u}_m)$ is the *Jacobian matrix* of partial derivatives,

$$
\begin{pmatrix}
\frac{\partial f_1}{\partial u_1} & \frac{\partial f_1}{\partial u_2} & \cdots & \frac{\partial f_1}{\partial u_n} \\
\frac{\partial f_2}{\partial u_1} & \frac{\partial f_2}{\partial u_2} & \cdots & \frac{\partial f_2}{\partial u_n} \\
\vdots & \vdots & & \vdots \\
\frac{\partial f_n}{\partial u_1} & \frac{\partial f_n}{\partial u_2} & \cdots & \frac{\partial f_n}{\partial u_n}
\end{pmatrix},
$$

evaluated at $\mathbf{u}_m$.

It is well-known that, in general, Newton's method is *locally quadratically convergent*. So if the initial guess is 'sufficiently close' to a solution $\mathbf{u}^\star$ of (5.2), then the Newton iterates converge very fast to $\mathbf{u}^\star$. In order to enlarge the domain of convergence the method may be modified. The idea of *damped Newton methods* is to take only a fraction of the *Newton update* $\mathbf{v}_m$ in (5.3). So rather than (5.3), we choose

$$\mathbf{u}_{m+1} := \mathbf{u}_m + \lambda_m \mathbf{v}_m, \tag{5.5}$$

with $0 < \lambda_m \leq 1$. Methods for choosing the *damping factors* λ_m are discussed in e.g. [2, Section 8.1],[59, Section 8.4]).

5.2 LOCAL DEFECT CORRECTION FOR NONLINEAR PROBLEMS

5.2.1 A Combination of Local Defect Correction and Newton's Method

We start by discretizing the nonlinear boundary value problem (5.1) on the uniform global coarse grid Ω^H from (2.2). This yields the *basic discretization*,

$$N^H(u_0^H) = 0 \qquad \text{on } \Omega^H, \tag{5.6}$$

which describes a system of nonlinear equations for the unknowns $\{u_0^H(\mathbf{x}) \mid \mathbf{x} \in \Omega^H\}$. In (5.6) N^H is a nonlinear mapping $N^H : \mathcal{F}(\Omega^H) \to \mathcal{F}(\Omega^H)$. The system of nonlinear equations (5.6) is solved by a damped Newton method. If (5.6) has at least one solution and if the damped Newton method converges, then an approximation $\tilde{u}_0^H$ of a solution of (5.6) results.

The approximation $\tilde{u}_0^H$ and a prolongation $p : \mathcal{F}(\Gamma^H) \to \mathcal{F}(\Gamma^h)$ (e.g. piecewise linear or piecewise quadratic interpolation on the interface) are used to define *artificial Dirichlet boundary values on the interface*. These values are defined in the same way as in the local defect correction approach for linear boundary value problems (see Section 2.2 and Section 3.1). The artificial Dirichlet boundary values are used for discretizing the boundary value problem (5.1) on the uniform local fine grid Ω_l^h. This yields the system of nonlinear equations,

$$N_l^h(u_{l,0}^h, p\tilde{u}_0^H|_\Gamma) = 0 \qquad \text{on } \Omega_l^h, \tag{5.7}$$

for the unknowns $\{u_{l,0}^h(\mathbf{x}) \mid \mathbf{x} \in \Omega_l^h\}$. In (5.7) N_l^h is a nonlinear mapping $N_l^h : \mathcal{F}(\Omega_l^h) \times \mathcal{F}(\Gamma^h) \to \mathcal{F}(\Omega_l^h)$. The system of equations (5.7) is the nonlinear counterpart of (2.13). A damped Newton method is used for approximately solving (5.7). If (5.7) has at least one solution and if the damped Newton method converges, then an approximation $\tilde{u}_{l,0}^h$ of a solution of (5.7) results. The local fine grid approximation $\tilde{u}_{l,0}^h$ is used to update the global coarse grid discretization (5.6) by *local defect correction*. We define

$$w^H(\mathbf{x}) := \begin{cases} \tilde{u}_{l,0}^h(\mathbf{x}) & \mathbf{x} \in \Omega_l^H \\ \tilde{u}_0^H(\mathbf{x}) & \mathbf{x} \in \Omega^H \backslash \Omega_l^H \end{cases},$$

with Ω_l^H the local coarse grid from (2.9). We substitute this approximation in the system of nonlinear equations (5.6) and define the defect as

$$d^H(\mathbf{x}) := \begin{cases} N^H(w^H)(\mathbf{x}) & \mathbf{x} \in \Omega_l^H \\ 0 & \mathbf{x} \in \Omega^H \backslash \Omega_l^H \end{cases}.$$

Then we solve the system of nonlinear equations

$$N^H(u_1^H) = d^H \qquad \text{on } \Omega^H, \tag{5.8}$$

using a damped Newton method. If (5.8) has at least one solution and if the damped Newton method converges, then an approximation $\tilde{u}_1^H$ of a solution of (5.8) results. The approximation
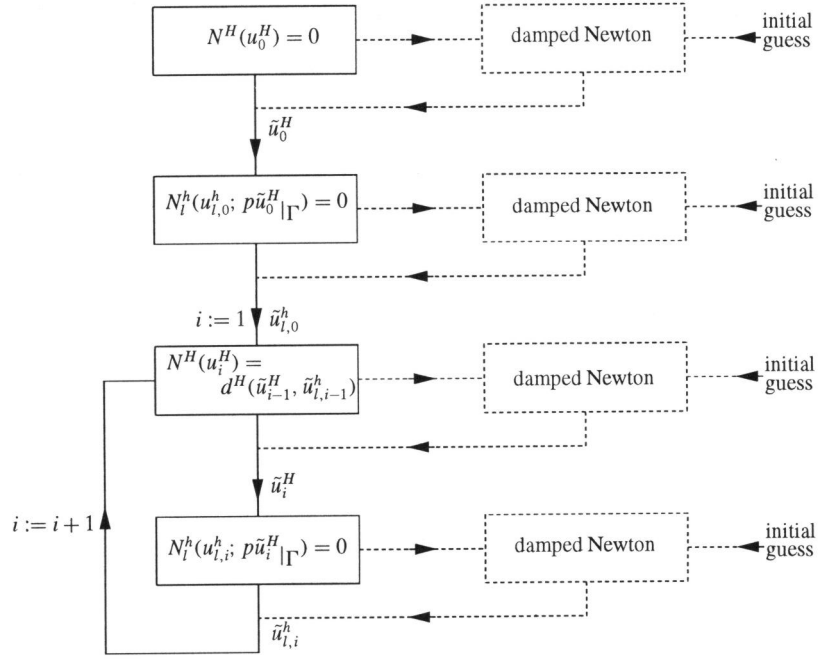
Figure 5.1   Schematic presentation of the nonlinear LDC method.

$\tilde{u}_1^H$ is used to define artificial Dirichlet boundary values on the interface. The related system of nonlinear equations (cf. (5.7)),

$$N_l^h(u_{l,1}^h, \, p\tilde{u}_1^H|_\Gamma) = 0 \qquad \text{on } \Omega_l^h, \tag{5.9}$$

is solved by a damped Newton method, resulting in an approximation $\tilde{u}_{l,1}^h$.

By solving (5.8) and (5.9), one local defect correction step has been carried out. By performing the local defect correction step iteratively, we obtain the *nonlinear LDC method*. We assume that the systems of nonlinear equations occurring in this method all have at least one solution. The nonlinear LDC method consists of an *initialization step* (5.6),(5.7), an *outer local defect correction iteration* and *inner Newton iterations*. In Figure 5.1 the method is presented schematically. The choice of suitable initial guesses for the damped Newton methods will be discussed in Subsection 5.2.2.

As the LDC method for linear boundary value problems (2.16), the nonlinear LDC method is a simple method which is relatively easy to implement. The linear Jacobian systems in the Newton processes are defined on uniform grids and they are relatively small. Hence they can be solved efficiently, for example using iterative solution methods.

5.2.2 Mathematical Formulation of the Nonlinear LDC Method

It is not a priori clear that for the systems of nonlinear equations which are obtained in the nonlinear LDC method a solution exists. In the description of the method in Subsection 5.2.1 it is simply assumed that each system of nonlinear equations occurring in the method has a solution. If a system occurs for which no solution exists, then the nonlinear LDC method breaks down. In this subsection we introduce certain reasonable conditions to assure that the nonlinear LDC method is well-defined in a neighbourhood of the desired continuous solution. For Newton's method such conditions are well-known. For the nonlinear LDC method the situation is somewhat more involved than for Newton's method since we have to deal with systems of nonlinear equations on two different grids and these systems result from the local defect correction process itself. In the approach below we assume that a fixed point of the nonlinear LDC iteration exists. We start with some preliminaries.

As in Section 3.1 we assume that the discretization process on the uniform grid Ω^H uses neighbouring grid points only. We introduce the operator $N_l^H : \mathcal{F}(\Omega_l^H) \times \mathcal{F}(\Gamma^H) \to \mathcal{F}(\Omega_l^H)$ which represents the operator N^H from (5.6) inside the subregion Ω_l (cf. (3.9)):

$$N_l^H(w^H|_{\Omega_l^H}, w^H|_\Gamma) := (N^H(w^H))|_{\Omega_l^H}, \qquad w^H \in \mathcal{F}(\Omega^H). \tag{5.10}$$

The system of nonlinear equations

$$N_l^H(u_l^H, u_\Gamma^H) = 0 \qquad \text{on } \Omega_l^H, \tag{5.11}$$

with $u_l^H \in \mathcal{F}(\Omega_l^H)$, $u_\Gamma^H \in \mathcal{F}(\Gamma^H)$, results from discretizing the differential equation $N(u) = 0$ on the local coarse grid Ω_l^H, using the Dirichlet boundary values $u = \varphi$ on $\partial\Omega_l \cap \partial\Omega$ and $u(\mathbf{x}) = u_\Gamma^H(\mathbf{x})$ at $\mathbf{x} \in \Gamma^H$. Using (5.10) and with u_{i-1}^H and $u_{l,i-1}^h$ given, a local defect correction step is formulated by:

$$\text{find a solution } u_i^H \text{ of} \qquad N^H(v^H) = \begin{bmatrix} N_l^H(u_{l,i-1}^h|_{\Omega_l^H}, u_{i-1}^H|_\Gamma) \\ \emptyset \end{bmatrix}, \tag{5.12a}$$

$$\text{find a solution } u_{l,i}^h \text{ of} \qquad N_l^h(v_l^h, pu_i^H|_\Gamma) = 0. \tag{5.12b}$$

In (5.12a) a block partitioning corresponding to the direct sum $\mathcal{F}(\Omega^H) = \mathcal{F}(\Omega_l^H) \oplus \mathcal{F}(\Omega_c^H)$ is used. We assume that the nonlinear boundary value problem (5.1) has an *isolated solution* $u^\star$, that is, there is a neighbourhood of $u^\star$ which contains no other solution of (5.1).

Definition 5.1 For given operators N^H, N_l^h, N_l^H, p, and norms $\| \ \|_{\Omega^H} : \mathcal{F}(\Omega^H) \to \mathbb{R}$ and $\| \ \|_{\Omega_l^h} : \mathcal{F}(\Omega_l^h) \to \mathbb{R}$, the grid function $u^H \in \mathcal{F}(\Omega^H)$ is called *LDC coarse grid approximation* of $u^\star$ if there exist balls

(a) $\qquad\qquad B_1 := \{v \in \mathcal{F}(\Omega^H) \mid \|v - u^\star|_{\Omega^H}\|_{\Omega^H} < r_1\},$

(b) $\qquad\qquad B_2 := \{v \in \mathcal{F}(\Omega_l^h) \mid \|v - u^\star|_{\Omega_l^h}\|_{\Omega_l^h} < r_2\},$

with $r_1 > 0$, $r_2 > 0$, such that the following conditions are fulfilled:

(i)   The system of nonlinear equations

$$N_l^h(v_l^h, pu^H|_\Gamma) = 0$$

has a unique solution $u_l^h \in B_2$.

(ii)   The system of nonlinear equations

$$N^H(v^H) = \begin{bmatrix} N_l^H(u_l^h|_{\Omega_l^H}, u^H|_\Gamma) \\ \emptyset \end{bmatrix},$$

with u_l^h from (i), has a unique solution $w^H \in B_1$, and $w^H = u^H$.

We assume that an LDC coarse grid approximation $\hat{u}^H$ of $u^\star$ exists. The corresponding local fine grid approximation (cf. condition (i) in Definition 5.1) is denoted by $\hat{u}_l^h$. We introduce the notation

$$B(\hat{u}^H, \varepsilon) := \{v \in \mathcal{F}(\Omega^H) \mid \|v - \hat{u}^H\|_{\Omega^H} < \varepsilon\},$$

$$B(\hat{u}_l^h, \varepsilon) := \{v \in \mathcal{F}(\Omega_l^h) \mid \|v - \hat{u}_l^h\|_{\Omega_l^h} < \varepsilon\},$$

where the same norms on Ω^H and Ω_l^h are used as in Definition 5.1. In the following theorem we give sufficient conditions for the systems of nonlinear equations in the local defect correction iteration to have a locally unique solution.

Theorem 5.2 *Assume that:*

A0.   An LDC coarse grid approximation $\hat{u}^H$ of $u^\star$ exists. The corresponding local fine grid approximation is denoted by $\hat{u}_l^h$.

A1. $\exists \varepsilon_1 > 0$ such that for all $\tilde{u}^H \in B(\hat{u}^H, \varepsilon_1)$ the system of nonlinear equations

$$N_l^h(v_l^h, p\tilde{u}^H|_\Gamma) = 0,$$

has a unique solution $w_l^h \in B_2$ and the mapping $\tilde{u}^H \to w_l^h$ is continuous.

A2. $\exists \varepsilon_2, \varepsilon_3 > 0$ such that for all $\tilde{u}_l^h \in B(\hat{u}_l^h, \varepsilon_2)$, $\tilde{u}^H \in B(\hat{u}^H, \varepsilon_3)$ the system of nonlinear equations

$$N^H(v^H) = \begin{bmatrix} N_l^H(\tilde{u}_l^h|_{\Omega_l^H}, \tilde{u}^H|_\Gamma) \\ \emptyset \end{bmatrix}$$

has a unique solution $w^H \in B_1$.

For $\varepsilon_4 > 0$ small enough the assumptions A1,A2 induce a mapping $B(\hat{u}^H, \varepsilon_4) \to B_1$ which is given by $\tilde{u}^H \to w_l^h \to w^H$, with w_l^h as in A1 and w^H as in A2 with $\tilde{u}_l^h = w_l^h$.
Assume that:

A3. $\|w^H - \hat{u}^H\|_{\Omega^H} \leq \|\tilde{u}^H - \hat{u}^H\|_{\Omega^H}.$

Then for all initial approximations $u_0^H \in B(\hat{u}^H, \varepsilon_0)$, with $\varepsilon_0 > 0$ sufficiently small, the following LDC iteration is well-defined:

$$\text{find} \qquad u_{l,0}^h \in B_2 \quad : \quad N_l^h(u_{l,0}^h, pu_0^H|_\Gamma) = 0, \tag{5.13a}$$

for $i \geq 1$:

$$\text{find} \qquad u_i^H \in B_1 \quad : \quad N^H(u_i^H) = \begin{bmatrix} N_l^H(u_{l,i-1}^h|_{\Omega_l^H}, u_{i-1}^H|_\Gamma) \\ \emptyset \end{bmatrix}, \tag{5.13b}$$

$$\text{find} \qquad u_{l,i}^h \in B_2 \quad : \quad N_l^h(u_{l,i}^h, pu_i^H|_\Gamma) = 0, \tag{5.13c}$$

and $(\hat{u}^H, \hat{u}_l^h)$ is a fixed point of this LDC iteration.

Proof. From A1 we have that if $\|\tilde{u}^H - \hat{u}^H\|_{\Omega^H} < \varepsilon_1$, then

$$N_l^h(u_l^h, p\tilde{u}^H|_\Gamma) = 0$$

has a unique solution $w_l^h \in B_2$ and

$$\forall \varepsilon > 0 \; \exists \delta > 0 : \|\tilde{u}^H - \hat{u}^H\|_{\Omega^H} < \delta < \varepsilon_1 \; \Rightarrow \; \|w_l^h - \hat{u}_l^h\|_{\Omega_l^h} < \varepsilon.$$

Take $0 < \delta_0 < \varepsilon_1$ such that $\|\tilde{u}^H - \hat{u}^H\|_{\Omega^H} < \delta_0$ implies $\|w_l^h - \hat{u}_l^h\|_{\Omega_l^h} < \varepsilon_2$, with ε_2 from A2. Define $\varepsilon_0 := \min\{\delta_0, \varepsilon_3, \varepsilon_4\}$, with ε_3 from A2, ε_4 from A3.
For $u_i^H \in B(\hat{u}^H, \varepsilon_0)$ we have by A1 that

$$N_l^h(u_l^h, pu_i^H|_\Gamma) = 0$$

has a unique solution $u_{l,i}^h \in B_2$, and by A2 that

$$N^H(u^H) = \begin{bmatrix} N_l^H(u_{l,i}^h|_{\Omega_l^H}, u_i^H|_\Gamma) \\ \emptyset \end{bmatrix}$$

has a unique solution $u_{i+1}^H \in B_1$ with, by A3, $\|u_{i+1}^H - \hat{u}^H\|_{\Omega^H} \leq \|u_i^H - \hat{u}^H\|_{\Omega^H} < \varepsilon_0$.
So $u_{i+1}^H \in B(\hat{u}^H, \varepsilon_0)$. If $u_0^H \in B(\hat{u}^H, \varepsilon_0)$ then it follows by induction that the systems of nonlinear equations in (5.13) have a (locally) unique solution and hence the LDC iteration (5.13) is well-defined.
Since $\hat{u}^H$ is an LDC coarse grid approximation of $u^\star$ the system of nonlinear equations

$$N_l^h(v_l^h, p\hat{u}^H|_\Gamma) = 0$$

has a unique solution $\hat{u}_l^h \in B_2$ (cf. Definition 5.1.i). By Definition 5.1.ii the system of nonlinear equations

$$N^H(v^H) = \begin{bmatrix} N_l^H(\hat{u}_l^h|_{\Omega_l^H}, \hat{u}^H|_\Gamma) \\ \emptyset \end{bmatrix}$$

has the unique solution $\hat{u}^H \in B_1$. Thus $(\hat{u}^H, \hat{u}_l^h)$ is a fixed point of (5.13). ∎

In the remark below we comment on the assumptions A1,A2,A3 in Theorem 5.2.

Remark 5.3 - Assumption A1 follows from the *implicit function theorem* (see e.g. [52, Section 5.2]) if the partial derivative

$$\frac{\partial N_l^h}{\partial u_l^h} : \mathcal{F}(\Omega_l^h) \times \mathcal{F}(\Gamma^h) \rightarrow L(\mathcal{F}(\Omega_l^h), \mathcal{F}(\Omega_l^h))$$

exists in a neighbourhood of $(\hat{u}_l^h, p\hat{u}^H|_\Gamma)$ and is continuous at $(\hat{u}_l^h, p\hat{u}^H|_\Gamma)$ and if

$$\frac{\partial N_l^h}{\partial u_l^h}(\hat{u}_l^h, p\hat{u}^H|_\Gamma)$$

is nonsingular. Here $L(\mathcal{F}(\Omega_l^h), \mathcal{F}(\Omega_l^h))$ denotes the space of linear mappings $\mathcal{F}(\Omega_l^h) \rightarrow \mathcal{F}(\Omega_l^h)$.
- Assumption A2 follows if N_l^H from (5.10) is continuous at $(\hat{u}_l^h|_{\Omega_l^H}, \hat{u}^H|_\Gamma)$ and if N^H is a local homeomorphism at $\hat{u}^H$. The latter follows from the *inverse function theorem* (see e.g. [52, Section 5.2]) if the derivative

$$\frac{\partial N^H}{\partial u^H} : \mathcal{F}(\Omega^H) \rightarrow L(\mathcal{F}(\Omega^H), \mathcal{F}(\Omega^H))$$

exists in a neighbourhood of $\hat{u}^H$ and is continuous at $\hat{u}^H$ and if

$$\frac{\partial N^H}{\partial u^H}(\hat{u}^H)$$

is nonsingular. Here $L(\mathcal{F}(\Omega^H), \mathcal{F}(\Omega^H))$ denotes the space of linear mappings $\mathcal{F}(\Omega^H) \rightarrow \mathcal{F}(\Omega^H)$.
- Assumption A3 states that the mapping $\tilde{u}^H \rightarrow w^H$, representing a well-defined nonlinear local defect correction step, is *non-expansive*: by performing a nonlinear local defect correction step one does not obtain a worse approximation of the coarse grid LDC approximation $\hat{u}^H$. □

In the nonlinear LDC method in Subsection 5.2.1 the initial approximation u_0^H results from the basic discretization

$$N^H(u^H) = 0 \qquad \text{on } \Omega^H. \tag{5.14}$$

Assume that (5.14) has a unique solution $w^H \in B_1$ and take $u_0^H := w^H$. This yields a suitable initial approximation for the local defect correction iteration (5.13) if u_0^H is sufficiently close to $\hat{u}^H$, i.e. if $\|u_0^H - \hat{u}^H\|_{\Omega^H} < \varepsilon_0$, with ε_0 as in Theorem 5.2.

The systems of nonlinear equations in (5.13) are *locally* uniquely solvable. Outside the ball B_2 the local fine grid problems in (5.13a,c) may have other solutions (see Example 5.4). If Newton's method is used for solving these local fine grid problems then a suitable initial guess is required such that the Newton iteration converges to the solution inside the ball B_2. For other initial guesses Newton's method may diverge or converge to a solution outside the ball B_2. This results in a breakdown of the nonlinear local defect correction iteration (5.13). In a similar way a breakdown of the nonlinear local correction iteration (5.13) may occur when solving the global coarse grid problems in (5.13b) by Newton's method. So, sufficiently good initial guesses for Newton's method are required for *all* systems of nonlinear equations in (5.13). For the systems of nonlinear equations (5.13b) and (5.13c), obvious initial guesses are provided by the LDC iteration itself,

namely the previously computed approximations u_{i-1}^H and $u_{l,i-1}^h$. Numerical results indicate that in general these approximations are indeed sufficiently good initial guesses. For the system

$$N_l^h(u_{l,0}^h, pu_0^H|_\Gamma) = 0 \qquad \text{on } \Omega_l^h, \tag{5.15}$$

an obvious initial guess is provided by interpolating the coarse grid approximation u_0^H on the local fine grid Ω_l^h. Often this interpolation approach yields a suitable initial guess. This approach shall be used in the numerical experiments in Chapter 6, where the nonlinear LDC method is applied to a concrete nonlinear problem resulting from combustion modelling. If the coarse grid approximation u_0^H is too inaccurate inside Ω_l to provide a suitable initial guess, both for (5.14) and for (5.15) initial guesses for Newton's method have to be specified explicitly.

In the following example the dependence of the nonlinear LDC method on the choice for the initial guess in Newton's method for (5.15) is illustrated.

Example 5.4 Consider the nonlinear two-point boundary value problem (in e.g., [51, Section 3.I], [57, Section 10.6])

$$\varepsilon u_{xx} = 1 - (u_x)^2, \quad 0 < x < 1,$$
$$u(0) = 0, \; u(1) = 1/2. \tag{5.16}$$

From [57] we have the result

$$\lim_{\varepsilon \downarrow 0} u(x, \varepsilon) = \begin{cases} -x & 0 \le x \le 1/4, \\ x - 1/2 & 1/4 \le x \le 1. \end{cases}$$

For $\varepsilon \ll 1$ this problem has a unique solution with a high activity region near $x = 1/4$. We take $\varepsilon = 0.01$, $\Omega_l = (0.15, 0.35)$, $H = 1/20$ and $\sigma = 8$. Both the first and second order derivative in (5.16) are discretized using central differences. The approximation u^h resulting from discretizing the boundary value problem (5.16) on a uniform global grid with grid size $h = 1/160$ is shown in Figure 5.2.a by the solid line.

As initial guess in the damped Newton method for the coarse grid problem (5.14) we use an approximation u_s^H of the solution of the boundary value problem (5.16) for $\varepsilon = \varepsilon_s = 0.1$. This approximation is shown in Figure 5.2.a. The corresponding solution $\tilde{u}^H$ of (5.14) is shown in Figure 5.2.b.

We consider *two* initial guesses for the damped Newton method for the local fine grid problem (5.15). The first is the linear interpolant of the approximation $\tilde{u}^H$ inside Ω_l. In Figure 5.2.c this initial guess and the corresponding solution of (5.15) are shown. The nonlinear LDC method converges to the approximations shown in Figure 5.2.d.

The second initial guess is the linear interpolant of u_s^H inside Ω_l. At the interface grid points $x = 0.15$ and $x = 0.35$ the values $\tilde{u}^H(0.15)$ and $\tilde{u}^H(0.35)$ are prescribed. In Figure 5.2.e this initial guess and the corresponding solution of (5.15) are shown. In this case the nonlinear LDC method (5.13) converges to the approximations shown in Figure 5.2.f, which are completely different from the approximations in Figure 5.2.d.

We observe that the local fine grid discretization (5.15) has at least two solutions. Only one of these two solutions is 'close' to the desired continuous solution (namely the solution in Fig-
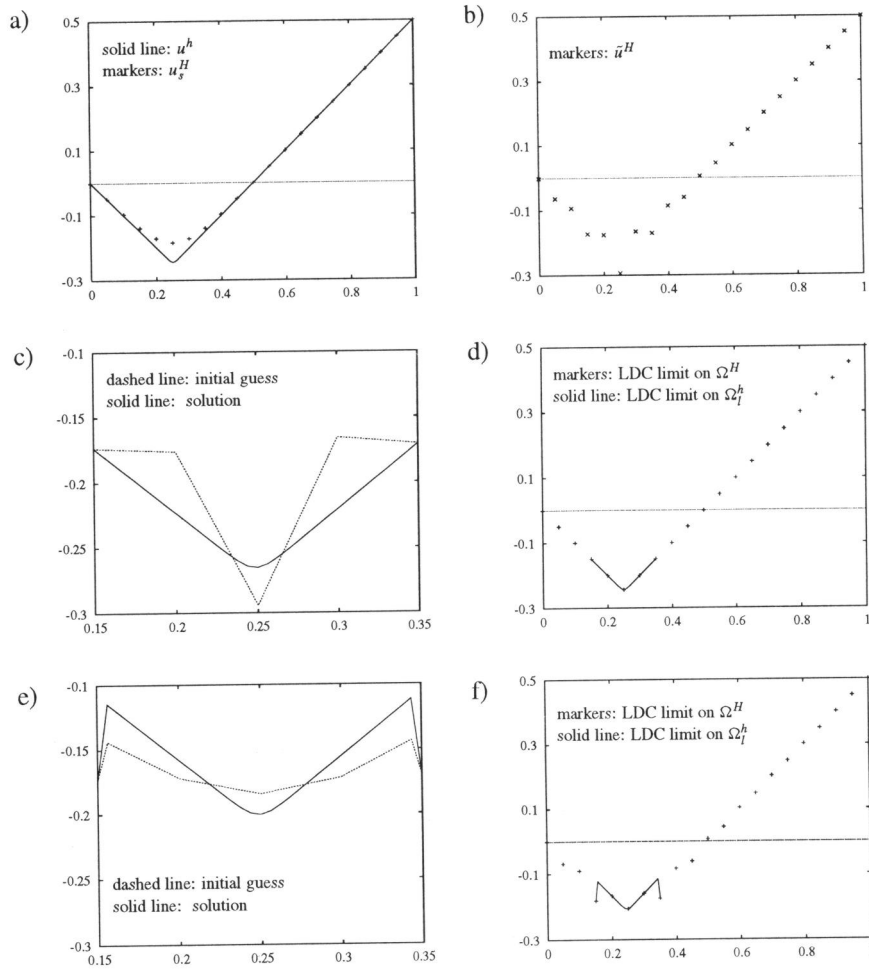
Figure 5.2 Approximations of the solution of the boundary value problem in Example 5.4; $H = 1/20$, $\sigma = 8$, $\Omega_l = (0.15, 0.35)$. a) global fine grid approximation u^h and Newton initial guess u_s^H; b) global coarse grid approximation $\tilde{u}^H$; c,e) Newton initial guess for local fine grid problem and corresponding solution; d,f) approximations resulting from nonlinear LDC method.

ure 5.2.c) and results in a satisfactory LDC process. We note that for $\varepsilon \leq 0.008$ the damped Newton method for (5.15) does not converge if the linear interpolant of $\tilde{u}^H$ inside Ω_l is used as initial guess.   □

In Chapter 6 the nonlinear LDC method is applied to a concrete nonlinear boundary value problem resulting from combustion modelling. For this problem the nonlinear LDC method performs well if the obvious initial guesses as described above are used.

As in the linear case, the LDC process is closely related to a system of nonlinear equations on the composite grid $\Omega^{H,h}$. We introduce the following system of nonlinear equations:

$$N^{H,h}(u^{H,h}) := \begin{bmatrix} N_l^h(u^{H,h}|_{\Omega_l^h}, pu^{H,h}|_\Gamma) \\ N_c^H(u^{H,h}|_{\Omega_c^H}, u^{H,h}|_{\tilde{\Gamma}^H}) \end{bmatrix} = 0 \qquad \text{on } \Omega^{H,h}, \qquad (5.17)$$

where a block partitioning corresponding to the direct sum $\mathcal{F}(\Omega^{H,h}) = \mathcal{F}(\Omega_l^h) \oplus \mathcal{F}(\Omega_c^H)$ is used. The operator $N_c^H : \mathcal{F}(\Omega_c^H) \times \mathcal{F}(\tilde{\Gamma}^H) \to \mathcal{F}(\Omega_c^H)$ represents the operator N^H outside the subregion Ω_l (cf. (3.13)):

$$N_c^H(w^H|_{\Omega_c^H}, w^H|_{\tilde{\Gamma}^H}) := (N^H(w^H))|_{\Omega_c^H}, \qquad w^H \in \mathcal{F}(\Omega^H), \qquad (5.18)$$

with Ω_c^H from (3.4) and $\tilde{\Gamma}^H$ from (3.3).

The composite grid problem (5.17) is the nonlinear counterpart of the composite grid problem (3.18). The system of nonlinear equations (5.17) results from discretizing the boundary value problem (5.1) on the composite grid $\Omega^{H,h}$ using uniform finite difference stencils at all grid points. So, the composite grid points on the interface are treated *as if they were grid points of the uniform grid* Ω^H. The composite grid points which lie inside the subregion Ω_l are discretized as uniform fine grid points using the interpolation operator $p : \mathcal{F}(\Gamma^H) \to \mathcal{F}(\Gamma^h)$ to eliminate the values at the slave points.

Theorem 5.5 *The composite grid function*

$$\bar{u}^{H,h} := \begin{bmatrix} \bar{u}_l^h \\ \bar{u}^H|_{\Omega_c^H} \end{bmatrix}, \qquad (5.19)$$

where $(\bar{u}^H, \bar{u}_l^h)$ is a fixed point of the nonlinear LDC iteration (5.13), is a solution of (5.17).

Proof. If $(\bar{u}^H, \bar{u}_l^h)$ is a fixed point of (5.13) we obtain:

$$N_l^h(\bar{u}_l^h, p\bar{u}^H|_\Gamma) = 0,$$
$$N^H(\bar{u}^H) = \begin{bmatrix} N_l^H(\bar{u}_l^h|_{\Omega_l^H}, \bar{u}^H|_\Gamma) \\ \emptyset \end{bmatrix}.$$

From the latter equation we obtain

$$N_c^H(\bar{u}^H|_{\Omega_c^H}, \bar{u}^H|_{\tilde{\Gamma}^H}) = 0.$$

Now $N^{H,h}(\bar{u}^{H,h}) = 0$ follows immediately from the definition of $\bar{u}^{H,h}$ in (5.19). ∎

5.3   A COMBINATION OF NEWTON'S METHOD AND THE FAC METHOD

As we have seen in Theorem 5.5 the nonlinear LDC method is closely related to the composite grid problem (5.17). In this section we assume that locally (5.17) has a unique solution. If one of the systems of nonlinear equations which are implicitly defined in the nonlinear LDC method does not have a solution, then the nonlinear LDC method breaks down and can not be used to solve the nonlinear boundary value problem (5.1) on the composite grid $\Omega^{H,h}$. In this section we describe a method for solving (5.1) on $\Omega^{H,h}$ which uses only *one* system of nonlinear equations, namely the composite grid problem (5.17). The method is a combination of the damped Newton method and the fast adaptive composite grid (FAC) method from Section 2.3.

In each Newton step a *system of linear equations* has to be solved:

$$\frac{\partial N^{H,h}}{\partial u^{H,h}}(\tilde{u}^{H,h})v^{H,h} = -N^{H,h}(\tilde{u}^{H,h}), \tag{5.20}$$

with $\tilde{u}^{H,h}$ a composite grid function and

$$\frac{\partial N^{H,h}}{\partial u^{H,h}} : \mathcal{F}(\Omega^{H,h}) \to L(\mathcal{F}(\Omega^{H,h}), \mathcal{F}(\Omega^{H,h})). \tag{5.21}$$

Here and in the remainder of this section we use the notation $L(V, W)$ to denote the set of linear mappings $V \to W$. In (5.20) $\frac{\partial N^{H,h}}{\partial u^{H,h}}(\tilde{u}^{H,h})$ denotes the Jacobian matrix evaluated at $\tilde{u}^{H,h}$. Below we shall show that the Jacobian matrix in (5.20) has a typical composite grid structure which is similar to the structure of $L^{H,h}$ in (3.18).

For the nonlinear operators $N_l^h : \mathcal{F}(\Omega_l^h) \times \mathcal{F}(\Gamma^h) \to \mathcal{F}(\Omega_l^h)$ and $N_c^H : \mathcal{F}(\Omega_c^H) \times \mathcal{F}(\tilde{\Gamma}^H) \to \mathcal{F}(\Omega_c^H)$ in (5.17) we introduce the *partial derivatives*:

$$
\begin{aligned}
\frac{\partial N_l^h}{\partial u_l^h} &: \mathcal{F}(\Omega_l^h) \times \mathcal{F}(\Gamma^h) \to L(\mathcal{F}(\Omega_l^h), \mathcal{F}(\Omega_l^h)), \\[4pt]
\frac{\partial N_l^h}{\partial u_\Gamma^h} &: \mathcal{F}(\Omega_l^h) \times \mathcal{F}(\Gamma^h) \to L(\mathcal{F}(\Gamma^h), \mathcal{F}(\Omega_l^h)), \\[4pt]
\frac{\partial N_c^H}{\partial u_c^H} &: \mathcal{F}(\Omega_c^H) \times \mathcal{F}(\tilde{\Gamma}^H) \to L(\mathcal{F}(\Omega_c^H), \mathcal{F}(\Omega_c^H)), \\[4pt]
\frac{\partial N_c^H}{\partial u_{\tilde{\Gamma}}^H} &: \mathcal{F}(\Omega_c^H) \times \mathcal{F}(\tilde{\Gamma}^H) \to L(\mathcal{F}(\tilde{\Gamma}^H), \mathcal{F}(\Omega_c^H)).
\end{aligned}
\tag{5.22}
$$

We introduce a short notation for the partial derivatives in (5.22), evaluated at a grid function $w \in \mathcal{F}(\Omega^{H,h})$:

$$
\begin{aligned}
\frac{\partial N_l^h}{\partial v}(w) &:= \frac{\partial N_l^h}{\partial v}(w_{|\Omega_l^h}, pw_{|\Gamma^H}), & v &= u_l^h, u_\Gamma^h, \\[4pt]
\frac{\partial N_c^H}{\partial v}(w) &:= \frac{\partial N_c^H}{\partial v}(w_{|\Omega_c^H}, w_{|\tilde{\Gamma}^H}), & v &= u_l^H, u_{\tilde{\Gamma}}^H.
\end{aligned}
\tag{5.23}
$$

In the following lemma we use a partitioning corresponding to $\mathcal{F}(\Omega^{H,h}) = \mathcal{F}(\Omega_l^h) \oplus \mathcal{F}(\Omega_c^H)$.

Lemma 5.6 *For $u^{H,h} \in \mathcal{F}(\Omega^{H,h})$ we have*

$$\frac{\partial N^{H,h}}{\partial u^{H,h}}(u^{H,h}) = \begin{bmatrix} \dfrac{\partial N_l^h}{\partial u_l^h}(u^{H,h}) & \dfrac{\partial N_l^h}{\partial u_\Gamma^h}(u^{H,h}) \, pr_\Gamma \\[3mm] \dfrac{\partial N_c^H}{\partial u_{\tilde{\Gamma}}^H}(u^{H,h}) \, r_{\tilde{\Gamma}} & \dfrac{\partial N_c^H}{\partial u_c^H}(u^{H,h}) \end{bmatrix}, \tag{5.24}$$

with r_Γ and $r_{\tilde{\Gamma}}$ the trivial injections from (3.17).

Proof. $N^{H,h}(u^{H,h})$ can be written as

$$N^{H,h}(u^{H,h}) = \begin{bmatrix} N_l^h(u^{H,h}|_{\Omega_l^h}, \, pr_\Gamma u^{H,h}|_{\Omega_c^H}) \\[3mm] N_c^H(u^{H,h}|_{\Omega_c^H}, \, r_{\tilde{\Gamma}} u^{H,h}|_{\Omega_l^h}) \end{bmatrix},$$

with r_Γ, $r_{\tilde{\Gamma}}$ as in (3.17).
By definition of the derivatives in (5.21) and (5.22), and using the notation from (5.23), we obtain

$$\frac{\partial N^{H,h}}{\partial u^{H,h}}(u^{H,h}) = \begin{bmatrix} \dfrac{\partial N_l^h}{\partial u_l^h}(u^{H,h}) & \dfrac{\partial N_l^h}{\partial u_\Gamma^h}(u^{H,h})\dfrac{d(pr_\Gamma u_c^H)}{du_c^H} \\[4mm] \dfrac{\partial N_c^H}{\partial u_{\tilde{\Gamma}}^H}(u^{H,h})\dfrac{d(r_{\tilde{\Gamma}} u_l^h)}{du_l^h} & \dfrac{\partial N_c^H}{\partial u_c^H}(u^{H,h}) \end{bmatrix}.$$

Now (5.24) follows since p, r_Γ, and $r_{\tilde{\Gamma}}$ are linear operators. ∎

For the nonlinear operator N_l^H from (5.10) we introduce the *partial derivatives*:

$$\begin{aligned} \frac{\partial N_l^H}{\partial u_l^H} &: \mathcal{F}(\Omega_l^H) \times \mathcal{F}(\Gamma^H) \to L(\mathcal{F}(\Omega_l^H), \mathcal{F}(\Omega_l^H)), \\[2mm] \frac{\partial N_l^H}{\partial u_\Gamma^H} &: \mathcal{F}(\Omega_l^H) \times \mathcal{F}(\Gamma^H) \to L(\mathcal{F}(\Gamma^H), \mathcal{F}(\Omega_l^H)). \end{aligned} \tag{5.25}$$

We introduce a short notation for the partial derivatives of N_l^H and N_c^H, evaluated at a grid function $w \in \mathcal{F}(\Omega^H)$:

$$\begin{aligned} \frac{\partial N_l^H}{\partial v}(w) &:= \frac{\partial N_l^H}{\partial v}(w|_{\Omega_l^H}, w|_{\Gamma^H}), & v &= u_l^H, u_\Gamma^H, \\[2mm] \frac{\partial N_c^H}{\partial v}(w) &:= \frac{\partial N_c^H}{\partial v}(w|_{\Omega_c^H}, w|_{\tilde{\Gamma}^H}), & v &= u_l^H, u_\Gamma^H. \end{aligned} \tag{5.26}$$

We define the *trivial injection* $\tilde{r}_{\tilde{\Gamma}} : \mathcal{F}(\Omega_l^H) \to \mathcal{F}(\tilde{\Gamma}^H)$ by

$$\tilde{r}_{\tilde{\Gamma}} w := w|_{\tilde{\Gamma}^H}, \qquad w \in \mathcal{F}(\Omega_l^H). \tag{5.27}$$

In the following lemma we use a partitioning corresponding to $\mathcal{F}(\Omega^H) = \mathcal{F}(\Omega_l^H) \oplus \mathcal{F}(\Omega_c^H)$.

Lemma 5.7 *For $u^H \in \mathcal{F}(\Omega^H)$ we have*

$$\frac{\partial N^H}{\partial u^H}(u^H) = \left[\begin{array}{cc} \dfrac{\partial N_l^H}{\partial u_l^H}(u^H) & \dfrac{\partial N_l^H}{\partial u_\Gamma^H}(u^H)\, r_\Gamma \\[2ex] \dfrac{\partial N_c^H}{\partial u_{\tilde{\Gamma}}^H}(u^H)\, \tilde{r}_{\tilde{\Gamma}} & \dfrac{\partial N_c^H}{\partial u_c^H}(u^H) \end{array} \right], \qquad (5.28)$$

with the trivial injections r_Γ from (3.17b) and $\tilde{r}_{\tilde{\Gamma}}$ from (5.27).

Proof. From (5.10) and (5.18) we find

$$N^H(u^H) = \left[\begin{array}{c} N_l^H(u^H|_{\Omega_l^H}, r_\Gamma u^H|_{\Omega_c^H}) \\[2ex] N_c^H(u^H|_{\Omega_c^H}, \tilde{r}_{\tilde{\Gamma}} u^H|_{\Omega_l^H}) \end{array} \right],$$

with r_Γ from (3.17b) and $\tilde{r}_{\tilde{\Gamma}}$ from (5.27).

By definition of the partial derivatives in (5.22) and (5.25), and using the notation from (5.23) and (5.26), we obtain

$$\frac{\partial N^H}{\partial u^H}(u^H) = \left[\begin{array}{cc} \dfrac{\partial N_l^H}{\partial u_l^H}(u^H) & \dfrac{\partial N_l^H}{\partial u_\Gamma^H}(u^H)\dfrac{d(r_\Gamma u_c^H)}{du_c^H} \\[3ex] \dfrac{\partial N_c^H}{\partial u_{\tilde{\Gamma}}^H}(u^H)\dfrac{d(\tilde{r}_{\tilde{\Gamma}} u_l^H)}{du_l^H} & \dfrac{\partial N_c^H}{\partial u_c^H}(u^H) \end{array} \right].$$

Now (5.28) follows since r_Γ and $\tilde{r}_{\tilde{\Gamma}}$ are linear operators.   ∎

Theorem 5.8 *Given a composite grid function $\tilde{u}^{H,h}$, the composite grid Jacobian matrix $L^{H,h} := \frac{\partial N^{H,h}}{\partial u^{H,h}}(\tilde{u}^{H,h})$ satisfies*

$$L^{H,h} = \left[\begin{array}{cc} L_l^h & L_\Gamma^h\, pr_\Gamma \\[1ex] L_{\tilde{\Gamma}}^H\, r_{\tilde{\Gamma}} & L_c^H \end{array} \right],$$

and the global coarse grid Jacobian matrix $L^H := \frac{\partial N^H}{\partial u^H}(\tilde{u}^{H,h}|_{\Omega^H})$ satisfies

$$L^H = \left[\begin{array}{cc} L_l^H & L_\Gamma^H\, pr_\Gamma \\[1ex] L_{\tilde{\Gamma}}^H\, \tilde{r}_{\tilde{\Gamma}} & L_c^H \end{array} \right],$$

with

$$L_l^h := \frac{\partial N_l^h}{\partial u_l^h}(\tilde{u}^{H,h}), \qquad L_\Gamma^h := \frac{\partial N_l^h}{\partial u_\Gamma^h}(\tilde{u}^{H,h}),$$

$$L_c^H := \frac{\partial N_c^H}{\partial u_c^H}(\tilde{u}^{H,h}), \qquad L_{\tilde{\Gamma}}^H := \frac{\partial N_c^H}{\partial u_{\tilde{\Gamma}}^H}(\tilde{u}^{H,h}),$$

$$L_l^H := \frac{\partial N_l^H}{\partial u_l^H}(\tilde{u}^{H,h}|_{\Omega^H}), \qquad L_\Gamma^H := \frac{\partial N_l^H}{\partial u_\Gamma^H}(\tilde{u}^{H,h}|_{\Omega^H}).$$

Proof. This follows immediately from Lemma 5.6 and Lemma 5.7.   ∎

From Theorem 5.8 we find that in each Newton step the fast adaptive composite grid (FAC) method from Section 2.3 can be used for solving the composite grid Jacobian system (5.20) if L^H and L_l^h are nonsingular.

FAC algorithm for solving (5.20)

initial approximation $v_0^{H,h}$ *given*

for $i \geq 1$

define $d^{H,h} := L^{H,h} v_{i-1}^{H,h} + N^{H,h}(\tilde{u}^{H,h})$

solve $L^H w^H = d^{H,h}|_{\Omega^H}$

solve $L_l^h w_l^h = d^{H,h}|_{\Omega_l^h} - L_\Gamma^h \, p w^H|_\Gamma$

define $v_i^{H,h} := v_{i-1}^{H,h} - \begin{bmatrix} w_l^h \\ w^H|_{\Omega_c^H} \end{bmatrix}.$

Remark 5.9 In the FAC method for solving (5.20) the trivial injection is used for restricting the composite grid defect $d^{H,h}$ to the global coarse grid Ω^H. In [22] it is shown that the trivial injection on the interface is optimal in case of a composite grid problem resulting from a discretization process in which interface grid points are treated as if they were grid points of the uniform grid Ω^H. From (5.24) and (5.28) it is clear that in the composite grid Jacobian $\frac{\partial N^{H,h}}{\partial u^{H,h}}(\tilde{u}^{H,h})$ the interface grid points are 'treated as if they were grid points of the uniform grid Ω^H'.   □

Remark 5.10 The composite grid problem (5.20) can also be solved using the LDC method from Section 2.2. We recall from Section 3.4 that the LDC method is actually a special case of the FAC method for solving a composite grid problem like (5.20).   □

The above described combination of the damped Newton method and the FAC method is called the *Newton-FAC* method. It consists of an *outer Newton iteration* for the system of nonlinear equations (5.17) and *inner FAC iterations* for solving the linear Jacobian systems. In Figure 5.3 the method is presented schematically. In practice it is not necessary to solve the Jacobian systems exactly. Often, under the assumption of a reasonable initial approximation $v_0^{H,h}$, a small number of FAC steps is sufficient (see Example 5.11). In Figure 5.3 the approximation of the solution of the Jacobian system in a damped Newton step is denoted by $\hat{v}^{H,h}$.

Contrary to the nonlinear LDC method, in the Newton-FAC method only *one system of nonlinear equations* (viz. (5.17)) is considered. For the damped Newton method to converge to the desired solution $u^{H,h}$ of this system, the initial guess $u_0^{H,h}$ has to be sufficiently close to $u^{H,h}$. In the following example we consider the performance of the Newton-FAC method for the nonlinear boundary value problem from Example 5.4.
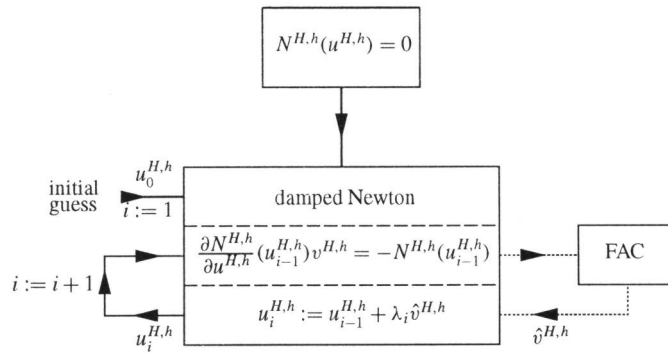
Figure 5.3   Schematic presentation of the Newton-FAC method.

Example 5.11 We consider the nonlinear boundary value problem (5.16). We take a composite grid composed of a uniform global grid with mesh size $H = 1/20$ and a local grid, covering $\Omega_l = (0.15, 0.35)$, with mesh size $h = 1/160$. Both the first and second order derivative in (5.16) are discretized using central differences. The interface grid points $x = 0.15$ and $x = 0.35$ are treated as if they were grid points of the uniform global grid (cf. (5.17)).

First we take $\varepsilon = 0.01$ and $\varepsilon_s = 0.1$ as in Example 5.4. The initial guess for the damped Newton method on the composite grid is obtained from the approximation u_s^H from Example 5.4 by linear interpolation inside Ω_l. We recall that u_s^H results from solving the boundary value problem (5.16) for $\varepsilon = \varepsilon_s$ on the global coarse grid Ω^H. In Table 5.1 the number of Newton steps required to obtain a composite grid function $u_i^{H,h}$ with $\|N^{H,h}(u_i^{H,h})\|_\infty < 10^{-6}$ is presented as a function of the number of FAC iterates used to solve the Jacobian systems. For the initial approximation in the FAC algorithm the grid function which is equal to 0 at all composite grid points is used. If 10 FAC steps are performed, the Jacobian systems are solved within machine precision. We observe that if less FAC steps are performed, the convergence rate of the outer Newton iteration does not become significantly worse. If the number of FAC steps becomes too small, the number of required Newton iterations does significantly increase, as expected.

In Example 5.4 we noticed that for $\varepsilon \leq 0.008$ both the 'first initial guess' and the 'second initial guess' do not yield a satisfactory LDC process. The problem of obtaining a suitable initial guess on the local fine grid does not occur in the Newton-FAC method. For example for $\varepsilon = 0.005$, the initial guess as described above and with 5 FAC steps per Newton step, 10 Newton steps are required to obtain a composite grid approximation $\tilde{u}_{10}^{H,h}$ with $\|N^{H,h}(\tilde{u}_{10}^{H,h})\|_\infty < 10^{-6}$. $\square$

number of FAC steps	10	5	4	3	2	1
number of Newton steps	4	5	5	6	9	18

Table 5.1   Number of outer Newton steps required in the Newton-FAC method as a function of the number of inner FAC steps for $\varepsilon_s = 0.1$.

6

NUMERICAL SIMULATION OF FLAT FLAMES ON COMPOSITE GRIDS

An important problem which is always met when modelling combustion processes, is the large difference between the size of the burner (typically ~ 10 cm) and the size of the chemically active layer (typically ~ 1 mm). Most chemical reactions occur in the chemically active layer and thus the field variables (e.g., the temperature) change rapidly inside this layer. Outside this layer the variations in the field variables are much smaller. Hence the numerical simulation of combustion processes requires the use of non-uniform grids in order to obtain accurate approximations and yet keep the number of grid points within reasonable bounds. In this chapter we consider the use of composite grids for the simulation of premixed laminar flat flames.

This chapter is organized as follows. In Section 6.1 a brief introduction to the field of combustion is given. In Section 6.2 we describe the governing equations for reacting gas flow and a one-step reaction mechanism for modelling the chemical reactions in a methane-air flame. The governing equations for the idealized, one-dimensional flame, which is one of the most studied topics in combustion research, are described in Section 6.3. In that section also a two-point boundary value problem for the temperature is derived. The nonlinear LDC method from Chapter 5 is applied to this combustion model problem. Composite grids with refinement factors 10-100 are used. In Section 6.4 characteristic properties of the nonlinear LDC method are illustrated by numerical results. For example, the error in the approximations resulting after 0, 1 and 2 local defect correction steps is considered. At the end of this chapter, in Section 6.5, a discussion of the results is presented.

6.1 INTRODUCTION

For many years, *laminar gas-phase combustion processes* have been the subject of both theoretical and experimental research. In this field, one distinguishes between combustion processes in which the fuel and the oxidizer (usually air) are initially separated (so-called *diffusion flames*) and the combustion of premixed gas mixtures (so-called *premixed laminar flames*). A Bunsen burner with its air hole closed supports a diffusion flame between the gas supplied through the tube and the surrounding oxygen-rich atmosphere. The structure of a diffusion flame is mainly determined

by the speed at which the fuel and oxygen diffuse into the reaction zone. For premixed laminar flames the reactants have already been mixed. A Bunsen burner with its air hole opened, so that a mixture of (natural) gas and air is supplied through the tube, supports a premixed laminar flame. The properties of this flame strongly depend on the composition of the gas mixture. This is due to the fact that if the composition of the gas mixture is varied, other chemical reactions may occur, and the properties of the premixed laminar flame mainly depend on the chemical reactions taking place.

Premixed laminar flames are encountered in industrial and domestic burners. At the Eindhoven University of Technology, premixed laminar flames have been studied since 8 years. The aim of this research is to investigate the influence of variations in the composition of natural gas on the combustion process in domestic applications. Topics such as the flame stability and the prediction the composition of exhaust gases are of main importance. In order to predict the effect of variations in the gas composition on these properties of the combustion process, numerical tools for simulating premixed laminar flames have been developed [17],[40],[58].

The physical basis of a combustion process is completely determined by the interaction between fluid dynamics and chemical reactions. The nature of the governing equations, which is nonlinear and strongly coupled, induces specific problems in the numerical simulation of premixed laminar flames. Two major problems originate from the *differences in time scales and in geometry scales*. In a flame many, often complicated, chemical reactions occur. Each reaction has its own typical time scale. When modelling flames using complex reaction mechanisms, many different orders of magnitude in time scales are present in the mathematical model. Due to this inherent stiffness, the computational costs for solving the governing combustion equations are very high when a detailed chemical model is used. Often combustion processes are modelled using simple reaction mechanisms. The most simple reaction mechanism is the *one-step overall chemical model* (see Subsection 6.2.4).

The differences in geometry scales occur both for simple and for complex reaction models, since the size of the chemically active layer is small (typically ~ 1 mm) compared to the size of the computational domain (typically ~ 10 cm). Almost all reactions take place in the chemically active layer, and the combustion variables (e.g., the mass fractions of the species in the gas mixture and the temperature) rapidly vary in a small part of the computational domain containing the chemically active layer. In this part of the domain very large gradients in the variables occur. For example for the temperature an increase of 10^3-10^4 °C/mm may occur. In order to obtain an accurate numerical solution of the governing combustion equations, a very small grid size is required in a neighbourhood of the chemically active layer. Away from the chemically active layer the variations in the variables are much smaller. So, in the greater part of the computational domain a much larger grid size can be used. If a single uniform grid were used, the number of unknowns would become excessive and the calculation would become inefficient. Therefore *non-uniform grids* have to be used when modelling premixed laminar flames.

In this chapter we use *composite grids* and the *composite grid methods* from Chapter 5 for the numerical simulation of combustion processes. For more-dimensional premixed laminar flames with detailed chemistry one has to deal with many different (numerical) problems. Here we restrict ourselves to the problem originating from the differences in the geometry scales and we consider a one-dimensional combustion process, the so-called *premixed laminar flat flame*, with

a one-step reaction mechanism. A composite grid composed of a global uniform coarse grid, covering the computational domain with a grid size H, and a local uniform fine grid, covering a small part of the domain, including the chemically active layer, with a grid size h, is used. Since the variations of the combustion variables are much larger inside the chemically active layer than outside this layer, the grid size h is taken much smaller than H.

First, in Section 6.2, we describe the governing equations for premixed laminar flames.

6.2 MODELLING OF PREMIXED LAMINAR FLAMES

6.2.1 The conservation equations for reacting gas flow

We consider a gas mixture consisting of N different chemical species, denoted by $\mathcal{M}_i$ ($i = 1, 2, \ldots, N$), in which M chemical reactions take place. For reacting gas flows, chemical reactions between the constituent species need to be modelled together with the fluid dynamics. Therefore, we consider the *conservation equations for reacting gas flow*. These equations represent the conservation of mass, momentum and energy of the total mixture and the balance of mass for the various species. The latter equations include source terms which describe the chemical reactions taking place. Below we briefly describe the conservation equations for reactive gas flow. For a detailed derivation of these conservations equations we refer to [60],[68].

Balance of mass for the various species requires

$$\partial(\rho Y_i)/\partial t + \nabla \cdot (\rho Y_i \mathbf{v}_i) = w_i, \quad i = 1, 2, \ldots, N, \tag{6.1}$$

where ρ is the *mass density of the mixture*, $\mathbf{v}_i$ the *flow velocity of species* $\mathcal{M}_i$, Y_i the *mass fraction of species* $\mathcal{M}_i$, and w_i the *rate of production of species* $\mathcal{M}_i$ (mass per unit volume per unit time) by the chemical reactions. The mass fractions Y_i satisfy

$$\sum_{i=1}^{N} Y_i = 1. \tag{6.2}$$

Since overall mass is neither created nor destroyed by chemical reactions, we have

$$\sum_{i=1}^{N} w_i = 0. \tag{6.3}$$

Summation of the mass balance equations over all species yields the overall **continuity equation**,

$$\partial \rho/\partial t + \nabla \cdot (\rho \mathbf{v}) = 0, \tag{6.4}$$

where $\mathbf{v} = \sum_{i=1}^{N} Y_i \mathbf{v}_i$ is the *mass-weighted average velocity of the mixture*. It is customary to write the flow velocity $\mathbf{v}_i$ of species $\mathcal{M}_i$ as

$$\mathbf{v}_i = \mathbf{v} + \mathbf{V}_i, \tag{6.5}$$

with $\mathbf{V}_i$ the *diffusion velocity of species* $\mathcal{M}_i$. Substituting (6.5) in (6.1) yields

$$\partial(\rho Y_i)/\partial t + \nabla \cdot (\rho Y_i \mathbf{v}) + \nabla \cdot (\rho Y_i \mathbf{V}_i) = w_i, \quad i = 1, 2, \ldots, N. \tag{6.6}$$

The diffusion velocities satisfy

$$\sum_{i=1}^{N} Y_i \mathbf{V}_i = 0. \tag{6.7}$$

Conservation of momentum for the mixture is governed by the Navier-Stokes equations,

$$\partial(\rho \mathbf{v})/\partial t + \nabla \cdot (\rho \mathbf{v} \mathbf{v}^T) = -\nabla p + \nabla \cdot \boldsymbol{\tau} + \rho \mathbf{g}, \tag{6.8}$$

with p the *hydrostatic pressure* in the gas mixture, $\boldsymbol{\tau}$ the *viscous stress tensor*, and $\rho \mathbf{g}$ the gravity force, assumed to be the only external force acting on the mixture.

Conservation of energy for the mixture requires

$$\partial(\rho E)/\partial t + \nabla \cdot (\rho E \mathbf{v}) = -\nabla \cdot \mathbf{q} - \nabla \cdot (p\mathbf{v}) + \nabla \cdot (\boldsymbol{\tau}\mathbf{v}) + \rho \mathbf{v} \cdot \mathbf{g}, \tag{6.9}$$

where E is the *specific total energy* and $\mathbf{q}$ is the *heat flux vector*. The specific total energy E is related to the *specific internal energy* e by the relation

$$E = e + \frac{1}{2}\mathbf{v} \cdot \mathbf{v}. \tag{6.10}$$

The term $\frac{1}{2}\mathbf{v} \cdot \mathbf{v}$ in (6.10) represents the specific kinetic energy of the gas mixture. Conservation of energy is often formulated in terms of the specific internal energy e. Taking the inner product of the momentum equation (6.8) with the flow velocity $\mathbf{v}$, and subtracting the resulting equation from (6.9) yields,

$$\partial(\rho e)/\partial t + \nabla \cdot (\rho e \mathbf{v}) = -\nabla \cdot \mathbf{q} - p\nabla \cdot \mathbf{v} + \nabla \cdot (\boldsymbol{\tau}\mathbf{v}) - (\nabla \cdot \boldsymbol{\tau}) \cdot \mathbf{v}. \tag{6.11}$$

6.2.2 Constitutive relations

The set of conservation equations for reacting gas flow has to be completed with *constitutive relations* for the diffusion velocities $\mathbf{V}_i$, the viscous stress tensor $\boldsymbol{\tau}$, the heat-flux vector $\mathbf{q}$, and the reaction rates w_i. In [68] very extensive models are presented. Here we shall use quite simple ones as is often done for laminar flames (see e.g. [11],[58],[62]).

For the **diffusion velocities** *Fick's law* (see e.g. [68]) is used,

$$Y_i \mathbf{V}_i = -D\nabla Y_i, \quad i = 1, 2, \ldots, N. \tag{6.12}$$

In Fick's law it is assumed that the mass diffusion caused by pressure and thermal gradients (known as the Soret effect) is negligible and that all binary diffusion coefficients D_{ij} are equal, i.e. $D_{ij} = D$

for $1 \leq i, j \leq N$.

If we assume that the mixture behaves like a Newtonian fluid for which the bulk viscosity can be neglected, then we obtain for the **viscous stress tensor**,

$$\boldsymbol{\tau} = \mu[(\nabla \mathbf{v}) + (\nabla \mathbf{v})^T] - \frac{2}{3}\mu(\nabla \cdot \mathbf{v})\mathbf{I}, \tag{6.13}$$

where μ is the viscosity coefficient of the gas mixture and $\mathbf{I}$ denotes the unit tensor.
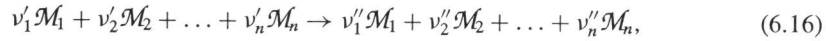
For the **heat flux vector q** of the gas mixture we take

$$\mathbf{q} = -\lambda \nabla T + \rho \sum_{i=1}^{N} h_i Y_i \mathbf{V}_i, \tag{6.14}$$

where T is the *(absolute) temperature of the gas mixture*, h_i the *specific enthalpy of species $\mathcal{M}_i$* and λ the *thermal conductivity of the gas mixture*. In (6.14) it is assumed that heat transfer caused by radiation and heat transfer caused by concentration gradients (known as the Dufour effect) are negligible. The specific enthalpy h_i is defined by the *caloric equation of state*

$$h_i := h_i^0 + \int_{T^0}^{T} c_{p,i}(\xi)d\xi. \tag{6.15}$$

The parameter h_i^0 is the standard heat of formation per unit mass at a reference temperature T^0 for species $\mathcal{M}_i$ and $c_{p,i} = c_{p,i}(T)$ is the specific heat at constant pressure for species $\mathcal{M}_i$. The coefficients D, μ, and λ in (6.12), (6.13), and (6.14) depend on the temperature and on the mixture composition.

A model for the **reaction rates** w_i can be obtained from chemical kinetics (see [68]). We consider only one reaction:

$$\nu_1' \mathcal{M}_1 + \nu_2' \mathcal{M}_2 + \ldots + \nu_n' \mathcal{M}_n \rightarrow \nu_1'' \mathcal{M}_1 + \nu_2'' \mathcal{M}_2 + \ldots + \nu_n'' \mathcal{M}_n, \tag{6.16}$$

where $\nu_i' - \nu_i''$ represents the number of molecules of species $\mathcal{M}_i$ converted in the reaction. The phenomenological law of mass action states that the reaction rates w_i are proportional to the products of the molar concentrations of the reactants ([68, Appendix B]):

$$w_i = (\nu_i' - \nu_i'')k \prod_{l=1}^{N}(\frac{\rho Y_l}{W_l})^{\nu_i'}, \quad i = 1, 2, \ldots, N, \tag{6.17}$$

with k the so-called specific reaction rate constant for reaction (6.16) and W_i the molecular weight of species $\mathcal{M}_i$. We assume that k satisfies *Arrhenius law*

$$k = Be^{-E_a/(RT)}. \tag{6.18}$$

The coefficients B and E_a in (6.18) are the *frequency factor* and the *activation energy*, respectively, and R is the universal gas constant. For the general situation of M reactions taking place in the mixture, we have to sum the reaction rates over all M reactions to obtain the total rate of production of each species $\mathcal{M}_i$.

The *conservation equations* (6.4), (6.6), (6.8), (6.11) in combination with the *constitutive relations* (6.12), (6.13), (6.14), (6.17) lead to a set of $N + 5$ equations for three-dimensional flow problems. However, only $N + 4$ of these are independent because the overall continuity equation (6.4) is the sum of the mass balance equations (6.6) for the individual species. The independent variables are : ρ, $\mathbf{v}$, Y_i ($i = 1, 2, \ldots, N - 1$), p, e, and T. So we have $N + 6$ unknowns for three-dimensional flow problems, and therefore two extra equations are required. We assume that the gas mixture behaves like an ideal gas. Then the two extra equations are the **equation of state**

$$p = \rho RT / W, \tag{6.19}$$

with $W := (\sum_{i=1}^{N} Y_i / W_i)^{-1}$, the *average molecular mass of the mixture*, and the **thermodynamic identity**

$$\sum_{i=1}^{N} Y_i h_i = e + p/\rho, \tag{6.20}$$

with $h := \sum_{i=1}^{N} Y_i h_i$ the *specific enthalpy of the mixture*.

6.2.3   Reformulation of the energy equation

In this subsection the energy equation (6.11) is written in terms of the absolute temperature explicitly. As is usually done in combustion modelling the contribution of the stress tensor to the energy equation, $\nabla \cdot (\boldsymbol{\tau} \mathbf{v}) - (\nabla \cdot \boldsymbol{\tau}) \cdot \mathbf{v}$, is neglected. Substituting $e = h - p/\rho$ (cf. (6.20)) into (6.11) then yields,

$$\partial(\rho h)/\partial t + \nabla \cdot (\rho h \mathbf{v}) = -\nabla \cdot \mathbf{q} + \partial p/\partial t + \nabla p \cdot \mathbf{v}. \tag{6.21}$$

Since $h = \sum_{i=1}^{N} Y_i h_i$ and $h_i = h_i^0 + \int_{T^0}^{T} c_{p,i}(\xi) d\xi$, we obtain:

$$\partial(\rho h)/\partial t = \sum_{i=1}^{N} h_i \partial(\rho Y_i)/\partial t + \rho c_p \partial T/\partial t, \tag{6.22a}$$

$$\nabla \cdot (\rho h \mathbf{v}) = \sum_{i=1}^{N} h_i \nabla \cdot (\rho Y_i \mathbf{v}) + \rho c_p \mathbf{v} \cdot \nabla T, \tag{6.22b}$$

where the *mixture heat capacity* is introduced as

$$c_p := \sum_{i=1}^{N} Y_i c_{p,i}. \tag{6.23}$$

Using the expression for the heat flux vector $\mathbf{q}$ in (6.14) we obtain:

$$-\nabla \cdot \mathbf{q} = \nabla \cdot (\lambda \nabla T) - \sum_{i=1}^{N} h_i \nabla \cdot (\rho Y_i \mathbf{V}_i) - \sum_{i=1}^{N} \rho Y_i c_{p,i} \mathbf{V}_i \cdot \nabla T. \qquad (6.22c)$$
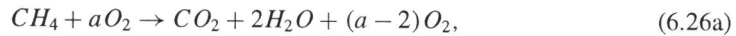
Substitution of (6.22a)-(6.22c) into (6.21) yields,

$$\rho c_p (\partial T/\partial t + \mathbf{v} \cdot \nabla T) - \nabla \cdot (\lambda \nabla T) = \partial p/\partial t + \nabla p \cdot \mathbf{v} - \sum_{i=1}^{N} \rho Y_i c_{p,i} \mathbf{V}_i \cdot \nabla T$$

$$- \sum_{i=1}^{N} h_i (\partial(\rho Y_i)/\partial t + \nabla \cdot (\rho Y_i \mathbf{v}) + \nabla \cdot (\rho Y_i \mathbf{V}_i)). \qquad (6.24)$$

If multiplied with the specific enthalpies, the sum of the mass balances (6.6) over all species yields,

$$\sum_{i=1}^{N} h_i (\partial(\rho Y_i)/\partial t + \nabla \cdot (\rho Y_i \mathbf{v}) + \nabla \cdot (\rho Y_i \mathbf{V}_i)) = \sum_{i=1}^{N} h_i w_i.$$

Using this equality to replace the last term on the right hand side of (6.24), we obtain

$$\rho c_p (\partial T/\partial t + \mathbf{v} \cdot \nabla T) - \nabla \cdot (\lambda \nabla T) = \partial p/\partial t + \nabla p \cdot \mathbf{v} - \sum_{i=1}^{N} h_i w_i$$

$$- \sum_{i=1}^{N} \rho Y_i c_{p,i} \mathbf{V}_i \cdot \nabla T. \qquad (6.25)$$

6.2.4 A one-step overall Arrhenius model

The reactions which occur in a flame are often numerous and complicated. For example even a simple hydrocarbon flame may involve about one hundred chemical species and several hundreds of reactions in the combustion process. The fuel species are transformed step by step into the final product species via numerous chain reactions [68, Appendix B]. However, the global chemical behaviour of a mixture can often be modelled quite adequately by a single one-step irreversible reaction:

$$\text{fuel} + \text{oxidizer} \rightarrow \text{products}.$$

In this chapter we consider methane-air mixtures. The one-step reaction mechanism of an arbitrarily composed methane-air mixture is given by (see e.g. [40]):

$$CH_4 + aO_2 \rightarrow CO_2 + 2H_2O + (a-2)O_2, \qquad (6.26a)$$

and

$$CH_4 + aO_2 \rightarrow (1 + 2a - 4)CO_2 + (4 - 2a)CO + 2H_2O, \qquad (6.26b)$$
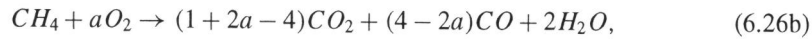
for $a \geq 2$ and $\frac{3}{2} < a \leq 2$, respectively. The methane-air mixture is called *stoichiometric* when CH_4 and O_2 are fully transformed into CO_2 and H_2O, i.e. for $a = 2$. In the remainder of this chapter the mass fractions of methane, oxygen and product species are denoted by Y_{fu}, Y_{ox} and Y_{pr}, respectively. These mass fractions and the mass fraction of the inert species sum up to 1. We note that (6.26) implies

$$
\begin{aligned}
Y_{\text{fu}}^{\text{b}} = 0, \; Y_{\text{ox}}^{\text{b}} = \tfrac{a-2}{a} Y_{\text{ox}}^{\text{u}} \quad &\text{if } a \geq 2, \\
Y_{\text{fu}}^{\text{b}} = 0, \; Y_{\text{ox}}^{\text{b}} = 0 \quad &\text{if } \tfrac{3}{2} < a \leq 2,
\end{aligned}
\tag{6.27}
$$

where the super script $^{\text{u}}$ indicates the unburnt mixture and the super script $^{\text{b}}$ indicates the burnt mixture. We shall use (6.27) in Subsection 6.3.2.

It is useful to introduce s_{ox} as the mass of oxygen consumed per unit mass of fuel:

$$
s_{\text{ox}} := \left\{
\begin{array}{ll}
2 W_{\text{ox}} / W_{\text{fu}} & \text{if } a \geq 2 \\
a W_{\text{ox}} / W_{\text{fu}} & \text{if } \tfrac{3}{2} < a \leq 2
\end{array}
\right. ,
\tag{6.28}
$$

with W_{ox} and W_{fu} the molecular weights of oxygen and methane, respectively. It follows from (6.26) that the rate of consumption of oxygen, w_{ox}, is related to the rate of consumption of methane, w_{fu},

$$
w_{\text{ox}} = s_{\text{ox}} w_{\text{fu}}.
\tag{6.29a}
$$

Since overall mass is neither created nor destroyed by chemical reactions, we have

$$
w_{\text{pr}} = -(1 + s_{\text{ox}}) w_{\text{fu}}.
\tag{6.29b}
$$

We assume that w_{fu} has the same form as (6.17), (6.18):

$$
w_{\text{fu}}(T, Y_{\text{fu}}, Y_{\text{ox}}) = -A \rho^{\alpha + \beta} (Y_{\text{fu}})^{\alpha} (Y_{\text{ox}})^{\beta} \exp(-E_a / (RT)),
\tag{6.30}
$$

with $(\alpha + \beta)$ the *overall reaction order* (see e.g. [11],[40]). The overall reaction 6.26 must include the effect of all possible reactions in the combustion process. Therefore non-integer values for the orders α and β are allowed in (6.30) (see e.g. [10]).

Remark 6.1 The 'constant' A has the unit $[\text{kgm}^{-3}]^{1-\alpha-\beta} s^{-1}$, where $\alpha + \beta$ may be a non-integer value. □

The chemical rate parameters A, α, β and E_a in (6.30) have to be determined from experimental results. In [40],[45] theoretical relations, derived using the expression in (6.30), are fitted to experimental data to determine the values of the parameters A, α, β, and E_a for atmospheric CH_4/air combustion.

6.3 BURNER STABILIZED FLAT FLAMES

For a first application of the composite grid methods from Chapter 5 to the field of combustion, we want to use a test case for which the governing equations become as simple as possible. Therefore we consider *premixed laminar flat flames*. The construction of a *flat flame burner* is such that it may be assumed that in a region near the burner axis all variables are constant in each plane parallel to the burner surface. In mathematical terms this means that any variable V obeys

$$|\frac{\partial V}{\partial y}(x, y, z)| \ll |\frac{\partial V}{\partial x}(x, y, z)|, \quad |\frac{\partial V}{\partial z}(x, y, z)| \ll |\frac{\partial V}{\partial x}(x, y, z)|,$$

for all (x, y, z) near the center of the burner, where (y, z) are the co-ordinates along the burner surface and x is the co-ordinate perpendicular to the burner surface. For premixed laminar flat flames the reacting flow equations are considered to be *one-dimensional*.

Experimentally the flat flames are stabilized near the cold burner surface at a fixed position in space. In the laboratory frame of reference this flame is in a steady state. For these stabilized laminar flat flames the reacting flow equations become *one-dimensional and stationary*.

6.3.1 Modelling of stabilized premixed laminar flat flames

The governing equations for stabilized premixed laminar flat flames result from the combustion equations from Section 6.2 when all terms involving $\partial/\partial t$ are put equal to zero and when only one spatial direction is considered. In order to obtain a manageable form of the governing equations, the following simplifying assumptions are made:

A1 The pressure is considered to be constant in the energy equation and in the equation of state, but not in the momentum equation. This is the so-called *combustion approximation* or *isobaric approximation* (see e.g. [11]). We write

$$p(x) = P_0 + \delta p(x),$$

with P_0 a constant pressure.

A2 The average molecular mass of the mixture, W, is constant.

A3 All chemical species have constant and equal specific heats at constant pressure:

$$c_{p,i} = c_p, \quad i = 1, 2, \ldots, N.$$

A4 The *Lewis number* is equal to unity,

$$Le := \frac{\lambda/c_p}{\rho D} = 1.$$

For a stabilized flat flame the *overall continuity equation* (6.4) reduces to

$$\rho u = \dot{m},$$
(6.31)

with u the velocity along the x-axis and $\dot{m}$ the given constant mass flux. The *Navier-Stokes equations* (6.8) reduce to a single equation,

$$\dot{m}\frac{du}{dx} = -\frac{d\delta p}{dx} + \frac{d}{dx}(\frac{4}{3}\mu\frac{du}{dx}) + \rho g,$$
(6.32)

with g the component of the gravity in the x-direction. In the combustion approximation the *energy equation* (6.25) reduces to

$$\dot{m}c_p\frac{dT}{dx} - \frac{d}{dx}(\lambda\frac{dT}{dx}) = -\sum_{i=1}^{N} h_i w_i - \sum_{i=1}^{N} \rho c_{p,i} Y_i U_i \frac{dT}{dx},$$
(6.33)

with U_i the diffusion velocity of species $\mathcal{M}_i$ along the x-axis. Under assumption A3 the second term on the right hand side of (6.33) vanishes since $\sum_{i=1}^{N} Y_i U_i = 0$ (cf. (6.7)). The first term on the right hand side of (6.33) reduces to $\sum_{i=1}^{N} h_i^0 w_i$ since $h_i = h_i^0 + c_p(T - T^0)$ and $\sum_{i=1}^{N} w_i = 0$ (cf. (6.3)). Now the energy equation reads

$$\dot{m}c_p\frac{dT}{dx} - \frac{d}{dx}(\lambda\frac{dT}{dx}) = -\sum_{i=1}^{N} h_i^0 w_i.$$
(6.34)

The thermal conductivity of the mixture (λ) is supposed to be ruled by the properties of the abundant nitrogen part in hydrocarbon-air mixtures [40]:

$$\lambda = \lambda_{\text{ref}}(T/T_{\text{ref}})^\gamma.$$
(6.35)

Using Fick's law (6.12), the *mass balance equations* (6.6) reduce to

$$\dot{m}\frac{dY_i}{dx} - \frac{d}{dx}(\rho D\frac{dY_i}{dx}) = w_i, \quad i = 1, 2, \ldots, N.$$
(6.36)

In the combustion approximation the *equation of state* becomes

$$P_0 = \rho R T / W.$$
(6.37)

Under assumption **A2** the mass density ρ is a function of the temperature only, since P_0, R and W are constants.

We specify the right hand sides of the energy equation (6.34) and the mass balance equations (6.36) for a stoichiometric methane-air flame with the one-step reaction mechanism from Subsection 6.2.2. For the right hand side of the energy equation (6.34) we obtain

$$
\begin{aligned}
-\sum_{i=1}^{N} h_i^0 w_i &= -(h_{\text{fu}}^0 w_{\text{fu}} + h_{\text{ox}}^0 w_{\text{ox}} + h_{\text{pr}}^0 w_{\text{pr}}) \\
&= -(h_{\text{fu}}^0 + s_{\text{ox}} h_{\text{ox}}^0 - (1 + s_{\text{ox}}) h_{\text{pr}}^0) w_{\text{fu}} \\
&=: -\Delta H \, w_{\text{fu}},
\end{aligned}
$$
(6.38)

with ΔH the so-called *heat of combustion*.

Remark 6.2 Consider an infinitely long tube with a fresh stoichiometric methane-air mixture. Some time after the mixture is ignited at $x = -\infty$ the flame will propagate towards $x = \infty$ with a constant velocity (a so-called *freely propagating flame*). Variables on the unburnt side of the mixture are denoted by a super script ^{u}; variables on the burnt side are denoted by a super script ^{b}. Integrating (6.34) over $(-\infty, \infty)$ yields,

$$\dot{m}c_p(T^b - T^u) = -\Delta H \int_{-\infty}^{\infty} w_{fu}(x)dx.$$

Integrating the mass balance for the fuel (cf. (6.36)) over $(-\infty, \infty)$ yields,

$$-\dot{m}Y_{fu}^u = \int_{-\infty}^{\infty} w_{fu}(x)dx,$$

where we have used $Y_{fu}^b = 0$. Now we obtain

$$\Delta H = \frac{(T^b - T^u)c_p}{Y_{fu}^u},$$

which gives the relation between the *adiabatic end temperature* T^b and the heat of combustion ΔH. □

Since the mass fractions of fuel, oxygen, products and inert species sum up to 1 and the mass fraction of the inert species is constant, we only have to consider the mass balances for fuel and oxygen. Summarizing we have the following system of equations for a *burner stabilized flat methane-air flame with a one-step reaction mechanism*:

$$\rho u = \dot{m}, \tag{6.39a}$$

$$\dot{m}\frac{du}{dx} = -\frac{d\delta p}{dx} + \frac{d}{dx}(\frac{4}{3}\mu\frac{du}{dx}) + \rho g, \tag{6.39b}$$

$$\dot{m}\frac{dT}{dx} - \frac{d}{dx}(\lambda/c_p\frac{dT}{dx}) = -\frac{\Delta H}{c_p}w_{fu}, \tag{6.39c}$$

$$\dot{m}\frac{dY_{fu}}{dx} - \frac{d}{dx}(\rho D\frac{dY_{fu}}{dx}) = w_{fu}, \tag{6.39d}$$

$$\dot{m}\frac{dY_{ox}}{dx} - \frac{d}{dx}(\rho D\frac{dY_{ox}}{dx}) = s_{ox}w_{fu}, \tag{6.39e}$$

$$\rho = \frac{P_0 W}{RT}, \tag{6.39f}$$

$$w_{fu} = -A\rho^{\alpha+\beta}(Y_{fu})^\alpha(Y_{ox})^\beta \exp(-\frac{E_a}{RT}). \tag{6.39g}$$

The system of equations (6.39) for the unknowns ρ, u, δp, T, Y_{fu}, Y_{ox} is not fully coupled. Since $\rho = \rho(T)$, the equations (6.39c), (6.39d), (6.39e) involve only the combustion variables T, Y_{fu} and Y_{ox}. So these equations decouple from the remaining (fluid dynamics) equations. After solving the combustion equations (6.39c), (6.39d), (6.39e) for T, Y_{fu} and Y_{ox}, the mass density ρ follows from (6.39f). Then the velocity u follows from (6.39a). Finally one can solve (6.39b) for the variation in the pressure δp. In the remainder of this chapter we only consider the combustion equations (6.39c), (6.39d), (6.39e).

6.3.2 Boundary conditions

The system of equations (6.39c),(6.39d),(6.39e) for the combustion variables T, Y_{fu}, Y_{ox} is not complete yet. We still have to specify the boundary conditions. We locate the burner surface at $x = 0$. The inside of the burner is identified with the interval $(-\infty, 0)$. The outside of the burner is identified with the interval $(0, \infty)$. We assume that *inside the burner no chemical reactions* take place and the *temperature of the mixture is constant*:

$$w_{fu} = 0 \qquad \text{inside the burner,}$$
$$T = T^u \qquad \text{inside the burner.}$$

If the temperature inside the burner is sufficiently low, so that the mixture is chemically inert, then $w_{fu} = 0$ is a good approximation. The assumption $T = T^u$ inside the burner implies an ideal cooling of the burner.

Since the temperature is constant inside the burner, we obtain from (6.39f) that the mass density is constant inside the burner, say $\rho = \rho^u$, and from (6.39a) that the velocity of the mixture is constant inside the burner, say $u = u^u$. Since $\lambda = \lambda(T)$ (cf. (6.35)) and the Lewis number is unity, the binary diffusion coefficient D does not depend on the mass fractions Y_{fu} and Y_{ox}. Thus D is constant inside the burner, say $D = D^u$.

At $x = -\infty$ the mass fractions of fuel and oxygen are given by:

$$\lim_{x \to -\infty} Y_{fu}(x) = Y_{fu}^u, \qquad \lim_{x \to -\infty} Y_{ox}(x) = Y_{ox}^u. \tag{6.40}$$

At $x = \infty$ the mixture is in chemical equilibrium:

$$\lim_{x \to \infty} \frac{dT}{dx}(x) = 0, \quad \lim_{x \to \infty} \frac{dY_{fu}}{dx}(x) = 0, \quad \lim_{x \to \infty} \frac{dY_{ox}}{dx}(x) = 0. \tag{6.41}$$

Now the *burner stabilized flame problem* is given by:

$$\dot{m}\frac{dY_{fu}}{dx} - \frac{d}{dx}(\rho^u D^u \frac{dY_{fu}}{dx}) = 0, \qquad -\infty < x < 0, \tag{6.42a}$$

$$\dot{m}\frac{dY_{ox}}{dx} - \frac{d}{dx}(\rho^u D^u \frac{dY_{ox}}{dx}) = 0, \qquad -\infty < x < 0, \tag{6.42b}$$

$$T = T^u, \qquad -\infty < x < 0, \tag{6.42c}$$

$$\dot{m}\frac{dY_{fu}}{dx} - \frac{d}{dx}(\rho D \frac{dY_{fu}}{dx}) = w_{fu}, \qquad 0 < x < \infty, \tag{6.42d}$$

$$\dot{m}\frac{dY_{ox}}{dx} - \frac{d}{dx}(\rho D \frac{dY_{ox}}{dx}) = s_{ox} w_{fu}, \qquad 0 < x < \infty, \tag{6.42e}$$

$$\dot{m}\frac{dT}{dx} - \frac{d}{dx}(\lambda/c_p \frac{dT}{dx}) = -\frac{\Delta H}{c_p} w_{fu}, \qquad 0 < x < \infty, \tag{6.42f}$$

with the boundary conditions (6.40) and (6.41).

If we prescribe the mass fractions of fuel and oxygen at the burner surface,

$$Y_{fu}(0) = Y_{fu}^0, \quad Y_{ox}(0) = Y_{ox}^0, \tag{6.43}$$

then the burner stabilized flame problem can be split into two parts: inside the burner and outside the burner.

Inside the burner analytical solutions of the governing equations, (6.42a) and (6.42b), exist. The mass fractions of fuel and oxygen inside the burner satisfy:

$$Y_i(x) = Y_i^u + (Y_i^0 - Y_i^u)\exp(\frac{u^u}{D^u}x), \quad -\infty < x < 0, \ i = \text{"fu"}, \text{"ox"}. \tag{6.44}$$

Outside the burner the equations for the mass fractions (6.42d),(6.42e) and the equation for the temperature (6.42f) have the same form. Since the Lewis number is unity, the differential operators on the left hand side of (6.42d), (6.42e) and (6.42f) are identical. The mass fractions Y_fu and Y_ox are dimensionless, while the temperature T is not. Here we define a *dimensionless temperature*,

$$\tau := \frac{T}{\Delta H/c_p}. \tag{6.45}$$

The equation for the dimensionless temperature τ reads,

$$\dot{m}\frac{d\tau}{dx} - \frac{d}{dx}(\lambda/c_p\frac{d\tau}{dx}) = -w_\text{fu}. \tag{6.46}$$

Simple relations between the mass fractions Y_fu and Y_ox and the dimensionless temperature τ can be derived. We introduce so-called *Shvab-Zeldovich variables*,

$$J_\text{fu} := Y_\text{fu} + \tau, \tag{6.47a}$$

$$J_\text{ox} := \frac{1}{s_\text{ox}}Y_\text{ox} + \tau. \tag{6.47b}$$

By (6.42d),(6.42e),(6.46) and with $Le = 1$ the Shvab-Zeldovich variables satisfy

$$\frac{dJ_i}{dx} - \frac{d}{dx}(\frac{\lambda}{\dot{m}c_p}\frac{dJ_i}{dx}) = 0, \quad 0 < x < \infty, \ i = \text{"fu"}, \text{"ox"}. \tag{6.48}$$

The general solution of (6.48) is

$$J_i(x) = C_{i,1} + C_{i,2}\exp(\int_0^x \frac{\dot{m}c_p}{\lambda}d\xi), \quad 0 \le x < \infty, \ i = \text{"fu"}, \text{"ox"}, \tag{6.49}$$

with $C_{i,1}$, $C_{i,2}$ constants. The only bounded solutions of (6.48) are constant functions. Thus we obtain

$$Y_\text{fu}(x) = Y_\text{fu}^0 + \tau^u - \tau(x), \qquad x \ge 0, \tag{6.50a}$$
$$Y_\text{ox}(x) = Y_\text{ox}^0 + s_\text{ox}(\tau^u - \tau(x)), \quad x \ge 0, \tag{6.50b}$$

where $\tau^u := T^u c_p/\Delta H$. Using (6.27) it follows from (6.50) that the mass fractions of fuel and oxygen at the burner surface are related:

$$Y_\text{ox}^0 = s_\text{ox}Y_\text{fu}^0 + Y_\text{ox}^b, \tag{6.51}$$

with Y_{ox}^b as in (6.27). Equation (6.51) gives a condition on the prescribed mass fractions Y_{fu}^0 and Y_{ox}^0. Note that (6.50) and (6.51) imply:

$$Y_{ox}(x) = Y_{ox}^b + s_{ox} Y_{fu}(x), \qquad x \geq 0. \tag{6.52}$$

Equation (6.50a) and (6.52) are substituted into (6.39g) to eliminate the mass fractions on the right hand side of the differential equation (6.46) for τ. Then we obtain a scalar equation for τ outside the burner,

$$\frac{d\tau}{dx} - \frac{d}{dx}\left(\frac{\lambda}{\dot{m}c_p}\frac{d\tau}{dx}\right) = S(\tau), \quad 0 < x < \infty, \tag{6.53a}$$

$$\tau(0) = \tau^u, \quad \lim_{x \to \infty} \frac{d\tau}{dx} = 0, \tag{6.53b}$$

with

$$S(\tau) := A\frac{(\rho^u \tau^u)^{\alpha+\beta}}{\dot{m}}\left(\frac{1}{\tau}\right)^{\alpha+\beta}(Y_{fu}^0 + \tau^u - \tau)^\alpha (Y_{ox}^b + s_{ox}(Y_{fu}^0 + \tau^u - \tau))^\beta \exp(-\tau_a/\tau). \tag{6.53c}$$

In (6.53c) the dimensionless activation temperature τ_a is defined by $\tau_a := E_a c_p/(R\Delta H)$. After solving (6.53) for τ, the mass fractions Y_{fu} and Y_{ox} outside the burner follow from (6.50).

Summarizing, for a prescribed value of $Y_{fu}(0)$ the mass fractions Y_{fu}, Y_{ox} and the dimensionless temperature τ inside the burner follow from (6.51), (6.44), (6.42c), while these combustion variables outside the burner follow from (6.53), (6.50a), (6.52). It is obvious that the resulting functions for the mass fractions and the temperature are continuous at $x = 0$. For an arbitrary choice of Y_{fu}^0 the first derivatives of these functions are discontinuous at $x = 0$. Such a discontinuity is to be expected for the temperature function because of the instantaneous cooling of the burner. However, in the burner stabilized flame problem (6.42) the first derivatives of the mass fractions are continuous at $x = 0$. If the burner stabilized flame problem (6.42) has a unique solution, then a unique value of Y_{fu}^0 exists for which the mass fraction functions inside and outside the burner connect properly at the burner surface.

6.4 NUMERICAL RESULTS

In this section the nonlinear LDC method from Chapter 5 is used to solve the scalar combustion equation (6.53) and the burner stabilized flame problem (6.42). First we consider (6.53). For numerically solving this two-point boundary value problem we introduce a computational domain extending from $x = 0$ (the burner surface) to a point $x = L$ downstream of the flame. At $x = L$ a homogeneous Neumann boundary condition is imposed,

$$\frac{d\tau}{dx}(L) = 0.$$

This implies that the length of the computational domain has to be 'large enough' (see e.g. [55],[58]). We take $L = 5$ cm, which is large compared to the size of the chemical active layer in a flame (typically ~ 1 mm). The length L is used to introduce the dimensionless space variable

$$\xi := x/L.$$

α	2.8		ΔH	$5.0\ 10^7$	J/kg	λ_{ref}	0.092	J/(m K s)
β	1.2		c_p	$1.4\ 10^3$	J/(kg K)	T_{ref}	$1.5\ 10^3$	K
A	$2.6\ 10^{15}$	$(\mathrm{kgm}^{-3})^{1-\alpha-\beta}\mathrm{s}^{-1}$	ρ^u	1.24	kg/m^3	γ	0.77	
E_a	$1.4\ 10^5$	J/mol	$\dot{m}$	0.37	kg/(m^2 s)	T^u	293	K

Table 6.1 Values for the physical and chemical parameters in (6.54).

With the thermal conductivity λ as in (6.35) and for a *stoichiometric* methane-air mixture, we obtain the two-point boundary value problem,

$$\frac{d\tau}{d\xi} - \frac{d}{d\xi}\left(a(\tau)\frac{d\tau}{d\xi}\right) = S(\tau), \quad 0 < \xi < 1, \tag{6.54a}$$

$$\tau(0) = \tau^u, \quad \frac{d\tau}{d\xi}(1) = 0, \tag{6.54b}$$

with

$$a(\tau) := \frac{\lambda_{ref}(\Delta H / T_{ref} c_p)^\gamma}{L\dot{m}c_p}\tau^\gamma, \tag{6.54c}$$

$$S(\tau) := AL\frac{(\rho^u\tau^u)^{\alpha+\beta}}{\dot{m}}s_{ox}^\beta\left(\frac{Y_{fu}^0 + \tau^u}{\tau} - 1\right)^{\alpha+\beta}\exp(-\tau_a/\tau). \tag{6.54d}$$

Typical values of the physical and chemical parameters[1] in (6.54) are given in Table 6.1. We take the mass fraction of fuel at the burner surface equal to the mass fraction of fuel in the fresh stoichiometric methane-air mixture:

$$Y_{fu}^0 = Y_{fu}^u = 0.0548.$$

In this section we use a composite grid $\Omega^{H,h}$, which is composed of the uniform grids Ω^H and Ω_l^h. The grid Ω^H is a uniform grid with grid size H, covering the computational domain $\Omega := (0, 1]$. We assume that $1/H \in I\!N$. Then $\xi = 1$ is a grid point of Ω^H. The grid Ω_l^h is a uniform grid with grid size $h < H$, covering the subregion $\Omega_l := (0, l) \subset \Omega$. We assume that $\sigma := H/h \in I\!N$ and $l/H \in I\!N$. These assumptions imply that the grid points of Ω^H inside Ω_l belong to Ω_l^h and that the *interface point* $\xi = l$ is a grid point of Ω^H. Examples of the grids Ω^H, Ω_l^h and $\Omega^{H,h}$ are shown in Figure 6.1. By Ω^h we denote the uniform grid with grid size h, covering the domain Ω.

For discretizing the boundary value problem (6.54) on the uniform grids Ω^H and Ω_l^h, finite difference methods are used. In particular, following Smooke [55],[56], the diffusion term is approximated using *central differences* and the convective term is approximated using *upwind differences*. For the grid points $y \in \Omega^H$ we use,

---

[1]The values for the physical and chemical parameters in this section have been supplied by the combustion research group at the Eindhoven University of Technology.

$$\frac{d}{d\xi}(a(\tau)\frac{d\tau}{d\xi})(y) \doteq \frac{1}{H^2}\{a(\tfrac{1}{2}\tau(y+H)+\tfrac{1}{2}\tau(y))\,(\tau(y+H)-\tau(y)) -$$
$$a(\tfrac{1}{2}\tau(y)+\tfrac{1}{2}\tau(y-H))\,(\tau(y)-\tau(y-H))\}, \qquad (6.55a)$$

$$\frac{d\tau}{d\xi}(y) \doteq \frac{1}{H}\{\tau(y)-\tau(y-H)\}. \qquad (6.55b)$$

The Dirichlet boundary condition at $\xi = 0$ yields $\tau(0) = \tau^u$. For the homogeneous Neumann boundary condition at the grid point $\xi = 1$, we use the approximation

$$\frac{1}{2H}\{\tau(1+H)-\tau(1-H)\} = 0. \qquad (6.55c)$$

For the grid points $y \in \Omega_l^h$ we use,

$$\frac{d}{d\xi}(a(\tau)\frac{d\tau}{d\xi})(y) \doteq \frac{1}{h^2}\{a(\tfrac{1}{2}\tau(y+h)+\tfrac{1}{2}\tau(y))\,(\tau(y+h)-\tau(y)) -$$
$$a(\tfrac{1}{2}\tau(y)+\tfrac{1}{2}\tau(y-h))\,(\tau(y)-\tau(y-h))\}, \qquad (6.56a)$$

$$\frac{d\tau}{d\xi}(y) \doteq \frac{1}{h}\{\tau(y)-\tau(y-h)\}. \qquad (6.56b)$$

The Dirichlet boundary condition at $\xi = 0$ yields $\tau(0) = \tau^u$. At $\xi = l$ the Dirichlet boundary condition $\tau(l) = \tau^*$ is used, with τ^* an artificial Dirichlet boundary value.

We use the *nonlinear LDC method* from Section 5.2 for solving the nonlinear boundary value problem (6.54) on the composite grid $\Omega^{H,h}$. We briefly recall the essential steps in the nonlinear LDC method. Starting point of the method is the system of nonlinear equations resulting from discretizing the boundary value problem (6.54) on the uniform global coarse grid Ω^H. As in Subsection 5.2.1 we refer to this system as the *basic discretization*. Discretizations of (6.54) on Ω^H and on Ω_l^h are coupled in the following way. After solving a discretization of (6.54) on Ω^H, where the solution is denoted by τ^H, the boundary value problem (6.54) is discretized on the uniform local fine grid Ω_l^h. In this discretization the Dirichlet boundary condition $\tau(l) = \tau^H(l)$ is used at the interface grid point $\xi = l$. After solving a discretization of (6.54) on Ω_l^h, where the solution is denoted by τ_l^h, the local defect of τ_l^h with respect to the basic discretization is computed. This local defect is added to the right hand side of the basic discretization to define an updated discretization of the boundary value problem (6.54) on Ω^H.
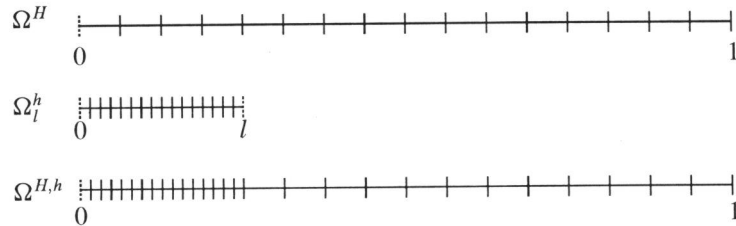
Figure 6.1 The grids Ω^H, Ω_l^h and $\Omega^{H,h}$ for $H = 1/16$, $l = 4/16$, $\sigma = 4$.

For solving the systems of nonlinear equations in the nonlinear LDC method a damped New-ton iteration is used. In each iteration step the damping factor (cf. (5.5)) is determined by a trial and error method. Starting with full Newton, i.e. the damping factor equal to 1.0, the damping factor is multiplied by $\frac{1}{2}$ until the condition

$$\|r^{j+1}\|_\infty \le a\|r^j\|_\infty \tag{6.57}$$

is satisfied. Here r^j and r^{j+1} denote the residual of the current and the updated Newton iterate. Note that these residuals are grid functions on a uniform grid. We shall use $a = 2$ in (6.57). The Newton iteration is stopped if the convergence criterion, $\|r^j\|_\infty < 10^{-6}$, is reached. The Jacobian matrices are evaluated analytically. The Jacobian systems are solved exactly using a tridiagonal solver.

In the examples below we present characteristic properties of the approximations of the di-mensionless temperature τ in (6.54), resulting from the nonlinear LDC method. We note that in the figures in this section the *dimensional* variables are plotted. The absolute temperature T is shown as a function of the distance to the burner surface x in cm. We recall that $T = \Delta H \tau / c_p$ and $x = L \xi$. Only the first 0.5 cm of the computational domain (of length 5 cm) is plotted in the figures.

The grid function τ_0^H is a solution of the basic discretization and the grid function $\tau_{l,0}^h$ is a solution of the local fine grid discretization with the artificial Dirichlet boundary value $\tau_0^H(l)$ at the interface grid point $\xi = l$. For solving the basic discretization, a piecewise linear tempera-ture profile is used as initial guess in the damped Newton method. For solving the local fine grid discretization related to τ_0^H, the linear interpolant of τ_0^H inside Ω_l is used as initial guess in the damped Newton method. The grid function τ_i^H with $i \ge 1$ results after i local defect correction steps and the grid function $\tau_{l,i}^h$ is a solution of the local fine grid discretization with the artificial Dirichlet boundary value $\tau_i^H(l)$ at the interface grid point $\xi = l$. For solving the systems of nonlin-ear equations on Ω^H and Ω_l^h in the i-th LDC step, the approximations τ_{i-1}^H and $\tau_{l,i-1}^h$, respectively, are used as initial guess in the damped Newton method.

Remark 6.3 A major problem for solving stationary combustion equations is the choice of a suit-able initial guess for Newton's method. For the combustion equation considered here, it is rela-tively easy to obtain a suitable initial guess on the global coarse grid by using the non-adiabatic end temperature resulting from (6.50a). □

The errors in the approximations resulting from the nonlinear LDC method are computed us-ing a *reference solution* $\hat{\tau}$ of (6.54). This reference solution is obtained on a global uniform grid with a grid size which is much smaller than the grid size h of the local fine grid Ω_l^h. The reference solution is shown in Figure 6.2. The (relative) errors are defined by

$$e_i^H(x_j) := \frac{|\tau_i^H(x_j) - \hat{\tau}(x_j)|}{|\hat{\tau}(x_j)|}, \qquad x_j \in \Omega^H, \ i \ge 0,$$

$$e_{l,i}^h(x_j) := \frac{|\tau_{l,i}^h(x_j) - \hat{\tau}(x_j)|}{|\hat{\tau}(x_j)|}, \qquad x_j \in \Omega_l^h, \ i \ge 0.$$
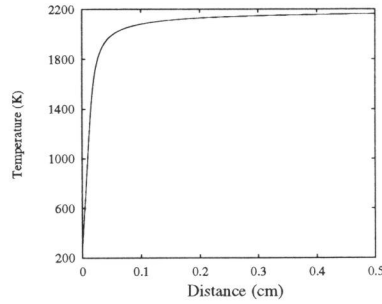
Figure 6.2   The reference solution for boundary value problem (6.54). Only the first 0.5 cm of the computational domain is plotted.

In Example 6.3 the global and local approximations τ_0^H and $\tau_{l,0}^h$ are compared with the approximations τ_1^H and $\tau_{l,1}^h$, resulting after 1 local defect correction step. It is shown that τ_1^H is significantly more accurate than τ_0^H both inside and outside the local region Ω_l, while $\tau_{l,1}^h$ is significantly more accurate than $\tau_{l,0}^h$ near the interface grid point $\xi = l$.

Example 6.4 In this example we take $H = 1/100$, $l = 5H$ and $\sigma = 10$. In Figure 6.3.a the approximations τ_0^H and $\tau_{l,0}^h$ are shown. In Figure 6.3.b the relative errors in the approximations τ_0^H and $\tau_{l,0}^h$ are plotted. The dashed line in this figure represents the error in the approximation τ^h, which results when the boundary value problem (6.54) is discretized on the global uniform fine grid Ω^h. We observe that τ_0^H, resulting from solving the basic discretization, approximates the reference solution $\hat{\tau}$ fairly well outside the local region Ω_l. Inside Ω_l the error in τ_0^H is large, but this error decays fastly when the distance increases. In a large part of the local region Ω_l the error in $\tau_{l,0}^h$ is comparable with the error in τ^h. Near the interface grid point the error in $\tau_{l,0}^h$ becomes much larger. This is due to the fact that at the interface grid point $\xi = l$ the value $\tau_0^H(l)$ is used to define an artificial Dirichlet boundary value. The behaviour of $\tau_{l,0}^h$ close to the interface grid point is shown in the insert in Figure 6.3.a.

In Figure 6.3.c the approximations τ_1^H and $\tau_{l,1}^h$, resulting after 1 local defect correction step, are shown. The global coarse grid approximation τ_1^H is accurate both *inside* and *outside* the local region Ω_l. Consequently, the error in $\tau_{l,1}^h$ near the interface grid point is much smaller than the error in $\tau_{l,0}^h$ near the interface grid point. This is shown in Figure 6.3.d where the relative errors in τ_0^H and $\tau_{l,0}^h$ and the relative errors in τ_1^H and $\tau_{l,1}^h$ are plotted. Both near the interface grid point and outside Ω_l, the errors in the approximations resulting after the local defect correction step are significantly smaller than the errors in the approximations before the local defect correction step.

For other values of the parameters H, σ and l, a similar improvement in accuracy for the global and local approximations is obtained after a local defect correction step. In Figure 6.4 the errors in the approximations τ_0^H and $\tau_{l,0}^h$ and in the approximations τ_1^H and $\tau_{l,1}^h$ are plotted for $H = 1/100$, $\sigma = 20$, $l = 5H$ (Figure 6.4.a) and for $H = 1/100$, $\sigma = 40$, $l = 3H$ (Figure 6.4.b). In this figure we use the same markers as in Figure 6.3.d. The error for the approximation τ^h, resulting when the boundary value problem (6.54) is discretized on the global uniform fine grid Ω^h, is indicated by the dotted line.   □
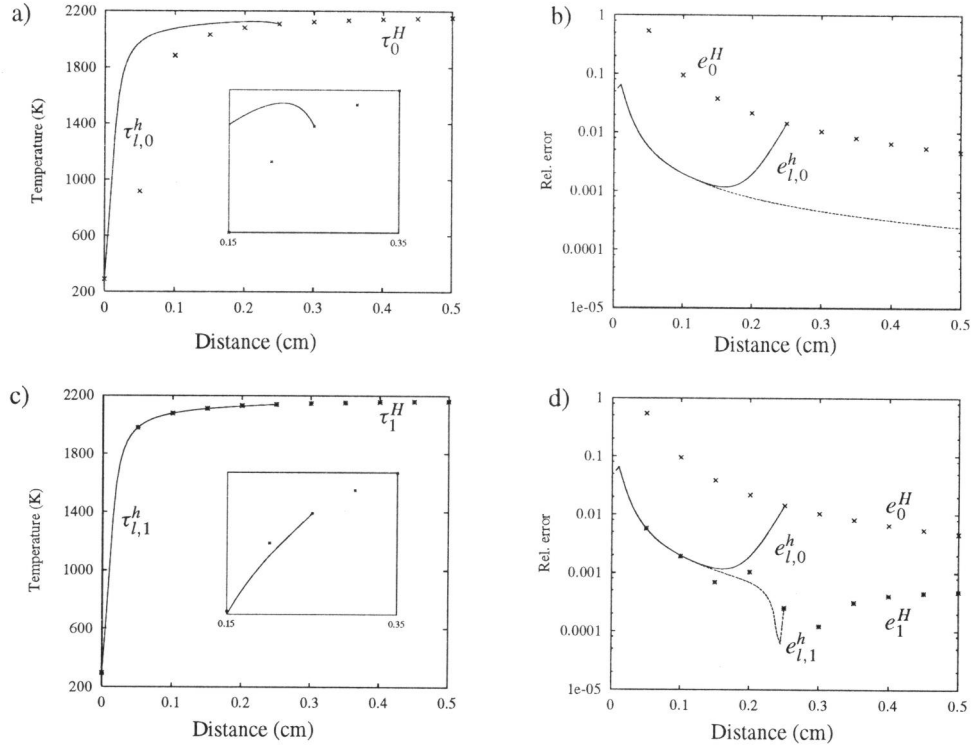
Figure 6.3 Temperature profiles and errors before a local defect correction step in a),b) and after a local defect correction step in c),d) in Example 6.4; $H = 0.05$ cm, $l = 5H$ and $\sigma = 10$. The region $[0.15, 0.35]$ is enlarged in the insert in a) and c).

In Example 6.4 only 1 local defect correction step is performed. In Example 6.5 and Example 6.6 we study the convergence behaviour of the nonlinear LDC method. Therefore we introduce the composite grid iterates

$$\tau_i^{H,h} := \begin{bmatrix} \tau_{l,i}^h \\ \tau_i^H|_{\Omega_c^H} \end{bmatrix}.$$

In Section 5.2 we have shown that the nonlinear LDC method is related to a system of nonlinear equations on a composite grid (cf. Theorem 5.5). Here we consider the following discretization of the boundary value problem (6.54) on the composite grid $\Omega^{H,h}$ (cf. (5.17)): At all grid points of $\Omega^{H,h}$ which lie inside Ω_l the finite difference approximations (6.56) are used. At all grid points of $\Omega^{H,h}$ which lie outside Ω_l the finite difference approximations (6.55) are used. The interface grid point $\xi = l$ is treated as if it was a grid point of the uniform grid Ω^H. In the remainder of this section we refer to the discretization above as the *composite grid discretization* of (6.54). The solution of this composite grid discretization is denoted by $\tau^{H,h}$.
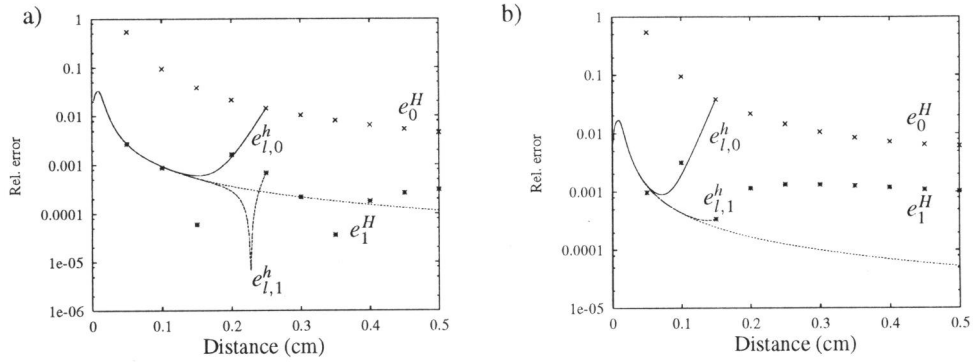
Figure 6.4   Relative errors before and after 1 local defect correction step in Example 6.4 for $H = 0.05$ cm, $l = 5H$, $\sigma = 20$ (a) and for $H = 0.05$ cm, $l = 3H$, $\sigma = 40$ (b).

i	$\dfrac{\|\tau_i^{H,h}-\tau^{H,h}\|_\infty}{\|\tau^{H,h}\|_\infty}$		σ	average error reduction
0	$1.35\ 10^{-2}$		5	0.082
1	$1.49\ 10^{-3}$		10	0.10
2	$1.57\ 10^{-4}$		20	0.11
3	$1.66\ 10^{-5}$		40	0.11
4	$1.76\ 10^{-6}$		80	0.11

Table 6.2   Convergence behaviour of the nonlinear LDC method in Example 6.6. Relative errors for $\sigma = 20$ and average error reduction factors for several values of σ.

Example 6.5 In this example we take $H = 1/100$ and $l = 5H$. The iterates $\tau_i^{H,h}$ in the nonlinear LDC method are compared with the solution $\tau^{H,h}$ of the composite grid discretization of (6.54). In Table 6.2 the relative errors

$$\frac{\|\tau_i^{H,h} - \tau^{H,h}\|_\infty}{\|\tau^{H,h}\|_\infty}$$

are presented for $\sigma = 20$. We observe a fast convergence of the iterates $\tau_i^{H,h}$ to the grid function $\tau^{H,h}$. The error reduction factors in the nonlinear LDC method are approximately 0.11 in this case. For other refinement factors a similar fast convergence of the LDC iterates to the grid function $\tau^{H,h}$ is obtained. In Table 6.2 the average error reduction factors in the nonlinear LDC method for $\sigma = 5, 10, 20, 40, 80$ are shown. The convergence rate is independent of the refinement factor σ.   □

In Example 6.5 we have seen that the composite grid iterates in the nonlinear LDC method converge fastly to the grid function $\tau^{H,h}$. In Example 6.6 the grid function $\tau^{H,h}$ and the approximations $\tau_1^{H,h}$ and $\tau_2^{H,h}$, resulting after 1, respectively 2 local defect correction steps, are compared with the reference solution $\hat{\tau}$ for several values of the refinement factor σ and for several values
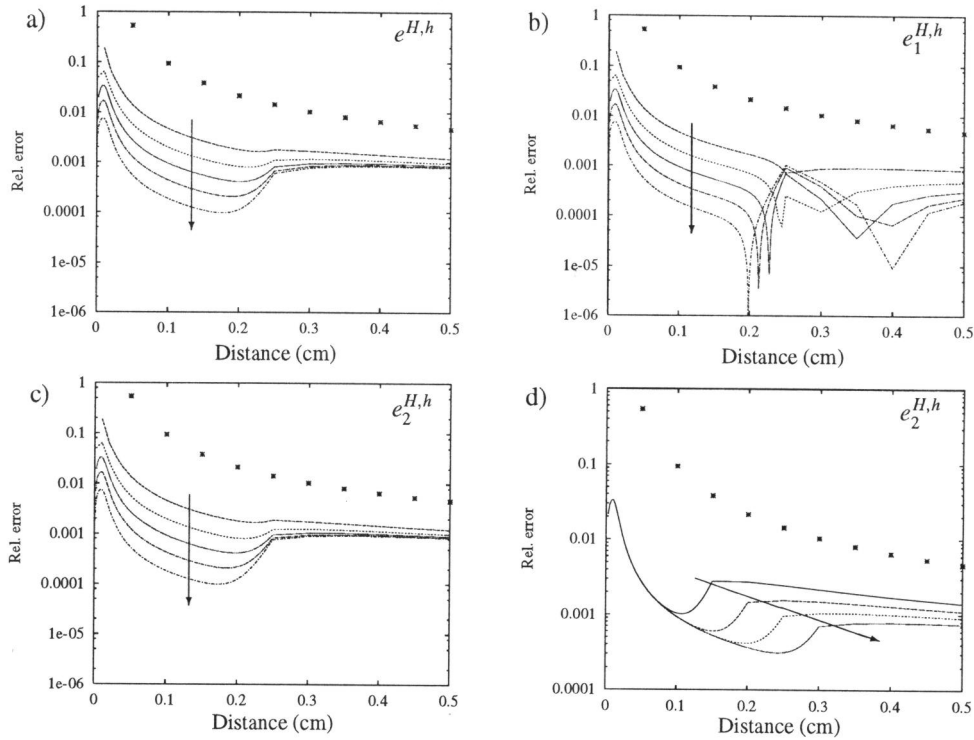
Figure 6.5 The errors in the grid functions $\tau^{H,h}$ (a), $\tau_1^{H,h}$ (b), and $\tau_2^{H,h}$ (c) for $H = 0.05$ cm, $l = 5H$, $\sigma = 1, 5, 10, 20, 40, 80$ and $\tau_2^{H,h}$ (d) for $H = 0.05$ cm, $\sigma = 20$, $l = 3H, 4H, 5H, 6H$. The arrows indicate the direction of increasing σ in a)-c) and increasing l in d).

of the interface grid point $\xi = l$. The errors in $\tau^{H,h}$, $\tau_1^{H,h}$ and $\tau_2^{H,h}$ are defined by

$$e^{H,h}(x_j) := \frac{|\tau^{H,h}(x_j) - \hat{\tau}(x_j)|}{|\hat{\tau}(x_j)|}, \qquad x_j \in \Omega^{H,h},$$

$$e_i^{H,h}(x_j) := \frac{|\tau_i^{H,h}(x_j) - \hat{\tau}(x_j)|}{|\hat{\tau}(x_j)|}, \qquad x_j \in \Omega^{H,h}, \quad i = 1, 2.$$

Example 6.6 We take $H = 1/100$. In Figure 6.5.a the error in the grid function $\tau^{H,h}$ is shown for $l = 5H$ and $\sigma = 1, 5, 10, 20, 40, 80$. For $\sigma = 1$ the grid $\Omega^{H,h}$ is a uniform grid with grid size H. The error for $\sigma = 1$ is indicated by an asterix ($*$). When σ increases, the error in $\tau^{H,h}$ inside the local region Ω_l decreases since the grid size of the composite grid $\Omega^{H,h}$ inside Ω_l becomes smaller. Outside the local region Ω_l the error in $\tau^{H,h}$ becomes constant for increasing σ, since the grid size of the composite grid $\Omega^{H,h}$ outside the local region Ω_l remains constant. For σ large enough, the size of the error outside Ω_l is in agreement with the grid size H and the variations

of the solution of (6.54) outside Ω_l. Note that this does not hold for the approximation $\tau_0^{H,h}$. In Figure 6.5.b the relative error in the grid function $\tau_1^{H,h}$, which results after 1 local defect correction step, is shown for the same set of refinement factors as in Figure 6.5.a. The relative error in $\tau_1^{H,h}$ displays a non-smooth behaviour in a neighbourhood of the interface grid point, but this error is nowhere significantly larger than the relative error in $\tau^{H,h}$. In Figure 6.5.c the relative error in the grid function $\tau_2^{H,h}$, resulting after 2 local defect correction steps, is shown for the same set of refinement factors as in Figure 6.5.a,b. The error in $\tau_2^{H,h}$ is comparable to the error in $\tau^{H,h}$, which is obtained in the limit by the nonlinear LDC method.

In Figure 6.5.d the relative error in $\tau_2^{H,h}$ is shown for $\sigma = 20$ and for $l = 3H, 4H, 5H, 6H$. When l decreases, the relative error in $\tau_2^{H,h}$ outside Ω_l becomes larger. This is due to the fact that for decreasing l the region $\Omega \backslash \Omega_l$, where a coarse grid size H is used, is extended in the direction of the burner surface and closer to the burner surface the variations in the solution τ are larger. □

In the previous examples we have shown some typical properties of the nonlinear LDC method for the boundary value problem (6.54). Due to the fact that a discretization of the boundary value problem on the global coarse grid Ω^H is used, the approximation u_0^H and $u_{l,0}^h$ in the initialization step of the nonlinear LDC method are relatively inaccurate near the interface grid point. Significantly more accurate approximations u_1^H and $u_{l,1}^h$ are obtained after only 1 local defect correction step. Performing more local defect correction steps yields significantly better approximations of the solution of a composite grid discretization of boundary value problem (6.54), but not of the solution of the boundary value problem itself. Since our goal is to approximately solve the boundary value problem (6.54) on the composite grid, one local defect correction step is sufficient. This holds for various (reasonable) values of σ and l.

In the next example we consider the amount of work required by the nonlinear LDC method. We compare the number of Newton iterations in this method with the number of Newton iterations in the Newton-FAC method from Section 5.3 applied to the composite grid discretization of (6.54) as defined above Example 6.5.

Example 6.7 We take $H = 1/100$, $l = 5H$, $\sigma = 20$. The Newton-FAC method consists of an outer Newton iteration on $\Omega^{H,h}$ and inner FAC iterations for solving the Jacobian systems. For the outer iteration we use the same damped Newton method as in the nonlinear LDC method. The initial guess is obtained from the solution τ_0^H of the basic discretization by linear interpolation inside Ω_l. Only *one* FAC step (cf. (2.20)), with the initial approximation equal to 0 at all composite grid points, is applied. Both for the nonlinear LDC method and for the Newton-FAC method we count the number of systems of linear equations which are solved on Ω^H and on Ω_l^h.

In Table 6.3 the number of Newton iterations in the nonlinear LDC method are shown. Each Newton step requires the solution of a system of linear equations on Ω^H or on Ω_l^h. In the local defect correction steps ($i = 1, 2, 3, 4, 5$) a small number of Newton iterations is sufficient since good initial guesses for the damped Newton method are available. In the Newton-FAC method 10 Newton steps are performed. If we take into account the cost for computing the initial guess, 16 systems of linear equations on Ω^H and 10 systems of linear equations on Ω_l^h have been solved. So in this case the amount of work required by the Newton-FAC method is comparable with the amount of work required for two steps in the nonlinear LDC method. □

i	0	1	2	3	4	5
Ω^H	6	3	2	1	1	1
Ω_l^h	9	3	2	2	1	1

Table 6.3 Number of Newton iterations on Ω^H and Ω_l^h required by the nonlinear LDC method in Example 6.7.
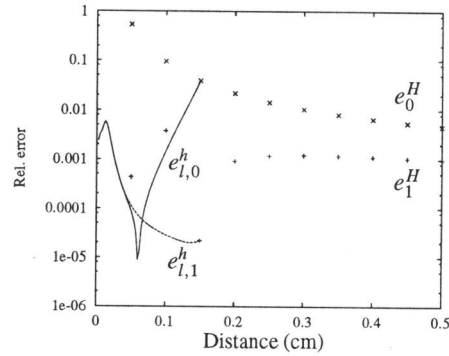

Figure 6.6 Errors before and after a local defect correction step in Example 6.8; $H = 0.05$ cm, $l = 3H$, $\sigma = 20$.

For approximating the solution of the boundary value problem (6.54) by the nonlinear LDC method, discretization processes on the uniform global coarse grid Ω^H and on the uniform local fine grid Ω_l^h have to be specified. In the examples above, both for discretizing (6.54) on Ω^H and on Ω_l^h, central differences are used for the diffusion term and upwind differences for the convective term. However, the discretization processes on Ω^H and Ω_l^h in the nonlinear LDC method may very well be different. In the Example 6.8 below we present results for the nonlinear LDC method for boundary value problem (6.54), where on the global grid the convective term is approximated using *upwind differences* and on the local grid the convective term is approximated using *central differences*,

$$\frac{d\tau}{d\xi}(y) \doteq \frac{\tau(y+h) - \tau(y-h)}{2h},$$

with $y \in \Omega_l^h$. On both grids the diffusion term in (6.54) is approximated using central differences.

Example 6.8 We take $H = 1/100$, $l = 3H$ and $\sigma = 20$. In Figure 6.6 the relative errors in the approximations τ_0^H, $\tau_{l,0}^h$ and τ_1^H, $\tau_{l,1}^h$ are plotted. Clearly, by using central differences instead of upwind differences for the convective term on the local grid, the quality of the discretization is improved (compare Figure 6.6 with Figure 6.5.d). Like in Example 6.4 we see that the error in $\tau_{l,0}^h$ is large near the interface grid point. Here the error at the interface grid point is larger than the maximum error inside Ω_l. After a local defect correction step a significant reduction of the relative error near the interface grid point results. We note that, like in Example 6.6, performing more local

defect correction steps does not significantly change the size of the errors in the approximations for τ. $\qquad\qquad\qquad\qquad\qquad\qquad\qquad\qquad\qquad\qquad\qquad\qquad\qquad$ $\square$

In Example 6.9 the burner stabilized flame problem (6.42) is solved on the composite grid $\Omega^{H,h}$. We make use of the fact that fine grid approximations before a local defect correction step are accurate near the burner surface.

Example 6.9 For solving the burner stabilized flame problem (6.42) we use the scalar combustion equation (6.54) and the fact that $\frac{dY_{fu}}{d\xi}$ is continuous at $\xi = 0$. With $Y_{fu}(0) = Y_{fu}^0$ given, the solution of the boundary value problem (6.54) is approximated on the composite grid $\Omega^{H,h}$. The composite grid approximation is denoted by $\tau^{H,h}$. By (6.50a) the approximation $\tau^{H,h}$ yields an approximation of Y_{fu} on $\Omega^{H,h}$. The first derivative $\frac{dY_{fu}}{d\xi}$ at $\xi = 0$ is approximated by

$$D_c := \frac{Y_{fu}^0 + \tau^u - \tau^{H,h}(h) - Y_{fu}(-h)}{2h},$$

where $Y_{fu}(-h)$ follows from (6.44). From (6.44) we find

$$\lim_{\xi\uparrow 0} \frac{dY_{fu}}{d\xi}(\xi) = (Y_{fu}^0 - Y_{fu}^u)\frac{u^u}{D^u} =: D_-.$$

While $|D_c - D_-| > tol$, the value of Y_{fu}^0 is adapted:

$$Y_{fu}^0 := Y_{fu}^u + \frac{D^u}{u^u}(D_c + D_-)/2.$$

As long as $|D_c - D_-| > tol$, the solution of (6.54) is approximated by solving the basic discretization on Ω^H and the related local fine grid discretization on Ω_l^h. No local defect correction steps are carried out, since the local fine grid approximation is sufficiently accurate near the burner surface. For the accepted value of Y_{fu}^0 a local defect correction step is carried out in order to improve the accuracy of the approximation outside the local region Ω_l.

In Figure 6.7 the results of this iterative process are shown for $H = 1/100$, $\sigma = 40$, $l = 3H$, $tol = 10^{-3}$. The dashed lines in Figure 6.7.a represent the approximations of the dimensionless temperature τ and the mass fraction Y_{fu} for the initial guess $Y_{fu}^0 = Y_{fu}^u$, while the solid lines represent the approximations of τ and Y_{fu} for the accepted value of Y_{fu}^0, obtained after 7 iteration steps. These approximations of τ and Y_{fu} are still inaccurate near the interface grid point $\xi = l$. By performing 1 local defect correction step the kink at $x = l$ in the approximations is removed. This is shown in Figure 6.7.b where the approximations of τ and Y_{fu} after 1 local defect correction step are plotted. $\qquad\qquad\qquad\qquad\qquad\qquad\qquad\qquad\qquad\qquad\qquad\qquad\qquad$ $\square$

6.5 DISCUSSION

In Section 6.4 we have presented results of the simulation of a one-dimensional premixed laminar flame on composite grids which are locally strongly refined. The use of locally strongly refined
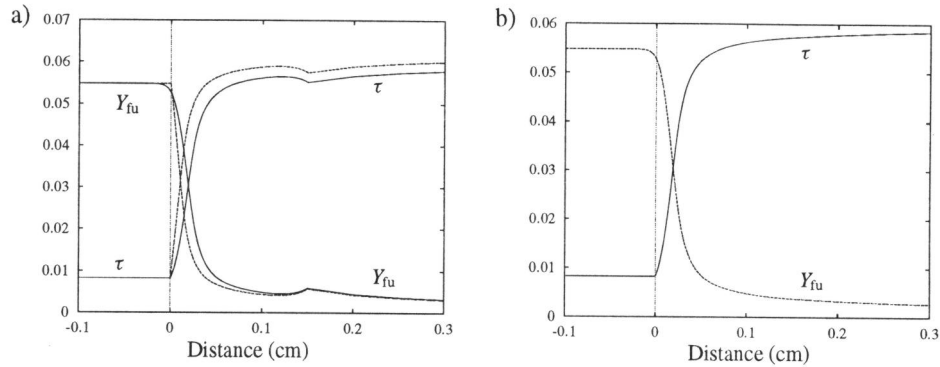
Figure 6.7 Approximations of τ and Y_{fu} for the burner stabilized flame problem in Example 6.9. a) The approximations for the initial value of Y_{fu}^0 (dashed line) and for the accepted value of Y_{fu}^0 (solid line). b) The approximations for the accepted value of Y_{fu}^0 after 1 local defect correction step.

grids is inevitable when numerically simulating combustion processes because of the large difference between the size of the burner and the size of the chemically active layer. Ratios of the largest distance between two neighbouring grid points to the smallest distance between two grid points of 10-100 are not unusual in combustion modelling. As we have seen, the local defect correction method is an attractive approach for solving the model combustion problem on such strongly refined composite grids. The boundary value problem is discretized on the uniform subgrids only. Also systems of algebraic equations need to be solved on the uniform subgrids only. Using very large refinement factors, accurate approximations of the solution result after only *one* local defect correction step.

Clearly the number of grid points in the composite grids in Section 6.4 is not minimal to obtain an approximation of boundary value problem (6.54) with a certain accuracy. For simulating one-dimensional flames, truly non-uniform locally refined grids, which need a smaller number of grid points to obtain approximations with a certain accuracy, can be used (e.g., [40],[55],[58]). Often the one-dimensional adaptive gridding techniques cannot be applied for two-dimensional problems. The concept of composite grids and the local defect correction method can easily be generalized for two space dimensions (and even for three space dimensions). For higher dimensional problems, this approach offers some clear advantages: locally strongly refined grids and yet simple data structures; also the fact that one can use uniform grids facilitates both the discretization process and the solution of the resulting algebraic equations considerably.

We realize that we only considered a fairly simple combustion problem. The latter was taken to demonstrate the versatility of our approach for real life problems. Of course, more research on the use of composite grids and local defect correction for more complex combustion problems is needed.

CONCLUSIONS

We have studied iterative methods for solving elliptic boundary value problems on composite grids which are locally strongly refined. This local refinement is obtained by using a small number of uniform grids with different grid sizes, covering different parts of the domain. For notational convenience a two-dimensional model composite grid composed of a uniform global coarse grid and only one uniform local fine grid has been used. The composite grids considered in this thesis have several attractive properties: data structures are simple and hence these grids are very manageable in a practical implementation; locally the grid can be refined to any scale required by the variations of the solution; since the composite grids are composed of uniform subgrids, discretization of the boundary value problem is standard in the greater part of the domain. These advantages are even more pronounced for three space dimensions. We have used finite difference methods for discretizing the boundary value problems on the composite grids.

In Chapter 2 and Chapter 3 we have given a presentation and analysis of three basic iterative methods for solving boundary value problems on composite grids: local defect correction (LDC, introduced by Hackbusch), the fast adaptive composite grid method (FAC, introduced by McCormick) and the multi-level adaptive technique (MLAT, introduced by Brandt). These methods have in common that in the iterative process only systems of algebraic equations on the uniform subgrids are solved. Often such systems can be solved very efficiently. By presenting the three methods in one framework, we have been able to discuss the similarities and the differences between these methods. We have shown that the composite grid discretizations which are actually solved by the LDC method and by the MLAT method are the same if the restriction, used in MLAT for restricting approximations on the local fine grid to grid points of the global coarse grid, is the trivial injection. Also we have shown that if the FAC method is applied to the composite grid discretization related to the LDC method, and if the restriction used in the FAC method is equal to the trivial injection on the interface, then the LDC method and the FAC method have the same iteration matrix. Unfortunately, we have not been able to derive satisfactory bounds for the norm or spectral radius of this iteration matrix. So a satisfactory convergence analysis of the LDC method and the FAC method in a finite difference setting is still lacking. Hence this topic is still

left for future research.

In Chapter 4 we have studied in detail the composite grid discretization related to the LDC method for the Poisson problem. For the one-dimensional Poisson problem this composite grid discretization is compared with two other reasonable finite difference discretizations on the composite grid. It is shown that already for this simple problem, the composite grid discretization related to the LDC method has important advantages compared to the other two discretization methods. For the two-dimensional Poisson problem we have derived a sharp global discretization error bound, which is valid without restrictions on the coarse grid size H, the fine grid size h and the refinement factor $\sigma = H/h$. This bound nicely separates the discretization error terms related to the high activity region, the low activity region and the interpolation on the interface. This is an important result, since up to now no results were known concerning finite difference discretization errors on composite grids.

Numerical results, both in this thesis and in the literature, show very fast convergence of the local defect correction iteration for several problems. Often accurate approximations of the solution of the boundary value problem are obtained after only one local defect correction step. In our opinion it would be worthwhile to analyse the solution method given by the LDC initialization step (consisting of a basic global coarse grid discretization and a corresponding local fine grid discretization) and one local defect correction step. Some first results in this direction are presented in [19].

In Chapter 5 we have shown how the LDC method and the FAC method can be applied to nonlinear boundary value problems. In Chapter 6 we have used the nonlinear LDC method for solving a concrete nonlinear boundary value problem, resulting from combustion modelling, on a composite grid. The numerical results for this (fairly simple) combustion problem indicate that for large refinement factors and after only one local defect correction step, accurate approximations of the solution of the boundary value problem can be obtained. These results and the attractive properties of composite grids as described in Section 1.2 make further research on the use of composite grids and local defect correction for more complex combustion problems worthwhile.

BIBLIOGRAPHY

[1] D.C. Arney and J.E. Flaherty, An adaptive local mesh refinement method for time-dependent partial differential equations, *Appl. Numer. Math.*, 5 (1989), pp. 257-274.

[2] U. M. Ascher, R.M.M. Mattheij and R.D. Russel, *Numerical Solution of Boundary Value Problems for Ordinary Differential Equations*, Classics In Applied Mathematics, Vol. 13, SIAM, Philadelphia (1995).

[3] R. Barret, M. Berry, T.F. Chan, J. Demmel, J. Donato, J. Dongarra, V. Eijkhout, R. Pozo, C. Romine and H. van der Vorst, *Templates for the Solution of Linear Systems: Building Blocks for Iterative Methods*, SIAM, Philadelphia (1994).

[4] M.J. Berger and P. Colella, Local adaptive mesh refinement for shock hydrodynamics, *J. Comput. Phys.*, 82 (1989), pp. 64-84.

[5] J.H. Bramble and B.E. Hubbard, A theorem on error estimation for finite difference analogues of the Dirichlet problem for elliptic equations, *Contributions to Differential Equations*, 2 (1963), pp. 319-340.

[6] J.H. Bramble and B.E. Hubbard, New monotone type approximations for elliptic problems, *Math. Comp.*, 18 (1964), pp. 349-367.

[7] A. Brandt, Multi-level adaptive solutions to boundary value problems, *Math. Comp.*, 31 (1977), pp. 333-390.

[8] A. Brandt, *Multigrid techniques: 1984 guide with applications to fluid dynamics*, GMD-Studien Nr 85, GMD (1984).

[9] A. Brandt and D. Bai, Local mesh refinement multilevel techniques, *SIAM J. Sci. Statist. Comput.*, 8 (1987), pp. 109-134.

[10] J.D. Buckmaster (ed.), *The Mathematics of Combustion*, SIAM, Philadelphia (1985).

[11] J.D. Buckmaster and G.S.S. Ludford, *Theory of Laminar Flames*, Cambridge University Press, Cambridge (1982)

[12] J.R. Bunch and D.J. Rose (eds), *Sparse Matrix Computations*, Academic Press, New York (1976).

[13] Z. Cai and S.F. McCormick, On the accuracy of the finite volume element method for diffusion equations on composite grids, *SIAM J. Numer. Anal.*, 27 (1990), pp. 636-655.

[14] P.G. Ciarlet, Discrete maximum principle for finite-difference operators, *Aequationes Math.*, 4 (1970), pp. 338-352.

[15] T.F. Chan, T.Y. Hou and P.L. Lions, Geometry related convergence results for domain decomposition algorithms, *SIAM J. Numer. Anal.*, 28 (1991), pp. 378-391.

[16] T.F. Chan and T.P. Mathew, Domain decomposition algorithms, *Acta Numerica* (1994), pp. 61-143.

[17] R.L.G.M. Eggels, *Modelling of Combustion Processes and NO Formation with Reduced Reaction Mechanisms*, Ph.D. Thesis, Eindhoven University of Technology, Eindhoven (1996).

[18] R.E. Ewing, Adaptive grid refinements for transient flow problems, in [25], pp. 194-205.

[19] P.J.J. Ferket, Coupling of a global coarse discretization and local fine discretizations, in [35], pp. 47-58.

[20] P.J.J. Ferket and A.A. Reusken, Further analysis of the local defect correction method, *Computing*, 56 (1996), pp. 117-139.

[21] P.J.J. Ferket and A.A. Reusken, A finite difference discretization method for elliptic problems on composite grids, *Computing*, 56 (1996), pp. 343-369.

[22] P.J.J. Ferket, The finite difference based fast adaptive composite grid method, RANA 95-19, Department of Mathematics and Computing Science, Eindhoven University of Technology (1995) (to appear in *Numerical Linear Algebra with Applications*).

[23] M. Fiedler, *Special Matrices and their Applications in Numerical Mathematics*, Nijhoff, Dordrecht (1986).

[24] J.E. Flaherty, P.K. Moore and C. Ozturan, Adaptive overlapping grid methods for parabolic systems, in [25], pp. 176-193.

[25] J.E. Flaherty, P.J. Paslow, M.S. Shephard and J.D. Vasilakis (eds.), *Adaptive Methods for Partial Differential Equations*, SIAM, Philapdelphia (1989).

[26] R.W. Freund, G.H. Golub and N.M. Nachtigal, Iterative solution of linear systems, *Acta Numerica* 1992, pp. 57-100.

[27] J.A. George and J. Liu, *Computer Solution of Large Sparse Positive Definite Systems*, Prentice Hall, Englewood Cliffs (1981).

[28] W.D. Gropp, Local uniform mesh refinement with moving grids, *SIAM J. Sci. Stat. Comput.*, 8 (1987), pp. 292-304.

[29] W.D. Gropp and D.E. Keyes, Domain decomposition with local mesh refinement, *SIAM J. Sci. Comput.*, 13 (1992), pp. 967-993.

[30] W. Hackbusch, Local defect correction method and domain decomposition techniques, *Computing*, Suppl 5 (1984), pp. 89-113.

[31] W. Hackbusch, *Multi-Grid Methods and Applications*, Springer Verlag, Berlin (1985).

[32] W. Hackbusch, *Elliptic Differential Equations. Theory and Numerical Treatment*, Springer-Verlag, Berlin (1992).

[33] W. Hackbusch, *Iterative Solution of Large Sparse Systems*, Springer-Verlag, Berlin (1994).

[34] W. Hackbusch and G. Wittum (eds.), *Fast Solvers for Flow Problems*, Notes on Numerical Fluid Mechanics, Vol. 49, Vieweg, Braunschweig (1995)

[35] W. Hackbusch and G. Wittum (eds.), *Numerical Treatment of Coupled Systems*, Notes on Numerical Fluid Mechanics, Vol. 51, Vieweg, Braunschweig (1995)

[36] L. Hart, S. McCormick, A. O'Gallagher and J. Thomas, The fast adaptive composite grid method (FAC): Algorithms for advanced computers, *Appl. Math. & Comp.*, 19 (1986), pp. 103-126.

[37] M. Heroux, S. McCormick, S. McKay and J.W. Thomas, Applications of the fast adaptive composite grid method, in *Proceedings of the Third Copper Mountain Conference on Multigrid Methods*, (1987), pp. 251-265.

[38] R.E. Ewing, R.D. Lazarov and P.S. Vassilevski, Local refinement techniques for elliptic problems on cell-centered grids. I: error analysis, *Math. Comp.*, 56 (1991), pp. 437-461.

[39] K. Khadra, P. Angot and J.-P. Caltagirone, A comparison of locally adaptive multigrid methods: LDC, FAC, and FIC, in *Proceedings of the Sixth Copper Mountain Conference on Multigrid Methods*, (1994), pp. 275-292.

[40] H.C. de Lange, *Modelling of Premixed Laminar Flames*, Ph.D. Thesis, Eindhoven University of Technology, Eindhoven (1992).

[41] P.L. Lions, On the Schwarz alternating method II: stochastic interpretation and order properties, in *Proceedings of the Second International Symposium on Domain Decomposition Methods*, (1989), pp. 47-70.

[42] J. Lorenz, Zur Inversmonotonie diskreter Probleme, *Numer. Math.*, 27 (1977), pp. 227-238.

[43] H.T.M. van der Maarel, *A Local Grid Refinement Method for the Euler Equations*, Ph.D. Thesis, University of Amsterdam, Amsterdam (1993).

[44] H.T.M. van der Maarel and P.W. Hemker, Structured adaptive finite-volume multigrid for compressible flows, in [34], pp. 14-37.

[45] A. van Maaren, *One-step chemical reaction parameters for premixed laminar flames*, Ph.D. Thesis, Eindhoven University of Technology, Eindhoven (1994).

[46] S. McCormick, Fast adaptive composite grid (FAC) methods: Theory for the variational case, *Computing*, Suppl. 5 (1984), pp. 115-121.

[47] S. McCormick and J. Thomas, The fast adaptive composite grid (FAC) method for elliptic equations, *Math. Comp.*, 46 (1986), pp. 439-456.

[48] S.F. McCormick, *Multilevel Adaptive Methods for Partial Differential Equations*, Frontiers in Applied Mathematics, Vol. 6, SIAM, Philidelphia (1989).

[49] S. McCormick and U. Rüde, A finite volume convergence theory for the fast adaptive composite grid methods, *Appl. Numer. Math.*, 14 (1994), pp. 91-103.

[50] A.R. Mitchell and D.F. Griffiths, *The Finite Difference Method in Partial Differential Equations*, John Wiley & Sons, New York (1980).

[51] R.E. O'Malley Jr., *Singular Perturbation Methods for Ordinary Differential Equations*, Springer-Verlag, New York (1991).

[52] J.M. Ortega and W.C. Rheinboldt, *Iterative Solution of Nonlinear Equations in Several Variables*, Academic Press, New York and London (1970).

[53] J.S. Otto, Multigrid convergence for convection-diffusion problems on composite grids, *Linear Algebra Appl.*, 190 (1993), pp. 39-70.

[54] G.L.G. Sleijpen and H.A. Van der Vorst, Optimal iteration methods for large linear systems of equations, in [66], pp. 291-320.

[55] M.D. Smooke, Solution of burner-stabilized premixed laminar flames by boundary value methods, *J. Comput. Phys.*, 48 (1982), pp. 72-105.

[56] M.D. Smooke, Fully adaptive solutions of one-dimensional mixed initial-boundary value problems with applications to unstable problems in combustion, *SIAM J. Sci. Stat. Comput.*, 7 (1986), pp. 301-321.

[57] D.R. Smith, *Singular-Perturbation Theory. An introduction with applications*, Cambridge University Press, Cambridge (1985).

[58] L.M.T. Somers, *The Simulation of Flat Flames with Detailed and Reduced Chemical Models*, Ph.D. Thesis, Eindhoven University of Technology, Eindhoven (1993).

[59] J. Stoer and R. Bulirsch, *Introduction to Numerical Analysis*, Second Edition, Springer-Verlag, New York (1993).

[60] R.A. Strehlow, *Combustion Fundamentals*, McGraw-Hill, New York (1984).

[61] K. Stüben and U. Trottenberg, *Multigrid methods: fundamental algorithms, model problem analysis and applications*, GMD-Studien Nr. 96, GMD (1984).

[62] J.H.M. ten Thije Boonkkamp, The conservation equations for reacting gas flow, *EUT Report* 93-WSK-01, Eindhoven (1993).

[63] J.W. Thomas, R. Schweitzer, M. Heroux, S. McCormick and A.M. Thomas, Application of the fast adaptive composite grid method to computational fluid dynamics, in *Numerical Methods in Laminar and Turbulent Flow*, (1987), pp. 1071-1082.

[64] R.A. Trompert, *Local Uniform Grid Refinement for Time-dependent Partial Differential Equations*, Ph.D. Thesis, University of Amsterdam, Amsterdam (1994).

[65] R.S. Varga, *Matrix Iterative Analysis*, Prentice Hall, Englewood Cliffs (1962).

[66] C.B. Vreugdenhil and B. Koren (eds.), *Numerical Methods for Advection-Diffusion Problems*, Notes on Numerical Fluid Mechanics, Vol. 45, Vieweg, Braunschweig (1993).

[67] P. Wesseling, *An Introduction to Multigrid Methods*, Wiley, Chichester (1992).

[68] F.A. Williams, *Combustion Theory*, Second Edition, Addison-Wesley, Redwood City (1985).

[69] D.M. Young, *Iterative Solution of Large Linear Systems*, Academic Press, New York (1971).

INDEX

SAMENVATTING

Veel fysische processen kunnen wiskundig gemodelleerd worden als een elliptisch randwaardepro-
bleem. Om een numerieke benadering van de oplossing van het randwaardeprobleem te krijgen,
wordt het randwaardeprobleem benaderd (gediscretiseerd) op een verzameling discrete punten
(het rooster), en wordt het resulterende stelsel algebraïsche vergelijkingen opgelost. Indien de
oplossing van het randwaardeprobleem sterk varieert is een fijn rooster nodig om een nauwkeurige
numerieke benadering te krijgen. Veelal is de variatie van de oplossing niet over het hele domein,
maar alleen lokaal groot. Om in dergelijke gevallen de oplossing van het randwaardeprobleem
nauwkeurig en efficiënt te benaderen is een lokaal verfijnd rooster nodig.

In dit proefschrift worden iteratieve methoden voor het oplossen van elliptische randwaardepro-
blemen op zogenaamde samengestelde roosters bestudeerd. Samengestelde roosters zijn lokaal
verfijnde roosters die zijn samengesteld uit een aantal uniforme roosters. Eén van de uniforme
roosters overdekt het hele domein en heeft een grove maaswijdte. De overige uniforme roosters
overdekken ieder slechts een deel van het domein en hebben een (veel) fijnere maaswijdte. Als
modelrooster wordt een samengesteld rooster gebruikt dat is samengesteld uit een globaal uni-
form grof rooster en één lokaal uniform fijn rooster. De maaswijdte van het lokale rooster zal
vaak veel fijner zijn dan de maaswijdte van het globale rooster. Om de randwaardeproblemen te
discretiseren worden eindige differenties gebruikt.

In de hoofdstukken 2 en 3 worden een drietal uit de literatuur bekende methoden voor het
oplossen van lineaire randwaardeproblemen op samengestelde roosters gepresenteerd en geana-
lyseerd. Bij de LDC methode ("local defect correction") en de MLAT methode ("multi-level
adaptive technique") wordt het randwaardeprobleem niet a priori gediscretiseerd op het samenge-
stelde rooster. In iedere iteratiestap worden stelsels algebraïsche vergelijkingen op de uniforme
deelroosters gedefinieerd en opgelost. Voor de LDC methode en de MLAT methode wordt het
discrete probleem op het samengestelde rooster, dat uiteindelijk wordt opgelost, afgeleid. De
verschillen tussen het discrete probleem gerelateerd aan de LDC methode en het discrete prob-
leem gerelateerd aan de MLAT methode worden besproken. Voor de LDC methode wordt een uit-
drukking voor de iteratiematrix afgeleid. De FAC methode ("fast adaptive composite grid method")

is een iteratieve methode voor het oplossen van a priori gegeven discrete problemen op het samengestelde rooster. De FAC methode wordt toegepast op het aan de LDC methode gerelateerde discrete probleem op het samengestelde rooster en de benaderingen in de FAC iteratie worden vergeleken met de benaderingen in de LDC iteratie.

In hoofdstuk 4 wordt het aan de LDC methode gerelateerde discrete probleem op het samengestelde rooster nader bestudeerd. Voor de één-dimensionale Poisson vergelijking wordt dit discrete probleem vergeleken met twee andere, aan de MLAT methode en de FAC methode gerelateerde, discrete problemen op het samengestelde rooster. De lokale en globale discretisatiefouten en eigenschappen van de differentiematrices worden vergeleken. Het blijkt dat het aan LDC gerelateerde discrete probleem een aantal gunstige eigenschappen heeft. Voor dit discrete probleem worden ook in geval van de twee-dimensionale Poisson vergelijking de lokale discretisatiefouten geanalyseerd en gunstige eigenschappen van de differentiematrix afgeleid. Uiteindelijk wordt een scherpe bovengrens voor de globale discretisatiefout afgeleid, die geldig is zonder beperking op de grove maaswijdte, de fijne maaswijdte en de verhouding tussen deze twee maaswijdten.

In de hoofdstukken 2, 3 en 4 worden lineaire randwaardeproblemen beschouwd. In hoofdstuk 5 wordt beschreven hoe de LDC methode kan worden gecombineerd met de Newton methode voor het oplossen van niet-lineaire randwaardeproblemen op een samengesteld rooster. Voor de niet-lineaire LDC methode wordt het discrete probleem op het samengestelde rooster, dat uiteindelijk wordt opgelost, afgeleid. Voor het oplossen van dit discrete probleem wordt ook een combinatie van de Newton methode en de FAC methode beschreven.

De niet-lineaire LDC methode wordt toegepast op een concreet niet-lineair probleem afgeleid uit de modellering van verbrandingsprocessen. Bij de numerieke simulatie van verbrandingsprocessen is het gebruik van lokaal sterk verfijnde roosters noodzakelijk omdat de afmeting van de brander in het algemeen een aantal ordes groter is dan de afmeting van de zone waarin de chemische reacties plaatsvinden. In hoofdstuk 6 worden de beschrijvende vergelijkingen voor reagerende gasmengsels in het algemeen, en voor één-dimensionale vlakke vlammen in het bijzonder, gegeven. Verder worden numerieke resultaten, verkregen met de niet-lineaire LDC methode, gepresenteerd en besproken.

DANKWOORD

CURRICULUM VITAE

De schrijver van dit proefschrift is geboren op 15 november 1968 te Clinge. Na het behalen van het diploma Gymnasium B aan de R.K. Jansenius Scholengemeenschap te Hulst is hij in 1987 wiskunde gaan studeren aan de Technische Universiteit te Eindhoven. In augustus 1992 is hij (met lof) afgestudeerd in de wiskunde na het schrijven van een scriptie over meerroostermethoden voor parabolische differentiaalvergelijkingen. Het afstudeerproject is uitgevoerd onder begeleiding van dr. A.A. Reusken bij de vakgroep Analyse. Tijdens zijn studie is hij een jaar als studentassistent werkzaam geweest bij de faculteit Wiskunde en Informatica van de Technische Universiteit Eindhoven.

Vanaf september 1992 is hij als assistent in opleiding in dienst geweest van de vakgroep Analyse van de faculteit Wiskunde en Informatica van de Technische Universiteit Eindhoven. In deze functie is onder leiding van prof.dr. R.M.M. Mattheij het onderzoek verricht dat geleid heeft tot dit proefschrift.